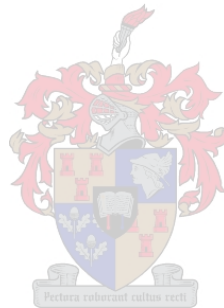


# **Machine learning for object-based crop classification using multi-temporal Landsat-8 imagery**

By  
JASON KANE GILBERTSON

Thesis presented in partial fulfilment of the requirements for the degree of Master  
of Science in the Faculty of Science at Stellenbosch University



Supervisor: Prof A van Niekerk

December 2017

## DECLARATION

By submitting this thesis electronically, I declare that the entirety of the work contained therein is my own, original work, that I am the sole author thereof (save to the extent explicitly otherwise stated), that reproduction and publication thereof by Stellenbosch University will not infringe any third-party rights and that I have not previously in its entirety or in part submitted it for obtaining any qualification.

Regarding Chapters 3 and 4, the nature and scope of my contribution were as follows:

Chapter	Nature of contribution	Extent of contribution (%)
Chapter 3	This chapter has been published as a journal article in <i>Computers and Electronics in Agriculture</i> (Gilbertson, Kemp & Van Niekerk 2017). It was co-authored by my supervisors who helped in the conceptualization and writing of the manuscript. I carried out the literature review, data collection, and analysis components	JK Gilbertson 80% A van Niekerk 15% J Kemp 5%
Chapter 4	This chapter has been published as a journal article in <i>Computers and Electronics in Agriculture</i> (Gilbertson & Van Niekerk 2017). It was co-authored by my supervisor who helped in the conceptualization and writing of the manuscript. I carried out the literature review, data collection, and analysis components.	JK Gilbertson 85% A van Niekerk 15%

Signature of candidate: Declaration with signature in possession of candidate and supervisor

Signature of supervisor: Declaration with signature in possession of candidate and supervisor

Date: 31 December 2017

## SUMMARY

Up-to-date and accurate crop maps are needed to update agricultural statistics, aid in yield forecasting, and are often used in environmental modelling. In situ methods are associated with high production costs and inefficient use of time, which hinder crop map production and reduce the usefulness of crop maps. Remote sensing offers an unbiased, cost-effective, and reliable way of mapping crops at a local, regional, and national scale. Currently, the use of multi-temporal optical imagery produces the most accurate crop maps. However, multi-temporal imagery often results in high feature dimensionality (large numbers of variables), which can negatively impact crop classification accuracy. It is therefore important to assess the benefits and limitations of using multi-temporal optical data for crop-type differentiation. This study undertakes this assessment by conducting several experiments based on multi-temporal Landsat-8 imagery in the Cape Winelands of the Western Cape, South Africa.

The first experiment assessed the effect of pansharpening (image fusion), a pre-processing technique, on supervised, multi-temporal classification of crops. A suitable number of Landsat-8 images was collected based on a crop calendar of the study area. Two separate datasets, (comprising a standard resolution set of imagery and a pansharpened set of imagery) were used to create a range of image features. The images were then classified using several machine learning classifiers. Results showed that pansharpening had a significant positive influence on classification accuracy and that the support vector machine (SVM) classifier produced the most accurate results (95.9%).

The second experiment utilized datasets produced in the first experiment to compare image analysis paradigms. The standard and pansharpened datasets were both segmented to produce image objects. Image object classification was then compared to the initial pixel-based classification to see which method was superior for crop differentiation with multi-temporal imagery. It was found that the object-based image analysis (OBIA) only slightly outperformed the pixel-based image analysis (PBIA), raising the question of whether the slight improvement in accuracy of the former approach is worth the effort of generating suitable image objects.

In the third experiment, the capability of feature selection and feature extraction methods to mitigate high feature dimensionality were tested. Informed by the findings of the previous experiments, an OBIA approach with pansharpened imagery was used as input to feature selection and feature extraction. Results showed that feature selection did not improve the accuracy of the best performing classifier (SVM). It was concluded that feature selection is not necessary for crop differentiation when a relatively small set of features (< 200) is used.

In general, multi-temporal Landsat-8 imagery shows much potential for producing accurate crop type maps. However, more research is required to evaluate the methodology in other areas and climates. Investigations into how crop type maps can be generated without collecting large numbers of training samples are also needed.

## **KEY WORDS**

Crop classification, machine learning, supervised classification, object-based image analysis, pixel-based image analysis, pansharpening, Landsat-8

## OPSOMMING

Bygewerkte en akkurate kaarte van gewasse word benodig om landbou statistieke op te dateer, opbrengs te voorspel, en word dikwels in omgewingsmodellering gebruik. Tradisionele in situ-metodes word met hoë produksiekoste en ondoeltreffende gebruik van tyd geassosieer, wat die produksie van gewaskaarte belemmer en die nut van daarvan verlaag. Afstandswaarneming bied 'n onbevooroordeelde, koste-effektiewe en betroubare manier om gewasse op plaaslike, streeks- en nasionale skaal te karteer. Tans word die akkuraatste gewaskaarte met die gebruik van multi-temporele optiese beelde geproduseer. Multi-temporele beeldmateriaal lei egter dikwels tot hoë-eienskapsdimensionaliteit (groot getalle veranderlikes), wat die akkuraatheid van gewasklassifikasie negatief kan beïnvloed. Dit is dus belangrik om die voordele en beperkings van die gebruik van multi-temporele optiese data vir die differensiasie tussen gewastipes te assesseer. Hierdie studie pak hierdie assessering aan deur verskeie eksperimente, gebaseer op multi-temporele Landsat-8 beelde in die Kaapse Wynland van die Wes-Kaap, Suid-Afrika, uit te voer.

Die eerste eksperiment beoordeel die effek van panverskerping (beeldfusie), 'n verwerkingstegniek wat vooraf uitgevoer word, op gekontroleerde, multi-temporele klassifikasie van gewasse. 'n Geskikte aantal Landsat-8 beelde is op grond van 'n gewasskalender van die studiegebied ingesamel. Twee afsonderlike datastelle (wat bestaan uit 'n stel beelde van standaard resolusie en 'n panverskerpte stel beelde) is gebruik om 'n verskeidenheid beeldkenmerke te skep. Die beelde is dan met behulp van verskeie masjienleerklassifiseerders geklassifiseer. Uitslae het getoon dat panverskerping 'n beduidende positiewe invloed op klassifikasie-akkuraatheid gehad het en dat die ondersteuningvektormasjien (OVM) die akkuraatste resultate (95.9%) opgelewer het.

Die tweede eksperiment het datastelle, wat in die eerste eksperiment geproduseer is, gebruik om beeldontledingsparadigmas te vergelyk. Die standaard en panverskerpte datastelle is albei gesegmenteer om beeldobjekte te produseer. Klassifikasie van beeldobjekte is dan vergelyk met die aanvanklike pixel-gebaseerde klassifikasie om die beste metode vir die differensiasie van gewasse met multi-temporele beelde te bepaal. Daar is bevind dat die objekgebaseerde-beeldontleding (OGBO) net effens beter as die pixelgebaseerde-beeldontleding presteer. Die vraag is of dié effense verbetering in die akkuraatheid die moeite om gepaste beeldobjekte te genereer regverdig.

In die derde eksperiment is kenmerkseleksie en kenmerk-ekstraksiemetodes se vermoë om hoë-kenmerk dimensionaliteit te versag, getoets. In die lig van die bevindinge van die vorige

eksperimente is 'n OGBO-benadering met panverskerpte beelde as inset vir kenmerkseleksie en kenmerk-ekstraksie gebruik. Resultate het getoon dat kenmerkseleksie nie die akkuraatheid van die beste presterende klassifiseerder (OVM) verbeter het nie. Daar is bevind dat, wanneer 'n relatief klein stel eienskappe ( $< 200$ ) gebruik word, kenmerkseleksie nie vir gewasdifferentiasie benodig word nie.

Oor die algemeen toon multi-temporele Landsat-8-beelde baie potensiaal vir die vervaardiging van akkurate gewastipekaarte. Meer navorsing is egter nodig om die metodologie in ander gebiede en klimaat te evalueer. Ondersoeke na hoe gewastipe-kaarte gegenereer kan word sonder om groot getalle opleidingsmonsters in te samel, is ook nodig.

## **SLEUTELWOORDE**

Gewasklassifikasie, masjienleer, gekontroleerde klassifikasie, objek-gebaseerde-beeldanalise, pixel-gebaseerde-beeldanalise, panverskerping, Landsat-8

## ACKNOWLEDGEMENTS

I sincerely thank:

- My father, mother, and brother for their endless emotional and financial support. Without them this would not have been possible;
- Prof Van Niekerk for a very long list of things over the past several years as well as his guidance for this thesis;
- The Water Research Commission for initiating and funding the project titled “Wide-scale modelling of water and water availability with Earth observation/satellite imagery” (contract number K5/2401//4) of which this work forms part;
- Ms Munch for her assistance with the tasseled cap and normalisation sections of my thesis, as well as her constant support and guidance;
- Gerrit and Maria for making me feel better about my work;
- [www.linguafix.net](http://www.linguafix.net) (Helene van Niekerk) for the language checking and editing services provided; and
- All my other friends who are not mentioned above that made my time at Stellenbosch University over the past few years a great experience.

## CONTENTS

<b>DECLARATION .....</b>	<b>ii</b>
<b>SUMMARY .....</b>	<b>iii</b>
<b>OPSOMMING .....</b>	<b>v</b>
<b>ACKNOWLEDGEMENTS.....</b>	<b>vii</b>
<b>CONTENTS.....</b>	<b>viii</b>
<b>TABLES .....</b>	<b>xi</b>
<b>FIGURES .....</b>	<b>xii</b>
<b>APPENDIX .....</b>	<b>xiii</b>
<b>ACRONYMS AND ABBREVIATIONS.....</b>	<b>xiv</b>
<b>CHAPTER 1: REMOTE SENSING AND CROP TYPE MAPPING.....</b>	<b>1</b>
<b>1.1 INTRODUCTION.....</b>	<b>1</b>
<b>1.1.1 Optical remote sensing.....</b>	<b>1</b>
<b>1.1.2 Pixel-based and Object-based image classification.....</b>	<b>2</b>
<b>1.1.3 Landsat imagery for crop type mapping.....</b>	<b>3</b>
<b>1.1.4 Pansharpening (image fusion).....</b>	<b>4</b>
<b>1.1.5 Image classification .....</b>	<b>5</b>
<b>1.1.6 Dimensionality reduction.....</b>	<b>6</b>
<b>1.2 PROBLEM FORMULATION.....</b>	<b>7</b>
<b>1.3 RESEARCH AIM AND OBJECTIVES .....</b>	<b>8</b>
<b>1.4 STUDY AREA AND PERIOD.....</b>	<b>9</b>
<b>1.5 METHODOLOGY AND RESEARCH DESIGN.....</b>	<b>10</b>
<b>CHAPTER 2: LITERATURE REVIEW .....</b>	<b>12</b>
<b>2.1 ACTIVE AND PASSIVE REMOTE SENSING .....</b>	<b>12</b>
<b>2.2 OPTICAL SENSORS .....</b>	<b>12</b>
<b>2.3 SPECTRAL SIGNATURES.....</b>	<b>14</b>
<b>2.4 GEOMETRIC AND ATMOSPHERIC CORRECTIONS.....</b>	<b>14</b>
<b>2.5 IMAGE FUSION.....</b>	<b>15</b>
<b>2.6 IMAGE TRANSFORMATIONS.....</b>	<b>16</b>
<b>2.6.1 Indices.....</b>	<b>16</b>
2.6.1.1 NDVI.....	17
2.6.1.2 SAVI.....	18



2.6.1.3	ARVI.....	18
2.6.1.4	EVI.....	19
2.6.1.5	GCI.....	19
2.6.1.6	GNDVI.....	20
2.6.1.7	GI.....	20
2.6.1.8	RGRI.....	20
2.6.1.9	SRI.....	21
2.6.1.10	NDWI.....	21
2.6.1.11	NDMI.....	22
<b>2.6.2</b>	<b>Principal component analysis.....</b>	<b>23</b>
<b>2.6.3</b>	<b>Tasseled cap transformation (TCT).....</b>	<b>23</b>
<b>2.6.4</b>	<b>Image texture.....</b>	<b>25</b>
<b>2.7</b>	<b>IMAGE SEGMENTATION.....</b>	<b>25</b>
<b>2.7.1</b>	<b>Multi-resolution segmentation (MRS).....</b>	<b>26</b>
<b>2.7.2</b>	<b>Estimation scale parameter tool (ESP).....</b>	<b>27</b>
<b>2.8</b>	<b>IMAGE CLASSIFICATION.....</b>	<b>28</b>
<b>2.8.1</b>	<b>Unsupervised classification.....</b>	<b>28</b>
<b>2.8.2</b>	<b>Supervised classification.....</b>	<b>28</b>
2.8.2.1	Decision tree (DT).....	29
2.8.2.2	k-Nearest neighbour (k-NN).....	29
2.8.2.3	Random forest (RF).....	30
2.8.2.4	Support vector machine (SVM).....	30
<b>2.8.3</b>	<b>Knowledge-based image classification.....</b>	<b>31</b>
<b>2.9</b>	<b>TRAINING DATA.....</b>	<b>32</b>
<b>2.10</b>	<b>DIMENSIONALITY REDUCTION.....</b>	<b>33</b>
<b>2.10.1</b>	<b>Classification and regression trees (CART).....</b>	<b>34</b>
<b>2.10.2</b>	<b>Random forest.....</b>	<b>35</b>
<b>2.11</b>	<b>ACCURACY ASSESSMENT.....</b>	<b>35</b>
<b>2.12</b>	<b>SUMMARY.....</b>	<b>36</b>
<b>CHAPTER 3: PANSHARPENED LANDSAT-8 IMAGERY FOR CROP</b>		
<b>DIFFERENTIATION WHEN USING MACHINE LEARNING AND OBIA</b>		
<b>3.1</b>	<b>ABSTRACT.....</b>	<b>38</b>
<b>3.2</b>	<b>INTRODUCTION.....</b>	<b>38</b>
<b>3.3</b>	<b>MATERIALS AND METHODS.....</b>	<b>41</b>
<b>3.3.1</b>	<b>Study area.....</b>	<b>41</b>

3.3.2	In situ data .....	41
3.3.3	Satellite data and image date selection.....	42
3.3.4	Pre-processing.....	42
3.3.5	Segmentation.....	43
3.3.6	Features .....	44
3.3.7	Classification and accuracy assessment .....	45
3.4	RESULTS AND DISCUSSION.....	45
3.5	CONCLUSION.....	48
<b>CHAPTER 4: VALUE OF DIMENSIONALITY REDUCTION FOR CROP DIFFERENTIATION WITH MULTI-TEMPORAL IMAGERY AND MACHINE LEARNING.....</b>		<b>49</b>
4.1	ABSTRACT .....	49
4.2	INTRODUCTION.....	49
4.3	MATERIALS AND METHODS.....	53
4.3.1	Study area and period.....	53
4.3.2	In situ data .....	54
4.3.3	Satellite data and image date selection.....	54
4.3.4	Pre-processing.....	55
4.3.5	Segmentation.....	55
4.3.6	Image feature-set generation.....	55
4.3.7	Feature selection .....	56
4.3.8	Classification and accuracy assessment .....	57
4.4	RESULTS.....	58
4.5	DISCUSSION .....	61
4.6	CONCLUSION.....	63
<b>CHAPTER 5: DISCUSSION.....</b>		<b>65</b>
5.1	REVISITING AIMS AND OBJECTIVES .....	65
5.2	MAIN FINDINGS AND VALUE OF RESEARCH.....	67
5.3	LIMITATIONS AND RECOMMENDATIONS FOR FUTURE RESEARCH....	69
5.4	CONCLUSIONS.....	70
<b>REFERENCES.....</b>		<b>71</b>

## TABLES

Table 1 Band allocation and description of Landsat-8 imagery.....	13
Table 2 TCT coefficients for Landsat-8 at satellite reflectance .....	24
Table 3 Identification of all classification scenarios.....	44
Table 4 Features used as input for the DT, NN, SVM, and RT classifiers .....	44
Table 5 Overall accuracies and kappa coefficients for each classification and dataset .....	46
Table 6 The average sum of pansharpened pixels per SIQ crop polygon/field .....	46
Table 7 Features considered in the classifications .....	56
Table 8 Overall accuracies and kappa coefficients for all classification scenarios .....	58

**FIGURES**

Figure 1 Location of the study area in the Cape Winelands, South Africa.....	9
Figure 2 Research design for evaluating the performances of crop differentiation .....	11
Figure 3 Spectral signatures of soil, vegetation, and water in comparison to Landsat-7 bands ...	14
Figure 4 Tasseled cap "transition zone" in imagery .....	24
Figure 5 SIQ vector crop data for the Western Cape, South Africa.....	33
Figure 6 Location of the study area in the Western Cape, South Africa.....	41
Figure 7 Phenological information for informational classes. ....	42
Figure 8 A canola field on which the five different classification methods were used. ....	43
Figure 9 Overall accuracies for all classifiers grouped by dataset .....	48
Figure 10 Location of the study area.....	53
Figure 11 Phenological information on crop types .....	54
Figure 12 Overall classification accuracies.....	60

## **APPENDIX**

Appendix: Classification results and confusion matrices for all experiments, provided on compact disk.

**ACRONYMS AND ABBREVIATIONS**

AI	artificial intelligence
ANN	artificial neural network
ARVI	atmospherically resistant vegetation index
CART	classification and regression trees
CDNGI	Chief Directorate National Geospatial Information
CV	coefficient of variance
DEM	digital elevation model
DT	decision tree
ESP	estimation scale parameter tool
EVI	enhanced vegetation index
GI	greenness index
GCI	green chlorophyll index
GCP	ground control point
GEOBIA	geographic object-based image analysis
GLCM	grey level co-occurrence matrices
GLS	global land survey
GNDVI	green normalised difference vegetation index
K	kappa
k-NN	k-Nearest neighbour
IR	infrared
LV	local variance
NASA	National Aeronautics and Space Administration
NDVI	normalised difference vegetation index
NIR	near-infrared
OA	overall accuracy
OBIA	object-based image analysis
OLI	operational land imager
PBIA	pixel-based image analysis
RGRI	red green ratio index
RF	random forest
RMSE	root mean square error
RS	remote sensing

RT	random trees
SAR	synthetic aperture radar
SAVI	soil-adjusted vegetation index
SPOT	satellite pour l'observation de la terre (satellite for observation of Earth)
SRI	simple ratio index
SVM	support vector machine
TM	thematic mapper
TIRS	thermal infrared sensor
USGS	United States Geological Survey

## **CHAPTER 1: REMOTE SENSING AND CROP TYPE MAPPING**

### **1.1 INTRODUCTION**

A successful agricultural sector is the foundation of developing economies and is critical to food security (Awokuse & Xie 2015). Accurate crop maps are needed as they can be used in environmental modelling (such as greenhouse gas variability in agro-ecosystems) and updating agricultural database statistics, and aid in yield forecasting (Monfreda, Ramankutty & Foley 2008). Knowledge of crop distribution is also important for the application of land cultivation policy actions such as subsidy payments or the implementation of agro-environmental measurements (Peña-Barragán et al. 2011).

Traditional methods of crop mapping and yield forecasting involve costly routine field visits, often based on biased sampling schemes (Castillejo-Gonzalez & López-Granados 2009). Remote sensing offers an unbiased, cost-effective, and reliable way of mapping crops at a local, regional, and national scale. However, the use of remotely sensed data to discriminate crops is complicated by agronomic factors, such as similar crop development patterns (similarities between different crop types) and varying crop development schedules (variability within the same crop) (Peña-Barragán et al. 2011). Financial and technical factors also limit the application of remote sensing for crop type mapping as suitable cost and quality relationships of imagery (with the right combinations of spatial, spectral, and temporal resolutions) are required (Castillejo-Gonzalez & López-Granados 2009). A sound methodology is needed to effectively deal with crop complexity and avoid high data costs.

#### **1.1.1 Optical remote sensing**

In recent years, optical remote sensing has gained popularity for its capacity to identify and monitor crop types (Vieira et al. 2012; Simms et al. 2014; Muller et al. 2015; Ozelkan, Chen & Ustundag 2015; Zheng et al. 2015). Optical remote sensing utilizes air- or space-borne sensors that take spectral readings of the Earth's surface. Combining theoretical knowledge of crops and modern Earth observation methods with these spectral readings enables accurate classification (Campbell & Wynne 2011). Crops were traditionally classified using single-date optical imagery, mainly due to high data and processing costs. Progress and development in the field of remote sensing has allowed for the use of optical imagery from multiple capture dates for image classification (i.e. multi-temporal image classification). This classification approach integrates image data from different acquisition dates into a single spatial location. Multi-temporal data have been shown to improve crop identification, with multi-temporal optical (as opposed to radio detection and ranging) data being the preferred source (Blaes, Vanhalle & Defourny 2005; Serra



& Pons 2008; McNairn et al. 2009). For instance, Serra and Pons (2008) developed a methodology to map and monitor six Mediterranean crops using Landsat-5 TM (thematic mapper) and Landsat-7 ETM+ (enhanced thematic mapper plus) data. They concluded that multi-temporal data and the consideration of crop phenology is essential for obtaining high classification accuracy. Ozelkan, Chen & Ustundag (2015) evaluated multi-temporal Landsat-8 data for the identification of agricultural vegetation and concluded that the sensor is an effective data source for such applications. Vieira et al. (2012) evaluated time-series Landsat TM and ETM+ data for crop discrimination and found that multi-temporal optical data is very effective for accurately mapping crops. They concluded that expert knowledge of crop phenology is critical to achieving good results. Zheng et al. (2015) and Muller et al. (2015), also utilizing multi-temporal Landsat data, made similar observations. As demonstrated by Simms et al. (2014), good results can even be obtained using low spatial resolution multi-temporal normalised difference vegetation index (NDVI) data derived from MODIS (Moderate Resolution Imaging Spectroradiometer) imagery.

Castillejo-Gonzalez & López-Granados (2009), Peña-Barragán et al. (2011), and Zheng et al. (2015) stated that the selection of suitable image dates is critical for ensuring good results. There is no set number of images required for crop classification, but the dates that are selected should cover the key phenological stages of the crops of interest (Vieira et al. 2012). Selecting key phenological dates involves collecting growth schedule data (i.e. sowing, establishment, pruning, harvest etc.) for the crops of interest and using this information to select imagery. The most common way of doing so is by creating crop calendar tables, as done by Sakamoto et al. (2005), Peña-Barragán et al. (2011), Vieira et al. (2012), and Muller et al. (2015). All of these authors used different image dates and a different number of input images because of unique crop identification goals. Serra & Pons (2008) acquired 36 Landsat images (from different missions), Ozelkan, Chen & Ustundag (2015) used 13 Landsat-8 OLI images, Vieira et al. (2012) acquired four Landsat images (two Landsat TM and two Landsat ETM+), and Peña-Barragán et al. (2011) used six ASTER scenes. Hao et al. (2015) compared different multi-temporal MODIS image sets for crop classification with the random forest (RF) classifier. They found that the use of more than five image dates did not improve their crop classification, and concluded that a multi-temporal image count of five is optimal if suitable image dates are selected.

### **1.1.2 Pixel-based and Object-based image classification**

Pixels are traditional building blocks of remote sensing-based image classification (known as pixel-based image analysis (PBIA)). PBIA involves the assignment of an informational class (e.g. crop type) to each individual pixel on an image. However, with recent advances in

technology and improvements in remote sensing, there has been an increasing interest in the use of object-based image analysis (OBIA) (Peña-Barragán et al. 2011; Li et al. 2015; Ozelkan, Chen & Ustundag 2015). OBIA groups pixels based on spectral and contextual information into readily usable objects. Classification methods are then applied to these newly created objects rather than to the individual pixels (Otukey & Blaschke 2010). OBIA has an advantage over pixel-based image classification as its use of topological concepts (Blaschke 2010) facilitates improved integration between geographic information systems (GIS) and remote sensing (Pauw & Van Niekerk 2012). Other advantages of OBIA include the reduction of the salt-and-pepper effect (where individual spectrally-distinct pixels in large spectrally homogenous areas are assigned to different classes than the pixels surrounding them) which is a common occurrence in pixel-based classification (Otukey & Blaschke 2010).

OBIA is the preferred paradigm when high spatial resolution data is used (Grzegozewski et al. 2016). Castillejo-Gonzalez & López-Granados (2009) compared the capability of PBIA and OBIA to identify crops with Quickbird imagery and concluded that OBIA clearly outperformed PBIA. Bhaskaran, Paramananda & Ramnarayan (2010), and Yan et al. (2015) drew similar conclusions with OBIA outperforming PBIA by overall accuracies of 20% and 36% respectively. Weih & Riggan (2010) used a combination of aerial photography and SPOT-5 imagery for land use and land cover (including cultivation types) classification. Their experiments showed that OBIA outperformed PBIA by 10% when high and medium spatial resolution imagery were merged for input to supervised and unsupervised classification. Unlike most other recent studies, Duro, Franklin & Dube (2015) compared OBIA and PBIA for classifying SPOT-5 data and concluded that neither paradigm was superior for the classification of agricultural landscapes. Although it is generally accepted that OBIA is only preferred when the objects of interest are significantly larger than the pixels of the imagery (Pesaresi & Benediktsson 2001; Mathieu, Freeman & Aryal 2007; Blaschke 2010), Schultz et al. (2015) showed that OBIA can be applied to medium spatial resolution Landsat-8 imagery for crop classification. They achieved an overall accuracy of over 80% with five crop types in a sub-tropical climate using bi-temporal imagery and the RF classifier and found that an accurate segmentation to create objects was essential for classification success. This may be attributed to OBIA's unique ability to deal with agricultural fields that are irregularly shaped and homogenous compared to other land cover features.

### **1.1.3 Landsat imagery for crop type mapping**

Oruc, Marangoz & Buyuksalih (2004) compared OBIA and PBIA for general land use and land cover mapping with Landsat ETM+ imagery. Their study evaluated different classifiers for the OBIA and PBIA scenarios. Three traditional classifiers (parallelepiped, minimum distance, and

maximum likelihood) were compared with eCognition's standard classifier, k-nearest neighbour (k-NN), by use of overall accuracy (OA) and kappa coefficient (K). The OBIA classifications outperformed the highest PBIA classifications by an OA of 14% and a K of 0.21, which lead to the conclusion that OBIA offers substantial advantages in terms of classification accuracy. This observation was shared by Yoon et al. (2003) who also tested OBIA for land cover and land use classification with Landsat ETM+ imagery. Although much work has been done on its predecessors, no published research has compared OBIA and PBIA for classifying Landsat-8 imagery. Landsat-8 has enhanced spectral capabilities, improved sensor signal-to-noise performance (with associated radiometric resolution enhancements), and an improved duty cycle that allows the collection of a significantly greater number of images per day compared to its predecessors (Roy et al. 2014). The enhanced capabilities of the Landsat-8 operational land imager (OLI) sensor and the value of the higher spatial resolution (15 m) panchromatic band (which was introduced with Landsat-7) for crop type mapping warrants further investigation.

#### **1.1.4 Pansharpening (image fusion)**

Pansharpening is the fusion of a multispectral and panchromatic image. It results in a product featuring the spectral resolution of the former and the spatial resolution of the latter (Campbell & Wynne 2011). There are many different pansharpening methods available, but not all are suitable for quantitative analyses. It is inevitable that some of the spectral fidelity of the original multispectral information is lost during the fusion process, but some algorithms are designed to maximize spectral preservation (Zhang & Mishra 2012). Pansharpening algorithms designed to maximize spectral preservation have been proven to be effective not only for the visual enhancements of imagery (Ghodekar, Deshpande & Scholar 2016), but also for quantitative analyses such as land cover mapping (Ai et al. 2016).

Johnson, Scheyvens & Shivakoti (2014) analysed the effects of pansharpening on two Landsat-8 vegetation indices (NDVI and simple ratio) using fast intensity-hue-saturation, Bovey transform, additive wavelet transform, and smoothing filter-based intensity modulation. The results showed that these pansharpening algorithms were able to downscale both single-date and multi-temporal Landsat-8 imagery without introducing significant distortions of index values, suggesting that pansharpening holds much potential for multi-temporal Landsat-8 image classification.

Finney (2004) and Lewinski (2007) compared the classification accuracies of standard and pansharpened Landsat ETM+ imagery for land cover mapping. Conflicting results were reported: Finney (2004) found that classification methods incorporating pansharpening achieved much higher classification results, whereas Lewinski (2007) found that pansharpening did not significantly improve classification accuracy. Other research on the effect of pansharpening on

classification accuracy include Kosaka et al. (2005) and Palsson et al. (2012), but to date nothing related to pansharpening of Landsat imagery for crop classification has been published.

### **1.1.5 Image classification**

A classifier is an algorithm that assigns informational classes to pixels or objects with certain attributes. Classification algorithms can be grouped into supervised or unsupervised classifiers, where the former is defined as the process of using samples of known identity (training data) to classify pixels or objects of unknown identity (Campbell 2008). The analyst usually selects training areas by identifying and digitizing homogenous areas on the image and assigning a class label to each.

Unsupervised classification is defined as the identification of natural groups of pixels within image data (Campbell & Wynne 2011). It involves clustering whereby spectral groups within an image are formed (Myburgh 2012). The analyst has the task of defining and/or merging the spectral classes into informational classes.

Supervised classifiers have two distinct advantages over unsupervised methods: the first is that the analyst has more control over the classification result because the informational categories are defined prior to the analysis. The second is that spectral classes are automatically matched to information classes during the classification process (Campbell & Wynne 2011). Supervised and unsupervised classification is explained in more detail in Section 2.12.

Supervised classification has been widely used for crop type mapping (Vieira et al. 2012; Simms et al. 2014; Muller et al. 2015; Ozelkan, Chen & Ustundag 2015; Zheng et al. 2015). Popular algorithms include decision trees (DTs), k-NN, RF, and support vector machine (SVM). DTs perform well for general land cover classification as demonstrated by Waheed et al. (2006) and Yang et al. (2003), while RF has been used successfully for crop identification, vegetation classification and change analysis (Pal 2005; Gislason, Benediktsson & Sveinsson 2006; Yuan et al. 2005). Myburgh & Van Niekerk (2013) found that SVM is a cost-effective solution for mapping land cover in large areas. Zheng et al. (2015) showed that SVM is also effective for the classification of agricultural land cover. K-NN has been used in many studies, partly because it used to be the only classifier available in the popular OBIA software eCognition. Examples include Myint et al. (2011), Mountrakis, Im & Ogole (2011), and Myburgh & Van Niekerk (2013).

Machine learning classifiers have been compared by Myburgh & Van Niekerk (2013), Peña et al. (2014), and Qian et al. (2015). Myburgh & Van Niekerk (2013) compared SVM, k-NN, and maximum likelihood for land cover mapping, while Qian et al. (2015) compared SVM, normal

Bayes, k-NN, and classification and regression trees (CART) for the same purpose. With the exception of Peña et al. (2014) who compared the multilayer perceptron, logistic regression, SVM, and DT for summer crop classification, no other research that compares the efficiency of machine learning classifiers for crop type mapping could be found in the published literature.

### **1.1.6 Dimensionality reduction**

The use of multi-temporal data often results in very high feature (variable) counts (Lu & Weng 2007; Heigl et al. 2009). Too many features can lead to the so-called “curse of dimensionality”, whereby classifiers perform poorly due to the presence of too many features (Rodriguez-Galiano et al. 2012). This is driven by the problem of sparsity, where training data becomes too sparse to cope with the increasing feature space brought on by large numbers of variables (Myburgh & Van Niekerk 2013). Sparsity is especially problematic for statistical classifiers (e.g. minimum distance and maximum likelihood), mainly because redundancy among features are too high, which makes it more difficult to find significant differences between classes (Myburgh 2012). Classifiers consequently require an increasing number of training samples as feature dimensionality increases.

High dimensionality can be mitigated by the application of feature selection and/or feature extraction (Guyon & Elisseeff 2003). Feature extraction is the replacement of the original data by a new collection of features representing most of the variance in the original data (Benediktsson JA & Sveinsson 1997). The most common feature extraction method is principal components analysis (PCA), which transforms the data into a new set of features (called principle components), that describes the underlying structure of the original dataset (Benediktsson JA & Sveinsson 1997). Feature selection involves selecting a subset of important features from the original dataset to reduce data dimensionality (Guyon & Elisseeff 2003; Yu et al. 2006; Saeys, Inza & Larrañaga 2007). A more in-depth overview of feature extraction and selection techniques is provided in Section 2.10.

Rodriguez-Galiano et al. (2012) assessed feature selection for Mediterranean land cover classification (including multiple crop classes) with multi-seasonal imagery. They found that feature selection using RF had a positive effect on image classification (OA increases of up to 10%) and concluded that feature selection reduced the effect of the “curse of dimensionality”. Hao et al. (2015), utilizing RF feature selection for crop classification with multi-temporal MODIS imagery, also claimed that RF selected the optimal portion of features to accurately discriminate between crop types. Similarly, Conrad et al. (2011) analysed the effect of CART feature selection for crop classification using multi-temporal MODIS imagery and found that CART was able to improve classification accuracy by up to 7%. They attributed this to CART’s

ability to prioritize segments representing active phases of the different crop class phenological stages.

## 1.2 PROBLEM FORMULATION

Pansharpening algorithms designed to maximize spectral preservation have proven to not only be effective for visual enhancements of imagery (Ghodekar, Deshpande & Scholar 2016), but also for quantitative analyses such as land cover mapping (Ai et al. 2016). Johnson, Scheyvens & Shivakoti (2014) found that pansharpening algorithms were able to downscale both single-date and multi-temporal Landsat-8 imagery without introducing significant distortions of index values, suggesting that pansharpening may be beneficial for multi-temporal Landsat-8 image classification. An investigation into the value of pansharpening Landsat multispectral imagery for use in crop classification is warranted as no such work has been published to date.

PBIA has traditionally been used for classifying remotely sensed images, but recent technological advances have led to an increase in the use of OBIA (Peña-Barragán et al. 2011; Li et al. 2015; Ozelkan, Chen & Ustundag 2015). Yoon et al. (2003) and Oruc, Marangoz & Buyuksalih (2004) showed that OBIA improves classification accuracy when imagery from the former Landsat sensors (TM and ETM+) were used. The radiometric and spectral improvements made to the latest Landsat sensor (OLI), coupled with OBIA, show much potential for crop classification as the target features (cultivated fields) are often regularly shaped and homogenous. To date no research that compares OBIA and PBIA for classifying Landsat-8 imagery has been published.

Machine learning has become popular in fields dealing with large and complex datasets and are increasingly being used for remote sensing applications. In spite of its clear potential, the efficiency of different machine learning classifiers for crop differentiation has received relatively little attention in the published literature. It is not known how well different algorithms will deal with the large number of (often redundant) features associated with multi-temporal imagery, especially within the context of classifying crop types that experience dynamic changes over time (within a season). Feature selection and reduction have been shown to reduce the negative effects of high dimensionality, but may compromise the temporal patterns (representing phenology) needed for differentiating different crops.

Taking into consideration all of these gaps in the current research, four research questions were formulated, namely:

1. Does pansharpening improve supervised crop classification accuracy when Landsat-8 imagery is used?

2. Is OBIA more effective (than PBIA) for classifying crops with multi-temporal Landsat-8 imagery?
3. Which of the popular machine learning algorithms (e.g. DT, k-NN, RF, or SVM) are most adept at handling the large number of (often redundant) features associated with multi-temporal imagery, and how successful are they in differentiating different crop types?
4. To what extent does dimensionality reduction benefit crop classification with multi-temporal Landsat-8 imagery?

### **1.3 RESEARCH AIM AND OBJECTIVES**

This research aims to evaluate the use of machine learning and multi-temporal Landsat-8 imagery for mapping crops in the Cape Winelands region of South Africa. To achieve this aim, the objectives are to:

1. carry out a literature review of the latest and most effective remote sensing techniques used for mapping crop types by means of multi-temporal satellite imagery;
2. collect suitable reference data for classifier training and validation purposes;
3. determine the value of increasing the spatial resolution of Landsat-8 imagery through pansharpening (image fusion);
4. evaluate a range of machine learning classifiers for producing crop maps with multi-temporal Landsat-8 imagery;
5. compare PBIA's and OBIA's capability to differentiate between crops using multi-temporal Landsat-8 imagery;
6. assess whether dimensionality reduction improves classification results when multi-temporal Landsat-8 imagery is used for mapping crop types; and
7. make recommendations on the use of Landat-8 imagery for crop type mapping within the context of finding an operational solution.

## 1.4 STUDY AREA AND PERIOD

This research was carried out in the Cape Winelands region of South Africa (Figure 1). The study site has an area of 1040 km<sup>2</sup>, which extends from 33°34'39" to 33°52'17" S and 18°32'24" to 18°54'43" E. The Cape Winelands has a Mediterranean climate with cool wet winters and warm dry summers, an average annual rainfall of 550 mm, and the mean annual temperature minima and maxima are 11°C and 22°C respectively (Tererai, Gaertner & Jacobs 2015). The area is generally mountainous, with multiple ranges, but also has broad, fertile valleys that are home to some of the country's finest vineyards (Tererai et al. 2013). This research focuses on the dominating crops within the study area.

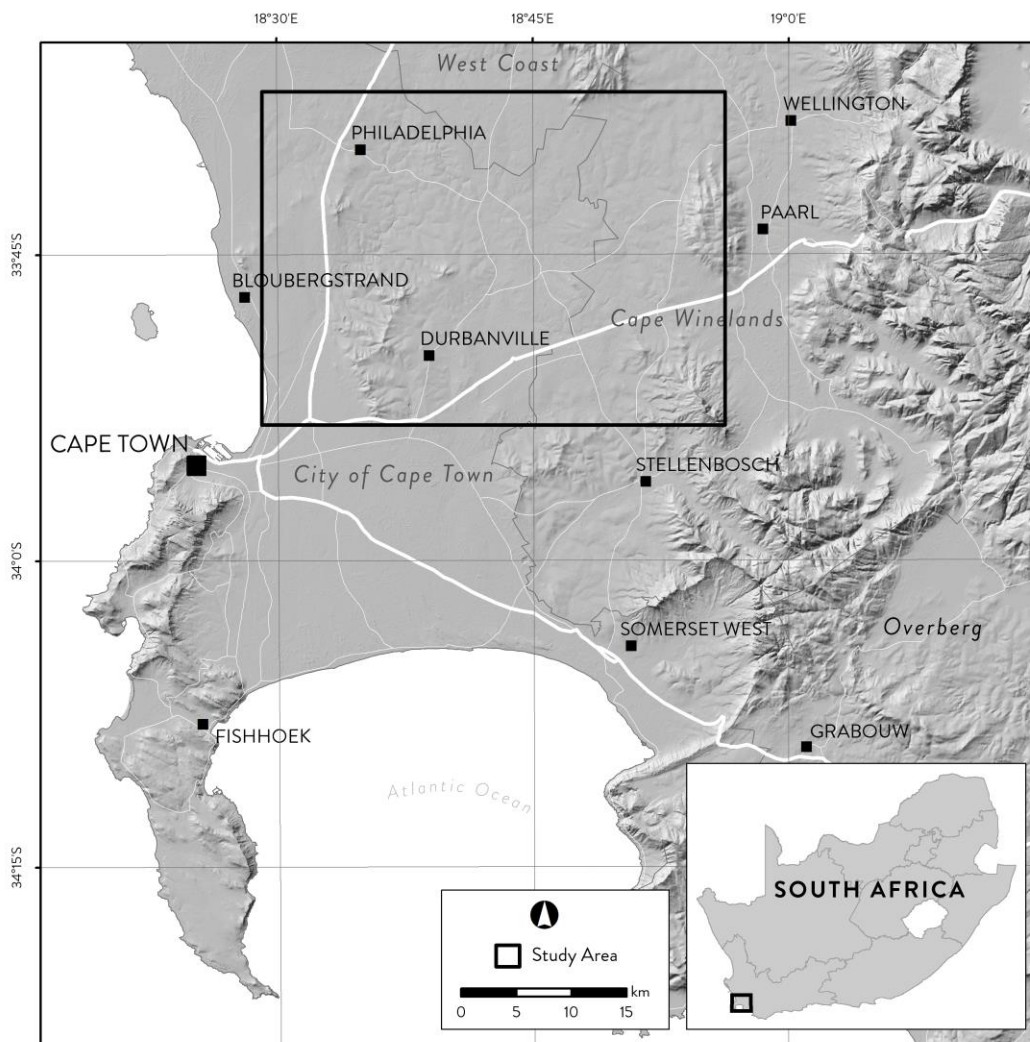


Figure 1 Location of the study area in the Cape Winelands, South Africa

The study site was chosen because of the availability of multi-temporal cloud-free Landsat-8 imagery and the variety of winter and summer crops produced in the region. The proximity to the research institution (Stellenbosch University), so as to make field visits more feasible, was also an important consideration. The period of study was 2015, as this was when field visits were carried out.



## 1.5 METHODOLOGY AND RESEARCH DESIGN

This study is quantitative in nature and was carried out in a positivistic paradigm. It experimented with multiple classifying techniques and scenarios, which were then assessed to determine their efficacy for differentiating crops within the study area. Qualitative methods (i.e. visual interpretation) were also used to assess the classification results. Classification accuracies for all scenarios were assessed against empirical crop type information collected during field surveys. Statistical techniques such as OA, kappa coefficient, and McNemar's test were used to assess classification results.

This section shows the research steps for achieving the aims and objectives outlined in Section 1.3 and illustrates the research design in Figure 2. Step 1 (overviewing the rationale and planning the research) is covered in Chapter 1. Chapter 2 is dedicated to the literature review (Step 2) and consists of an in-depth review of modern literature relating to crop type mapping using remote sensing methods and data. The literature review laid the foundation for data collection and processing overviewed in Chapter 3 (Step 3). The details in Chapter 3 relate directly to the subsequent experiments.

Steps 4.1, 4.2, and 4.3 are represented in Chapters 4 and 5 and serve as the structural framework for answering the research questions posed in Section 1.2. Step 4.1 attempts to answer the first research question by comparing the accuracies of separate classifications using standard resolution imagery and pansharpened imagery. Step 4.2 addresses the second question, by comparing the classification accuracies of different machine learning algorithms when employed in the pixel-based and object-based paradigms. The fourth research question is the focus of Step 4.3, in which OA, kappa coefficient, and McNemar's test are used to compare the classifications produced by different feature-sets generated by employing different dimensionality reduction techniques. The third research question is addressed in all three of the above-mentioned steps.

Step 5 (covered in Chapter 5) involves summarizing all the results obtained in this study, after which the research questions, as well as the aim and objectives are revisited. The thesis concludes with a discussion of the contributions and limitations of the research. Recommendations for further research are also made.

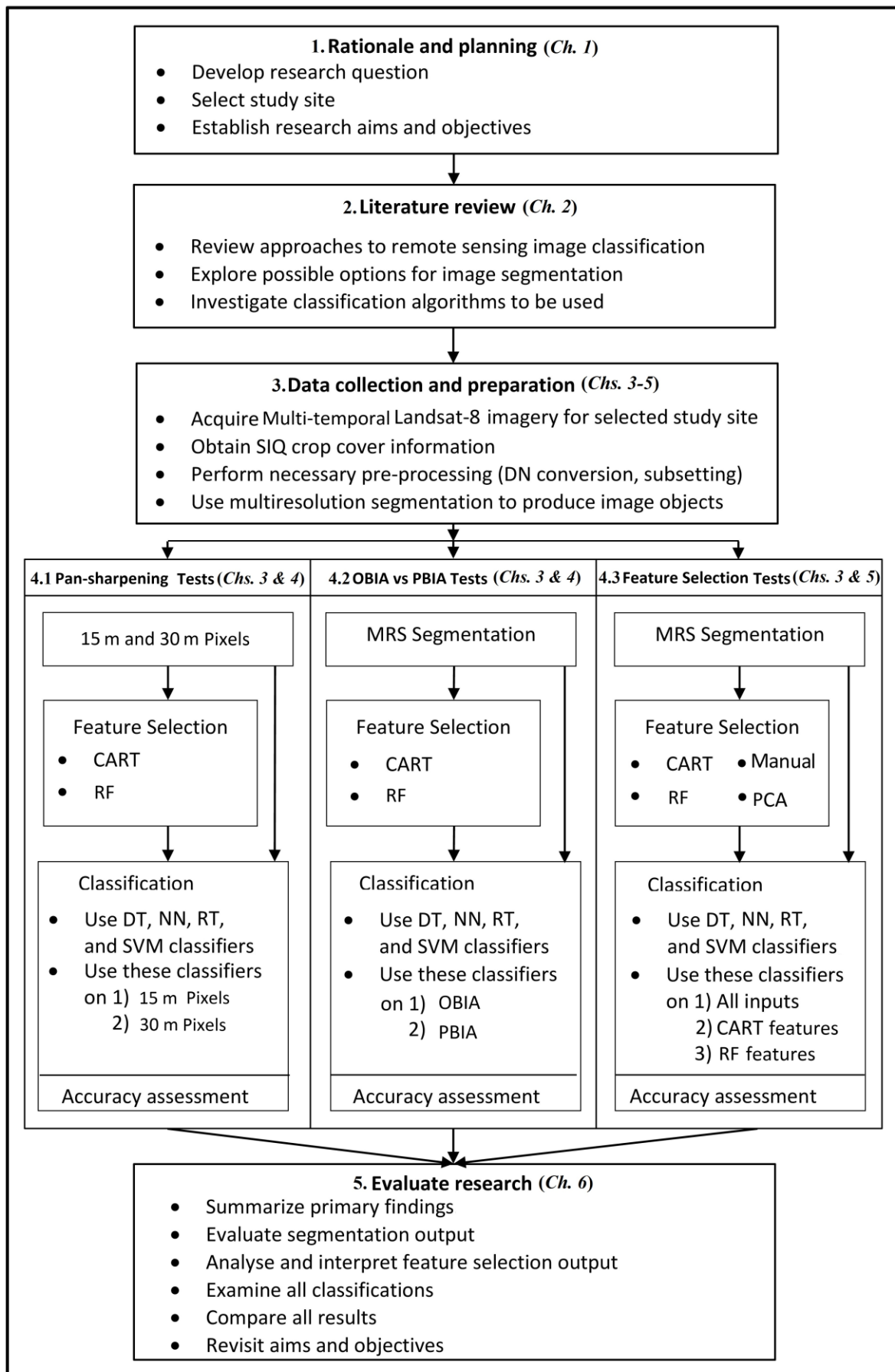


Figure 2 Research design for evaluating the performances of crop differentiation using pansharpened vs standard data, OBIA vs PBIA, and different feature selection methods.

## **CHAPTER 2: LITERATURE REVIEW**

The adoption of a well-structured and appropriate classification approach is critical for the successful classification of satellite imagery. This chapter overviews aspects related to the data and methods associated with the discrimination of crops. A brief background of the fundamentals of remote sensing is given, followed by an in-depth review of the technical aspects of crop discrimination (including data and processing techniques). The chapter concludes with a summary that synthesises the most important information relating to the successful classification of crop types using remotely sensed imagery.

### **2.1 ACTIVE AND PASSIVE REMOTE SENSING**

Energy emitted from the sun is either reflected or absorbed when it interacts with the Earth's surface and objects on it. Remote sensing systems that record emitted and reflected energy are known as passive sensors. Passive sensors are only able to detect and measure energy when naturally occurring energy is available; therefore, they are only able to produce imagery during the day (when the Earth is being illuminated by the sun) (Campbell & Wynne 2011). Alternatively, active sensors are capable of functioning day and night as they produce their own source of energy by emitting radiation towards the object being investigated. The sensor then detects and records this energy once it has been reflected. Although these systems are capable of operating efficiently day and night, they require large amounts of energy to adequately illuminate their targets (Campbell 2008). Passive sensors are more commonly referred to as optical sensors, whereas examples of active sensors include LIDAR (light detection and ranging) and SAR (synthetic aperture radar).

### **2.2 OPTICAL SENSORS**

Optical sensors have a long history of being employed for monitoring crops (Hoffer, Johannsen & Baumgardner 1966; Bauer 1975; Wardlow, Egbert & Kastens 2007; Zheng et al. 2015). Data from optical sensors are capable of representing the properties of vegetation and crop fields. These properties include the retrieval of surface characteristics that can be used for crop classification. The recorded reflection of visible and infrared energy from vegetation is directly related to plant structure, plant pigmentation, as well as leaf and canopy moisture (McNairn et al. 2009). Since this information is produced by passive sensors, optical imagery has been widely used for the classification of crops (Vieira et al. 2012; Simms et al. 2014; Muller et al. 2015; Ozelkan, Chen & Ustundag 2015; Zheng et al. 2015).

The most commonly used modern optical instruments for agricultural applications include MODIS (moderate-resolution imaging spectroradiometer), SPOT (Satellite for observation of Earth), and Landsat. For this study, Landsat-8 imagery was used for analysis since it is freely available and easily accessible. The imagery generated in the Landsat programme has improved greatly in spatial, spectral, radiometric, and temporal resolution (USGS 2014). The first sensor, Landsat-1, was launched in 1972 and recorded data in four spectral bands (Green, Red, NIR 1, NIR 2). It had a spatial resolution of 60 m, a temporal resolution of 18 days, and a radiometric resolution of 6 bits (64 grey values). Landsat-8, launched in 2013, records data in 11 spectral bands (optical and thermal), has a spatial resolution of 30 m and a radiometric resolution of 16-bit images (55000 grey levels), and scans the entire Earth every 16 days (USGS 2015).

Landsat-8 carries two instruments, namely the operational land imager (OLI) and thermal infrared sensor (TIRS). OLI includes refined heritage bands along with three new bands (USGS 2015) (Table 1). The data from Landsat-8 is available at no cost, making it ideal for crop type mapping over large areas.

Table 1 Band allocation and description of Landsat-8 imagery

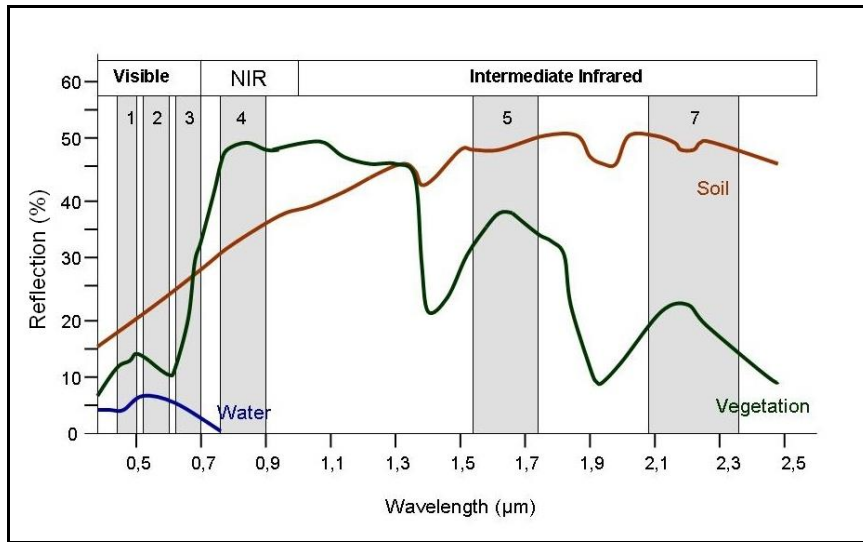
Bands	Wavelength ( $\mu\text{m}$ )	Resolution (m)
Band 1 – Coastal aerosol	0.43 - 0.45	30
Band 2 – Blue	0.45 - 0.51	30
Band 3 – Green	0.53 - 0.59	30
Band 4 – Red	0.64 - 0.67	30
Band 5 – Near-infrared (NIR)	0.85 - 0.88	30
Band 6 – SWIR 1	1.57 - 1.65	30
Band 7 – SWIR 2	2.11 - 2.29	30
Band 8 – Panchromatic	0.50 - 0.68	15
Band 9 – Cirrus	1.36 - 1.38	30
Band 10 – Thermal infrared (TIRS) 1	10.60 - 11.19	100 * (30)
Band 11 – Thermal infrared (TIRS) 2	11.50 - 12.51	100 * (30)

Source: USGS (2015)

All of the Landsat-8 bands represent different portions of the electromagnetic spectrum (Table 1). These portions (or bands) will interact differently with different material on the Earth and in the atmosphere (Campbell 2008). By combining these bands, spectral signatures for target objects can be generated.

## 2.3 SPECTRAL SIGNATURES

All material on Earth has a unique spectral signature, therefore this spectral information can be used to discern one entity from another during image classification (Campbell & Wynne 2011). An object's spectral signature can be visualized using spectral reflectance curves, which are functions of wavelengths. Figure 3 shows the typical spectral curves of three basic materials found on Earth, namely soil, vegetation, and water.



Source: Siegmund & Menz (2005)

Figure 3 The spectral signatures of soil, vegetation, and water in comparison to Landsat-7 bands

The differences in vegetation's response to electromagnetic energy are brought on by leaf pigment, cell structure and water content (McNairn et al. 2009). The pigment found in leaves (chlorophyll) strongly absorbs radiation in the visible wavelength, and the cell structure strongly reflects radiation in the near-infrared region (Campbell 2008). The absorption and reflection of plants or crops are not consistent during the year owing to different phenological stages (Peña-Barragán et al. 2011). As crops grow and enter different phenological stages, their leaf chlorophyll content, cell structure, and water content change. Individual crop types may not all be in the exact same growth stage on a single image, but will exhibit similar growth patterns over multiple images (Vieira et al. 2012). By capturing images on multiple dates (also known as multi-temporal data), it is possible to build temporal spectral profiles of individual crop types.

## 2.4 GEOMETRIC AND ATMOSPHERIC CORRECTIONS

Pre-processing is defined as the operations prior to the main analysis (Campbell 2008). It is done to correct distorted or degraded data and create a more accurate representation of the original image. It typically involves the initial processing of raw image data to correct for issues such as geometric distortion, atmospheric effects, and image noise (Campbell & Wynne 2011).

Geometric correction is the process of manipulating a digital image so that the image's projection precisely matches a specific projection surface or shape (Barret 2013). It corrects for variations in altitude, panoramic distortion, Earth rotation, and Earth curvature. Radiometric correction is performed to adjust digital values for the effect of the atmosphere such as haze, changes in scene illumination, and instrument response characteristics (Elachi & Van Zyl 2006). Noise reduction removes unwanted disturbances in image data caused by limitations in the sensor, signal processing, digitization, or data-recording process. Sources of noise include: malfunction of a detector, electronic interference between sensor components, and intermittent errors in the data transmission and recording sequence (Elachi & Van Zyl 2006). The last type of pre-processing – geo-referencing – is the process of assigning spatial coordinates to an image that has no explicit geographic coordinate system (Campbell 2008).

Landsat-8 imagery can be acquired from the USGS (United States Geological Survey) as level 1T data in top of atmosphere reflectance. This level of data processing provides systematic geometric and radiometric accuracy by using ground control points (GCPs), while employing a digital elevation model (DEM) for topographic accuracy. The geodetic accuracy of the data is dependent on the accuracy of the GCPs and resolution of the DEM used (DEM resolution varies due to different DEM data sources, which include Shuttle Radar Topography Mission, NED (National Elevation Dataset), CDED (Canadian Digital Elevation Data), GTOPO30 (Global 30 Arc-Second Elevation), and the Greenland Ice Mapping Project. The GCPs used originate from the global land survey (GLS), which was a collaboration between the USGS and NASA (National Aeronautics and Space Administration).

Song et al. (2001) tested the effects of atmospheric correction for classification and change detection using Landsat-5 TM imagery and found that all classifications in which atmospheric correction were used improved accuracy. However, according to the authors, atmospheric correction is not always necessary for image classification but is recommended when training data from one time or place is applied to another time or place. Liang et al. (2002), evaluating a custom atmospheric correction algorithm on Landsat-7 enhanced thematic mapper plus (ETM+) imagery, found that atmospheric correction is always desirable and that it clearly improved the imagery (based on visual analysis or haze reduction).

## **2.5 IMAGE FUSION**

Pansharpening is an image enhancement technique that essentially combines the superior spatial resolution of a panchromatic band (required for an accurate description of texture and shapes) with the spectral information of the lower resolution multispectral bands (required for an accurate discrimination of informational classes) (Ghassemian 2016). As discussed in Section

1.1.4, pansharpening has proven to be effective not only for the visual enhancements of imagery (Ghodekar, Deshpande & Scholar 2016), but also for quantitative analyses such as land cover mapping (Ai et al. 2016). But not all pansharpening algorithms are suitable for quantitative analyses. It is inevitable that some of the spectral fidelity of the original multispectral information is lost during the fusion process, but some algorithms are designed to maximize spectral preservation. Zhang and Mishra (2012) reviewed a range of commercially available pansharpening techniques and concluded that the Pansharp algorithm, available in the software package PCI Geomatica, retained most of the spectral information of the original imagery and consistently produced superior results for all types of sensors, images and spectral bands considered (Zhang 2002a; Zhang 2002bB). MS-split, a pansharpening technique introduced by Guo-dong et al. (2015), also shows promise, but the technique is not yet available in commercial software.

## **2.6 IMAGE TRANSFORMATIONS**

Image transformation is the method whereby the spectral information captured in an image is changed or modified to emphasize specific features (Campbell & Wynne 2011). This is usually done with local or neighbourhood raster operators and is created to enhance visual results and improve image classification (Campbell 2008). The image classification improvement is brought about by reduced data dimensionality, emphasized variation between features, new dimensions, and the reduction of noise. Common image transforms used for classification include indices, principal components, texture measures, and tasseled cap transforms (Heinl et al. 2009). These common transforms have been shown to have a positive effect on the accuracy of remote sensing classifications (Lu & Weng 2007).

### **2.6.1 Indices**

Spectral indices are combinations of reflectance at two or more wavelengths that indicate relative abundance of features of interest (Jackson & Huete 1991). The most common group of spectral indices is vegetation indices (VIs), although other indices are available for water, geologic features, man-made features, and burnt areas (Campbell 2008). VIs are composites of two or more wavelengths designed to emphasize a certain property of vegetation (Huete, Justice & Liu 1994). Numerous VIs have been formulated and published in scientific literature, but only a few have been systematically tested. Some of the most popular and systematically tested VIs include: NDVI (normalised difference vegetation index), ARVI (atmospherically resistant VI), EVI (enhanced VI), GCI (green chlorophyll index), GNDVI (green normalised VI), GI (greenness

index), RGRI (red green ratio index), SAVI (soil-adjusted VI), SRI (simple ratio index), NDWI (normalised difference water index), and NDMI (normalised difference moisture index).

#### 2.6.1.1 NDVI

The NDVI is the most commonly used VI (Benedetti & Rossini 1993). It normalises green leaf scattering in the NIR wavelength and chlorophyll in the red wavelength, allowing it to effectively quantify green crops (Wardlow & Egbert 2008). NDVI is used extensively in modern research to monitor crops (Wardlow & Egbert 2008; Peña-Barragán et al. 2011; Simms et al. 2014; Campbell et al. 2015; Zheng et al. 2015). It has also been used in conjunction with other features to successfully (90%+ accuracy) identify irrigated and cultivated crops using temporal Landsat-5 and Landsat-7 data (Zheng et al. 2015). NDVI is formulated as:

$$NDVI = \frac{(NIR) - (RED)}{(NIR) + (RED)} \quad \text{Equation 1}$$

where NDVI is the normalised difference vegetation index;  
 NIR is the near-infrared image band; and  
 RED is a red image band.

NDVI is related to a large number of attributes (e.g. biomass, percentage of bare ground and vegetation), but it is not a direct measure of any of these attributes (Benedetti & Rossini 1993). NDVI is a general indicator of plant “vigour”, and several factors can influence the measurements or readings that it produces, including image scale, atmospheric conditions, plant moisture, soil moisture, overall vegetation cover, and soil type and management (Wardlow & Egbert 2008).

Two of the primary factors that limit the use of NDVI include a loss of sensitivity to change in the amount of vegetation at the high biomass conditions and sensitivity to light reflected from the soil surface. The former limitation means that, as biomass increases, the changes in NDVI becomes unnoticeable. Therefore, for high NDVI values, a small change in reading may actually represent a very large change in vegetation (Wardlow & Egbert 2008) often referred to as the NDVI “saturation problem”. The effect of soil reflectance on NDVI is particularly problematic in arid and semi-arid regions that tend to have larger areas of exposed soil and rock in vegetated areas (Jackson & Huete 1991). This limitation of NDVI was the main reason for the development of the SAVI.



### 2.6.1.2 SAVI

SAVI, developed by Huete, Justice & Liu (1994), was designed to minimize soil brightness influences from spectral indices of red and NIR wavelengths. This is done by shifting the origin of reflectance spectra in the NIR region to account for first-order soil-vegetation interactions and differential red and NIR flux extinction through vegetation canopies (see Equation 2).

$$SAVI = \frac{NIR - RED}{NIR + RED + L} \times (1 + L) \quad \text{Equation 2}$$

where *SAVI* is the soil-adjusted vegetation index;  
*NIR* is the near-infrared image band;  
*RED* is the red image band; and  
*L* is the relative soil constant.

The L-value in Equation 2 is a constant added by Huete, Justice & Liu (1994), to help account for soil variation, known as the soil brightness correction factor. An L-value of 0 is used when there is minimal influence of soil in the area being analysed. Once L reaches 1, the influence of soil is minimized. Huete, Justice & Liu (1994) found that an L-value of 0.5 was able to minimize soil brightness variation and eliminate the need for additional calibration for different soils. SAVI is often used in modern research that seeks to monitor vegetation health, as seen in the work of Hunt et al. (2013) and Taghvaeian et al. (2015).

### 2.6.1.3 ARVI

ARVI uses reflective measurements in the blue wavelengths. It corrects for atmospheric scattering effects that register in the red region of the reflectance spectrum, therefore making it more resistant to atmospheric factors such as aerosols (Rondeaux, Steven & Baret 1996). ARVI has been utilized for the classification of vegetation when atmospheric effects had to be reduced (Rondeaux, Steven & Baret 1996). ARVI has been tested with Landsat TM (Kaufman & Tanr 1992), but is yet to be tested on Landsat-8 imagery for the use of crop identification. The formula for ARVI is:

$$ARVI = \frac{NIR - ((2 \times RED) - BLUE)}{NIR + ((2 \times RED) - BLUE)} \quad \text{Equation 3}$$

where *ARVI* is the atmospherically resistant vegetation index;  
*NIR* is the near-infrared image band;  
*RED* is the red image band; and  
*BLUE* is the blue image band.

#### 2.6.1.4 EVI

The EVI leverages information from the blue region of the electromagnetic spectrum in areas with dense leaf canopy to address the saturation problem often experienced with NDVI (Jiang et al. 2008). The EVI enhances the vegetation signal with improved sensitivity in high biomass regions and improved vegetation monitoring through a de-coupling of background canopy signals and a reduction in atmosphere effects (Jiang et al. 2008). The enhancement of vegetation signal is done by using the blue band to correct for aerosol influences in the red band and addressing non-linear, differential NIR and red radiant transfer through a canopy with a canopy background adjustment ( $L$ ) (Hess et al. 2009). The formula for EVI is:

$$EVI = G \times \frac{(NIR - RED)}{NIR + C1(RED) - C2(BLUE) + L} \quad \text{Equation 4}$$

where

$EVI$	is the enhanced vegetation index;
$G$	is canopy background adjustment;
$NIR$	is the near-infrared image band;
$RED$	is the red image band;
$BLUE$	is the blue image band;
$C1$	is the first aerosol resistance coefficient;
$C2$	is the second aerosol resistance coefficient; and
$L$	is a canopy background adjustment.

Hess et al. (2009) utilized the EVI with MODIS imagery to detect seasonal patterns of leaf phenology. They showed that effective values for the algorithms coefficients are:  $L = 1$ ,  $C1 = 6$ ,  $C2 = 7.5$ , and  $G = 2.5$ . EVI has been used to successfully identify individual crops using temporal data (Wardlow & Egbert 2008) and to monitor the different growth stages of rice crops using Landsat-5 TM and Landsat-7 ETM+ data (Oguro & Sura 2003; Jiang et al. 2008).

#### 2.6.1.5 GCI

The GCI was developed by Gitelson, Gritz & Merzlyak (2003a) to indicate the total pigment content of a plant and estimate chlorophyll content. The GCI has shown promise for monitoring vegetation in Gitelson et al. (2003a), Gitelson et al. (2003b), Gitelson et al. (2005) and Viña et al. (2011). GCI is defined as:

$$GCI = (NIR \div GREEN) - 1$$

Equation 5

where *GCI* is the green chlorophyll index;  
*NIR* is the near-infrared image band; and  
*GREEN* is the green image band.

#### 2.6.1.6 GNDVI

GNDVI is similar to NDVI, but uses both the red and green bands (Gitelson et al. 2003a), which makes it more sensitive to chlorophyll concentration than NDVI. The formula for GNDVI is:

$$GNDVI = \frac{NIR - GREEN}{NIR + RED}$$

Equation 6

where *GNDVI* is the green NDVI;  
*NIR* is the near-infrared image band;  
*RED* is the red image band; and  
*GREEN* is the green image band.

As with most of the indices discussed in this section, GNDVI is often used (in combination with other features) for vegetative analysis (Hunt et al. 2013; Mulla 2013; Hunt et al. 2014).

#### 2.6.1.7 GI

The GI is a simple index used to monitor vegetation leaf pigments and greenness (Peña-Barragán et al. 2011). It has been used and refined by Gitelson et al. (2002) and adapted for ASTER by Peña-Barragán et al. (2011). The formula is given as:

$$GI = \frac{GREEN}{RED}$$

Equation 7

Where *GI* is the greenness index;  
*GREEN* is the green image band; and  
*RED* is the red image band.

#### 2.6.1.8 RGRI

The RGRI is a measurement of reflectance that is useful for making foliage development estimations, indicating leaf stress and production, as well as indicating flowering in certain canopies (Gamon & Surfus 1999). Originally created by Gamon & Surfus (1999) as a narrow-

band light use efficiency index, it has been modified for broad-band use (Yang, Willis & Mueller 2008). RGRI is formulated as:

$$RGRI = \frac{\text{mean}(RED)}{\text{mean}(GREEN)} \quad \text{Equation 8}$$

Where *RGRI* is the red green ratio index;  
*RED* is the red image band; and  
*GREEN* is the green image band.

#### 2.6.1.9 SRI

SRI is a commonly used index that monitors vegetation status and canopy structure (Jordan 1969). It describes the ratio of light scattered in the NIR range to the light that is absorbed in the red range. The formula for the SRI is:

$$SRI = \frac{NIR}{RED} \quad \text{Equation 9}$$

where *SRI* is the simple ratio index;  
*NIR* is the near-infrared band; and  
*RED* is the red image band.

Although SRI was not used as the primary index of any recent work, it has been used in combination with other more common indices for agricultural observations by Peña-Barragán et al. (2011), Hunt et al. (2013), Mulla (2013), and Zhao et al. (2016).

#### 2.6.1.10 NDWI

NDWI is a commonly used index for monitoring water status and tree canopy. There are several variations of this popular index. The index (and its variations) are designed to maximize reflectance of water by minimizing the low reflectance of NIR by water features, and taking advantage of high reflectance in the NIR region by vegetation and soil features (Xu 2006). The version in Equation 10 (McFeeters 1996) gives positive values for water (i.e. emphasizing water), while vegetation and soil usually have values less than or equal to zero (suppressing vegetation and soil) (McFeeters 1996).

$$NDWI = \frac{GREEN - NIR}{GREEN + NIR} \quad \text{Equation 10}$$

where  $NDWI$  is the normalised difference water index;  
 $GREEN$  is the green image band; and  
 $NIR$  is the near-infrared image band.

Xu (2006) noticed that the mean digital number of the Landsat TM band 5 (which represents middle infrared (MIR) radiation), is much greater than that of the Landsat TM band 2 (green band). Using this information, Xu (2006) developed a modified NDWI.

$$MNDWI = \frac{GREEN - MIR}{GREEN + MIR} \quad \text{Equation 11}$$

where  $GI$  is the modified NDWI;  
 $GREEN$  is the green image band; and  
 $MIR$  is the middle infrared image band.

Another version of the NDWI is (Gao 1996):

$$NDWI = \frac{RED - SWIR}{RED + SWIR} \quad \text{Equation 12}$$

where  $NDWI$  is the normalised difference water index;  
 $RED$  is the red image band; and  
 $SWIR$  is the short wave infrared image band.

#### 2.6.1.11 NDMI

NDMI is an index commonly used to monitor the moisture content of vegetation. It was proposed by Wilson & Sader (2002) and is defined as:

$$NDMI = \frac{NIR - SWIR}{NIR + SWIR} \quad \text{Equation 13}$$

Where  $NDMI$  is the normalised difference moisture index;  
 $NIR$  is the near-infrared image band; and  
 $SWIR$  is the short wave infrared image band.

The NDMI has been used to classify agricultural areas and crops as done by Collingwood et al. (2009) and Singh, Agrawal & Singh et al. (2011).

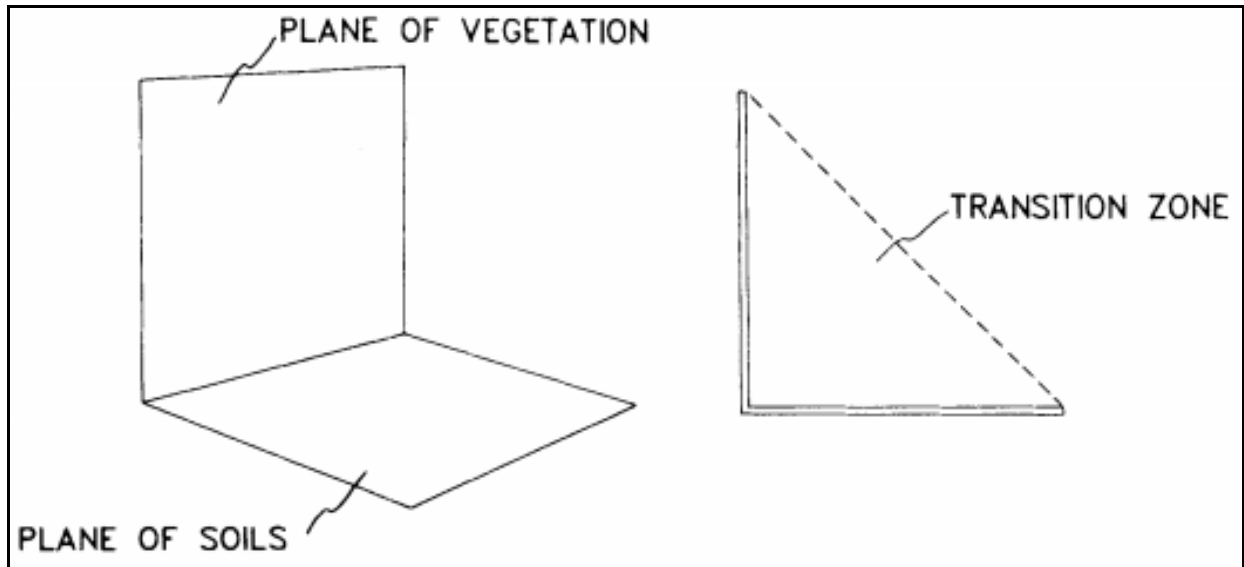
### **2.6.2 Principal component analysis**

Principal component analysis (PCA) is a statistical procedure that identifies patterns in data and then expresses the information in a way that highlights inherent similarities and differences (Smith 2002). This is done by using orthogonal projections to convert the possibly correlated data into a set of linearly uncorrelated variables called principle components. The number of components generated from the transformation is less than or equal to the original number of variables, with the first principal component representing the largest possible variance (Smith 2002). The variance of the components is a measure of the data's information content (Da Silva et al. 2015). By compressing the variance from all the image layers into a smaller composite of images (components), PCA can be used to reduce the number of dimensions in data (Smith 2002). PCA has been used successfully for spatial applications ranging from general land cover mapping to crop monitoring (Bell, Caviglia-Harris & Cak 2015; Da Silva et al. 2015; Lee et al. 2016). Bell, Caviglia-Harris & Cak (2015) characterized land use change using a temporal dataset in Amazonia with a focus on agricultural classes. They used PCA to produce new features from their original dataset, and used Eigenvalues to remove components to further reduce feature dimensionality. They commented that PCA allowed for effective comparison of variation within the informational classes. Da Silva et al. (2015) used PCA on time-series MODIS imagery to produce new features from the original dataset. This was done to aid in identifying soybean fields in Brazil. They selected the first three components and achieved satisfactory classification accuracies. Eigenvalues were also used select the most important components. Similarly, Lee et al. (2016) utilized PCA for feature extraction to differentiate individual tree species with multi-sensor imagery. They applied PCA to the imagery to prune the data and select the most important features for the classification. Lee et al. (2016) concluded that a robust PCA with machine learning has the potential to distinguish individual tree species using hyperspectral data.

### **2.6.3 Tasseled cap transformation (TCT)**

The TCT is a process whereby spectral data from an optical sensor is compressed into a few bands associated with a scene's physical characteristics while suffering minimal information loss (Huang et al. 2002). It was originally developed for the Landsat multispectral scanner, but has now been widely adapted to other sensors due to its value for developing insight into plant growth patterns in spectral space when using combinations of different bands (Kauth & Thomas

1976). When used on Landsat-8 data, the transformation produces six new components in a four-dimensional space: brightness, greenness, wetness, fourth (haze), fifth, and sixth (Baig et al. 2014). The Landsat-8 TCTs occupy a space described as a “transition zone” (Crist & Cicone 1984) in three dimensions (Figure 4), which define two planes when used in the context of soils and vegetation. The process of creating these components involves the rotation of the Landsat-8 spectral data in these three dimensions to tasseled cap coordinates (Crist & Cicone 1984).



Source: Crist & Cicone (1984)

Figure 4 Tasseled cap "transition zone" in imagery

Because TCT was originally developed for the Landsat multispectral scanner, the coefficients used had to be adapted to the bands of later sensors. The Landsat-8 coefficients are provided in Table 2 (Baig et al. 2014).

Table 2 TCT coefficients for Landsat-8 at satellite reflectance

Component	Band 2	Band 3	Band 4	Band 5	Band 6	Band 7
Brightness	0.3029	0.2786	0.4733	0.5599	0.508	0.1872
Greenness	-0.2941	-0.243	-0.5424	0.7276	0.0713	-0.1608
Wetness	0.1511	0.1973	0.3283	0.3407	-0.7117	-0.4559
TCT4	-0.8239	0.0849	0.4396	-0.058	0.2013	-0.2773
TCT5	-0.3294	0.0557	0.1056	0.1855	-4349	0.8085
TCT6	0.1079	-0.9023	0.4119	0.0575	-0.0259	0.0252

It is best to apply these coefficients to calibrated Landsat-8 reflectance data rather than to raw digital numbers (Huang et al. 2002).

#### **2.6.4 Image texture**

Texture represents the surface and structure of an image; it can be defined as a regular repetition, or pattern of an element, or pattern on a surface (Srinivasan & Shobha 2008). Texture measures can be grouped into two general approaches, namely statistical and structural (Long, Zhang & Feng 2002). Statistical texture measures entail the computation of values based on the statistical distribution of observed combinations and intensities at specified positions relative to other positions in the image (Kusumaningrum & Arymurthy 2011). By considering the number of pixels defining a local feature, the statistical approach can be further categorized into sub-classes, namely first-order (one pixel), second-order (two pixels), and higher-order (three or more pixels). The structural approach views image texture as a set of pixels in a regular or repeated pattern (Srinivasan & Shobha 2008). Image texture derived from this approach represents the spatial relationship of pixels by using Voronoi tessellation. Examples of structural texture measures include image edges, shapes, and Voronoi polygons (Long, Zhang & Feng 2002).

The most commonly used texture extraction methods for remotely sensed data are two statistical approaches, namely grey level co-occurrence matrices (GLCM) and grey level difference vectors (GLDV) (Clausi 2002; Srinivasan & Shobha 2008). GLCM and GLDV have shown potential for remote sensing applications (Peña-Barragán et al. 2011; Vieira et al. 2012; Myburgh & Van Niekerk 2013; Avci & Sunar 2015). GLCM is a two-dimensional matrix made up of joint probabilities between adjacent pairs of pixels (Kusumaningrum & Arymurthy 2011). It is produced by forming a co-occurrence matrix of the image and then extracting the GLCM descriptors from the co-occurrence matrix. GLDV is an estimation of the probability density function for differences between image functions at locations based on specified pixel distances and angles (Khazenie & Richardson 1993). The resultant GLDV texture measure is based on a first-order statistic, whereas GLCM estimates the joint grey level distribution for two grey levels (second-order statistic). The most commonly extracted texture parameters from these two methods are GLCM contrast, GLCM correlation, GLCM entropy, GLCM homogeneity, GLDV correlation, GLDV entropy, and GLDV mean (Clausi 2002; Peña-Barragán et al. 2011; Vieira et al. 2012; Myburgh & Van Niekerk 2013; Avci & Sunar 2015).

### **2.7 IMAGE SEGMENTATION**

The core concepts relating to OBIA and PBIAs were covered in Section 1.1.2. Image segmentation is an essential step in OBIA and can be described as the process of partitioning an image into objects with point-based, edge-based, or region-based algorithms, as well as combinations of them all (Blaschke 2010).



Point-based image segmentation uses global threshold values to find groups of homogenous pixels within an image. It is done in two steps: 1) all pixels in the image are categorized based on a global threshold value; and 2) all of the spatially connected elements that fall into the same category are grouped into separate regions (Pesaresi & Benediktsson 2001). This approach is not favoured in RS applications as the spectral properties of a particular object may vary greatly at different locations within an image scene (Schiewe 2002).

Edge-based image segmentation regards image element edges as boundaries. These boundaries are identified with an edge detection filter and are then transformed into object outlines by a contour-generating algorithm. This segmentation shows a very high sensitivity to image noise (Schiewe 2002).

Region-based image segmentation compares pixels or objects with other pixels or objects to determine if they are similar (Mathieu, Freeman & Aryal 2007). It is done in one of two ways: region growing (bottom-up) or region splitting (top-down). Region growing starts with randomly sampled seed pixels that grow into bordering elements, whereas region splitting starts with the entire image and recursively splits it into smaller elements (Mathieu, Freeman & Aryal 2007). An advantage of randomly generated seeds is that the process is autonomous and requires no input from the user. Of all the available segmentation methods, region growing is the most popular (Van Niekerk 2010). One of the most commonly used region-based segmentation algorithms is multi-resolution segmentation (MRS).

### **2.7.1 Multi-resolution segmentation (MRS)**

MRS is a region-merging, bottom-up algorithm that can perform segmentation on a pixel or object level (Blaschke 2010). Its input (pixel or object) is merged into a set of objects in such a way that the average heterogeneity of the set is minimized and the homogeneity within objects maximized (Benz et al. 2004). It merges using a mutual best-fit approach by which a seed element is located and best-fit neighbours identified (Blaschke & Lang 2006). The merging is only performed if the element falls under the specified range defined during the preparation of the segmentation (Tang et al. 2000). The algorithm will continue checking for neighbours to merge until the homogeneity threshold has been reached. MRS takes scale, shape, and compactness parameters as input. The scale factor determines the maximum change in total heterogeneity allowed when merging pixels into an object (Drăguț & Blaschke 2006). The shape value determines how much importance is allocated to the shape of an object, compared to its spectral properties. Compactness will determine how much influence an object's compactness will have on the resulting segmentation (Li et al. 2015).

MRS has been used in numerous remote sensing applications, including crop and vegetation classification. Castillejo-Gonzalez & López-Granados (2009) used MRS on Quickbird imagery while comparing OBIA and PBIA for crop classification (OBIA outperformed PBIA in classification accuracy). The authors emphasized the importance of the correct selection of segmentation parameters, a notion shared by many other authors using this method (Drăguț & Blaschke 2006; Peña-Barragán et al. 2011; Schultz et al. 2015). Peña-Barragán et al. (2011) used an empirical discrepancy method to evaluate their segmentations and ended up using colour, shape, smoothness, and compactness parameters of 0.4, 0.6, 0.2, and 0.8 at a scale value of 50, while 0.9, 0.1, 0.3, and 0.7 were used at a scale value of 100. Using these parameters with multi-seasonal ASTER data and the DT classifier, OAs of over 80% were achieved. Schultz et al. (2015) also emphasized the importance of selecting suitable segmentation parameters. They used bi-annual Landsat-8 data and attempted to automate the process of crop discrimination. Their results showed that their best segmentation outperformed their worst segmentation by an OA of 20%.

Authors working on segmentation accuracy have employed different approaches to finding “optimal” segmentations. Factors contributing to the challenge of achieving optimal segmentation include the size of the image (due to a great amount of processing time needed for region growing algorithms), the aim of the classification, the type of landscape, the variation in objects being classified, and the imagery being used. The next section overviews a tool developed to assist analysts in the process of setting a suitable MRS scale value.

### **2.7.2 Estimation scale parameter tool (ESP)**

The ESP tool is a procedure (developed for use in eCognition software by Drăguț et al. (2014)) that automates the parameterisation of MRS. It utilizes the concept of local variance to detect scale transitions in geospatial data by first identifying the number of layers present in an eCognition project. It then iteratively segments the layers with MRS in a bottom-up approach, where the scale parameter value of the segmentation increases with every iteration. The local variance is calculated and used to determine when iterations are to be stopped (when the current scale level records a local variance lower than or equal to the previous iterations value). The output of ESP includes a graph that displays local variance, scale, and rate of change. By analysing the peaks and plateaus of the graph, one is able to judge which scale settings are most likely to produce suitable segmentations. According to Drăguț et al. (2014), the ESP tool produces satisfactory results with very high resolution imagery.

## **2.8 IMAGE CLASSIFICATION**

Digital image classification is the process of grouping pixels or objects with certain spectral, textural, or image transform values into informational classes (Campbell 2008). There are three main techniques, namely unsupervised, supervised, and knowledge-based image classification. Each of these techniques are briefly overviewed in the following subsections.

### **2.8.1 Unsupervised classification**

Unsupervised classification can be defined as the identification of natural groups of pixels within multispectral data (Campbell 2008). It uses clustering whereby natural groups within an image are identified (Myburgh 2012). Clustering involves the identification and labelling of distinct classes based on the information present in the feature-set (Campbell & Wynne 2011). Once these distinct classes have been identified, the user or expert assigns these natural groups of pixels or objects to more meaningful or appropriate informational classes (Mather 2004). Unsupervised classification is convenient when there is no information available on the study area prior to classification (Campbell & Wynne 2011). Because no user input is required, unsupervised image classification is quick and relatively easy to implement (Gao 2009). It is important to note that, although the process of creating classes by clustering is easy, it does not always correspond to informational classes of interest (Stephenson & Van Niekerk 2009). Popular unsupervised classification algorithms include ISODATA, k-means, and modified k-means. These three unsupervised classifiers have been applied to a variety of classification problems (Nolin & Payne 2007; Lang et al. 2008)

### **2.8.2 Supervised classification**

As explained in Section 1.1.5, supervised classification is the process of using samples of known identity (training data) to classify pixels or objects of unknown identity (Campbell & Wynne 2011). There are many supervised classifiers available, ranging from traditional statistical (parallelepiped, minimum distance, and maximum likelihood) to modern machine learning algorithms. Statistical classifiers require training data to be normally distributed and are parametric. This means they rely on statistical measures such as mean, standard deviation, and probability to perform properly (Mather 2004). Machine learning classifiers often incorporate artificial intelligence into their learning process, and iteratively learn how to classify images (Campbell & Wynne 2011). They do not require training data to be normally distributed and are non-parametric. Because of this, they are considered to be more robust and tend to perform better than traditional classifiers (Myburgh 2012). Widely used machine learning classifiers include

decision trees (DT), k-nearest neighbour (k-NN), random forest (RF), and support vector machines (SVM).

#### 2.8.2.1 Decision tree (DT)

A DT is a machine learning classifier that evaluates the given training samples and creates a set of thresholds used for binary separation (Brown et al. 2013). Brown et al. (2013) used the commercial DT classifier, See5, with time-series MODIS vegetation index data to classify agricultural land use. They managed to achieve overall classification accuracies of over 80%, but presented evidence that the DT models were overfitting the training data despite their best efforts to mitigate this through parameter tweaking. Overfitting occurs when a classifier describes random error to noise instead of the underlying relationship. Peña et al. (2014) used the C4.5 DT algorithm with OBIA to map summer crops. The C4.5 DT was only capable of achieving 79%, a relatively low score when compared to the logistic regression, SVM, and multilayer perceptron classifiers also tested in the same study. The authors did, however, note that the DT was computationally less expensive than the other methods. Salmon et al. (2015) also employed the DT4.5 decision tree to produce global irrigation maps at 500 m resolution using multiple RS sources. They did not specify the OA or kappa scores of their results, but showed that the DT4.5 DT produced thematic maps that were very similar to the reference data.

#### 2.8.2.2 k-Nearest neighbour (k-NN)

k-NN is a simple, non-parametric machine learning classifier (Campbell & Wynne 2011) that classifies unknown pixels or objects based on the k-nearest known values (Myburgh 2012). Objects or pixels are classified by a majority vote of its neighbours, with the object or pixel being assigned to the class most common among its k-nearest neighbours. If  $k = 1$ , then the object is simply assigned to the class of the single nearest neighbour (Mather 2004). Myburgh & Van Niekerk (2013) tested the effect of feature dimensionality on k-NN, maximum likelihood (ML), and SVM for object-based land cover classification. Their research showed that k-NN outperformed the ML classifier in scenarios with higher feature dimensionality. Richardson, Goodenough & Chen (2014) used k-NN for land cover classification using SAR time-series data with a hierarchical unsupervised approach. They found that k-NN is suitable for this application, provided that a suitable k-value is selected. Guan et al. (2016) suggested that classification systems utilizing other classification algorithms can be combined with the k-NN classifier to produce satisfactory crop monitoring results when dealing with multi-temporal satellite data.

### 2.8.2.3 Random forest (RF)

RF is an ensemble learning method for classification, regression, and other tasks. Ensemble classifiers use a divide-and-conquer approach to improve performance. The principle behind ensemble methods is that a group of “weak learning algorithms” can be combined to form a “strong learning algorithm” (Liaw & Wiener 2002). RF functions by creating a set of DTs during model training and outputs the class that appears most often (for classification) or mean prediction (for regression) (Breiman 2001). RF input parameters include *ntree* and *mtry*. The *ntree* parameter represents the number of trees to grow and *mtry* represents the number of variables randomly sampled as candidates at each split. Benefits of using RF include its runtime being computationally effective, and its ability to deal with unbalanced and missing data. Weaknesses include the inability to predict beyond the range in the training data for regression, and overfitting in datasets that are particularly noisy (Liaw & Wiener 2002).

RF is one of the leading classification methods when multi-source data is used (Gislason, Benediktsson & Sveinsson 2006). Duro, Franklin & Dube (2015) compared RF to SVM for crop type identification using SPOT-5 data and found that, although SVM outperformed RF, the latter algorithm achieved a very high accuracy (OA of 93%). Long et al. (2013) used RF and Landsat ETM+ imagery for crop classification (comparing object-based image analysis and pixel-based image analysis) and achieved an OA of 89% using PBIA. They concluded that RF is suitable for multi-temporal crop classification because of its ability to create multiple paths with different variable choices to classify the same class. Hao et al. (2015), using RF for crop classification with time-series MODIS data, achieved an OA of 88% and concluded that the RF algorithm is suitable for selecting features and classifying crops when large volumes of data are being used.

### 2.8.2.4 Support vector machine (SVM)

A SVM is a supervised, non-parametric statistical learning technique (Mountrakis, Im & Ogole 2011). The SVM training algorithm aims to find a hyperplane that divides the input data into two discrete predefined classes similar to the training classes (Steinwart & Christmann 2008). However, it is often not possible to separate classes using a plane. Instead of attempting to define a complex separation surface in the datasets' feature space, the SVM algorithm transforms the feature space using a kernel (a mathematical function) until a hyperplane can be used as separator (Myburgh 2012). SVMs are effective in high dimensional feature space, are memory efficient (as they use a subset of training points in the decision function), and are also very versatile due to their ability to utilize different kernel functions (Suykens & Vandewalle 1999). Issues with SVMs include the inability to directly provide probability estimates. If needed, it has to be calculated using expensive cross-validations. SVMs are also designed to separate two

classes (Suykens & Vandewalle 1999), whereas classification schemes with multiple classes are frequently used in remote sensing. SVM deals with multiple classes by using either the one-against-all or the one-against-one approach (Steinwart & Christmann 2008). In the one-against-all approach, several binary classifiers are trained to separate each class from all the others. This results in multiple binary classifiers being trained for a multi-class problem. A decision value is calculated for each class from these classifiers and data objects are assigned to the class for which the largest decision value was determined (Myburgh 2012). The one-against-one approach utilizes multiple binary classifiers for each pair of classes, resulting in several classification outputs. A majority vote is then applied to decide on the final class allocation for each data object (Steinwart & Christmann 2008). Duro, Franklin & Dube (2015) found that an object-based implementation of SVM outperformed several other image analysis methods and achieved an OA of 94% for mapping crop types. Zheng et al. (2015), employing SVMs with multi-temporal Landsat-5 and Landsat-7 NDVI data, demonstrated that they were very successful at differentiating nine main crop types, with an OA of over 90%. Kumar et al. (2015) managed to accurately map crops with an OA of 88% and concluded that SVM should be able to accurately map crop types in other areas and environments.

### **2.8.3 Knowledge-based image classification**

Knowledge-based image classification makes use of an expert system approach. Expert systems are computer systems that emulate human decision making (a.k.a. artificial intelligence) by considering a predefined set of rules (Campbell & Wynne 2011). Rules are often ordered in a DT-like structure, but unlike in machine learning classification, the decision trees are built by humans and not machines. An expert system DT is essentially a hierarchical set of “if” statements that classifies objects or pixels into different informational classes based on expert knowledge of features (Campbell & Wynne 2011). Knowledge-based systems consist of three components: a knowledge base, an inference engine, and a database. The knowledge base stores expert knowledge in the form of a rule-set defined by the expert, while the inference engine stores protocols relating to how the rules in the knowledge base are applied. The database is a set of raw and transformed datasets.

Stephenson & Van Niekerk (2009) compared an expert system approach to supervised classification for forest mapping using SPOT-5 imagery. They found that the accuracy of the knowledge-based rule-set classifier was high and comparable to that of a supervised classifier. Although it was very time-consuming to produce the knowledge base, it was deemed superior to supervised classification because of the potential of the former approach to be transferred to other areas without the need to collect training data. Similarly, Pauw & Van Niekerk (2012)

compared an expert system and supervised approach for wetland mapping using SPOT-5 and SAR imagery. They found that the k-NN classifier produced slightly more accurate results than the expert system approach.

## 2.9 TRAINING DATA

Training data is a set of data used to discover potentially predictive relationships between features. The training sets are selected by the user or expert, and represent the informational classes present in classification (Campbell & Wynne 2011). Campbell & Wynne (2011) proposes using at least 100 training pixels per class, whereas Mather (2004) suggests a minimum of  $30p$  per class, where  $p$  is the number of features used in the classification. GEOBIA changes the nature of training data used by learning algorithms as it groups pixels into objects, thereby effectively reducing the number of training samples available to the classifier (Myburgh 2012). Classifiers that perform well under conditions of limited training set size are consequently needed. Myburgh & Van Niekerk (2013) tested the use of various sizes of sample sets as input into the ML, NN, and SVM classifiers within a GEOBIA environment. They found that larger sample sets produced substantially higher classification accuracies compared to smaller sets, showing that an increase of information provided during training significantly improves classification results. High quality agricultural survey data could therefore be used as large sample sets for crop mapping.

According to the land cover field guide of the Chief Directorate: National Geospatial Information, (Lück et al. 2010) agricultural land refers to areas where the natural vegetation is replaced by other types of vegetative cover of anthropogenic origin. This vegetation is artificial and requires human involvement to maintain it in the long term. In between the human activities, or before starting crop cultivation, the surface can be temporarily without vegetative cover.

Spatialintel (SIQ) (Pty), a leading provider of agricultural and other surveys in South Africa, has created agricultural census datasets for Gauteng (2009), Limpopo (2011), and recently the Western Cape (2013). These datasets contain crop information for each individual cultivated field and were generated through an extensive aerial survey, supported by field surveys. The agricultural census dataset includes orchards and vegetables, as well as annual and perennial pastures. Crop datasets from SIQ are provided in vector format (Figure 5), with detailed attribute information linked to each individual field.

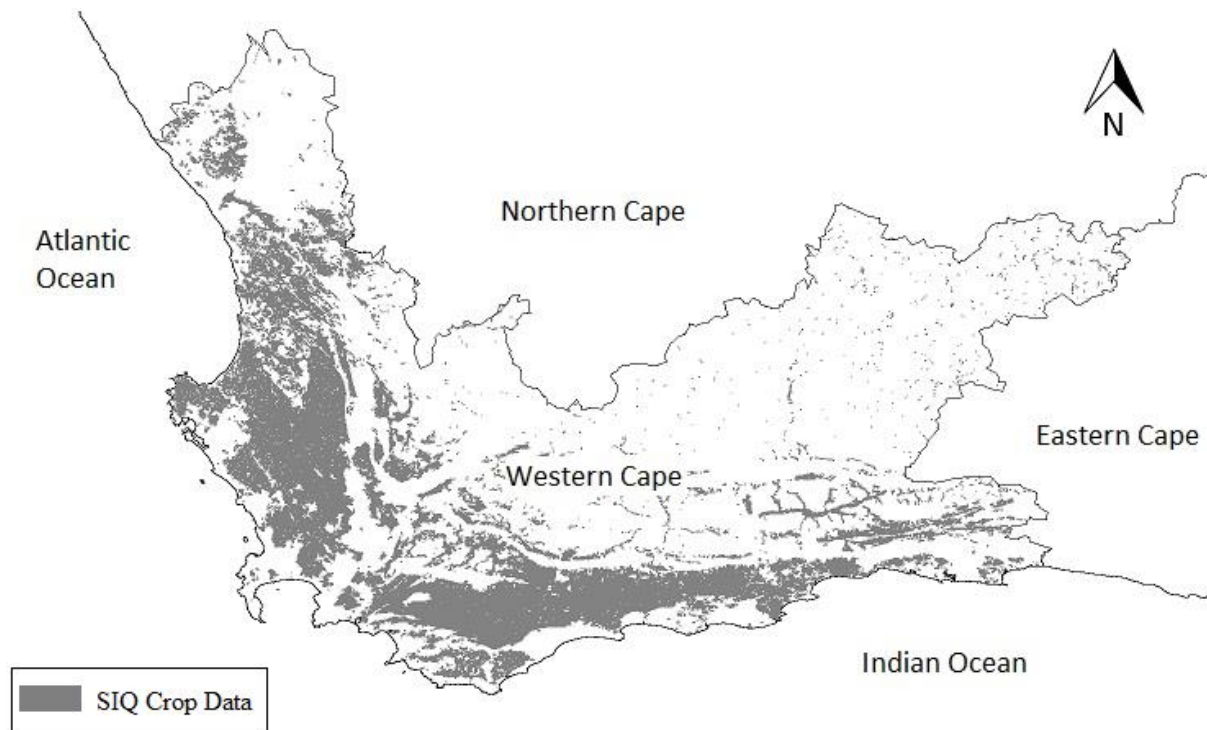


Figure 5 SIQ vector crop data for the Western Cape, South Africa

The crop data acquired from SIQ are highly accurate and have a coefficient of variance (CV) of less than 2% on a national level (SIQ 2014).

## 2.10 DIMENSIONALITY REDUCTION

As introduced in Section 1.1.6, the term “feature dimension” refers to the number of features (image bands, image transforms, ancillary data) considered in a classification. When too many features are considered (i.e. high feature dimensionality), classification algorithms tend to perform poorly (Rodriguez-Galiano et al. 2012). One way of mitigating high dimensionality is to reduce the number of features used for classification. This can be done by extracting or selecting features (Gislason, Benediktsson & Sveinsson 2006).

Feature extraction is the building of a new set of features from the original feature-set, while feature selection is the selection of a subset of features from the original feature-set. Feature extraction involves transforming the original feature space to yield an entirely new set of features. Examples of feature extraction methods include PCA and TCT, both of which were covered in Sections 2.6.2 and 2.6.3 respectively. These methods help classification algorithms to achieve maximum performance by limiting model variance and aid in the reduction of sparsity (Guyon & Elisseeff 2003).

Feature selection can be categorized into four approaches: filters, wrappers, embedded methods, and semantic feature selection. Filter feature selection is a classifier independent pre-processing



step that uses a common (objective) measure to score each feature's importance (e.g. variable importance) (Guyon & Elisseeff 2003). Once features have all received an importance score, they can be selected and used for classification (Guyon & Elisseeff 2003). Examples of filter methods include CART and RF.

A wrapper selects features during the classification procedure and is considered superior to the filter approach because a particular filter algorithm may not be appropriate for all classifiers. However, wrappers are very computationally expensive and slow because they must be iteratively applied for each individual learning algorithm (when multiple learning algorithms are used). Wrappers randomly select a subset of features and apply a learning algorithm to it. The output is then compared against reference data to determine the subset's performance. This process is repeated on many different subsets of features to determine which features consistently performed well. Examples of wrappers include recursive feature elimination, sequential feature selection algorithms, and genetic algorithms.

Embedded feature selection methods are similar to wrappers in that they are also used to optimize the performance of a learning algorithm. They learn which features contribute the most to the accuracy of the classification while the model is being created. The difference between the embedded approach and wrappers is that in the first approach, an intrinsic model-building metric is used during learning. Examples of embedded methods include L1 (LASSO) regularization and DTs (Huang et al. 2016).

The final approach, semantic feature selection, is simply the selection of features deemed most important by an expert. For instance, an analyst might decide to exclude the original image bands and only use indices instead.

### **2.10.1 Classification and regression trees (CART)**

CART is a decision tree machine learning algorithm used for data mining, predictive modelling, and data pre-processing. It uses binary recursive partitioning to grow DTs while the Gini and Twoing methods search for important relationships and patterns, allowing better insight into data (Breiman et al. 1984). The binary recursive partitioning can be viewed as a DT. Classification trees are designed for dependent variables with a finite number of unordered values. Prediction error is measured in terms of misclassification cost (Loh 2011). Regression trees are suitable for classifying dependent variables with continuous or ordered discrete values. Prediction error is typically measured by the squared difference between the observed and predicted values (Breiman et al. 1984).

CART has frequently been used for feature selection in the field of remote sensing (Lawrence & Wright 2001; Bittencourt & Clarke 2004). It can be used as a filter or wrapper feature selection method. In the former approach, CART is applied to identify suitable features (by assigning variable importance values to features), after which the selected features are used as input to other learning algorithms (e.g. SVM, DT, RF, and k-NN) (Loh 2011). The same features can also be used as input to CART for producing a DT (which results in the wrapper feature selection approach). When CART is used as filter, there is no guarantee that it will produce a subset of predictor variables that will optimize other classifiers. However, many studies have shown that feature selection using CART also improves modelling using alternative classifiers (Miner, Nisbet & Elder 2009). For instance, CART has been successful in improving the accuracy of vegetation classifications when used as a filter feature selection method for input to k-NN, ML, SVM, and RF classifiers (Yu et al. 2006).

### **2.10.2 Random forest**

RF, overviewed in Section 2.8.2.3, produces a variable importance score that can be used for feature selection. It has been used in remote sensing as a filter method by Guan et al. (2012), Rodriguez-Galiano et al. (2012), Abdel-Rahman, Ahmed & Ismail (2013), and Hao et al. (2015). Guan et al. (2012) used RF as a filter for land use classification with LIDAR and orthoimagery. Using 48 DEM derivatives, VIs, and textural features ranked by variable importance, they concluded that feature selection with RF can be used to facilitate accurate land use classification. Abdel-Rahman, Ahmed & Ismail (2013) used RF to select spectral bands from hyperspectral imagery for sugar cane leaf nitrogen detection. They found that RF successfully reduced redundancy in the data, but that more research is needed to better understand what *n*tree and *m*try settings will achieve optimal algorithm performance. Rodriguez-Galiano et al. (2012) and Hao et al. (2015) used RF to filter multi-temporal data to monitor crops. Both recommended the use of RF for selecting multi-temporal features, claiming that it has positive effects on classification accuracy.

## **2.11 ACCURACY ASSESSMENT**

Research on crop mapping using remote sensing methods usually aim to improve the speed and accuracy of the process. Two commonly used methods to assess the accuracy of thematic maps generated through classification are OA and kappa coefficient (K). OA is derived from a confusion (error) matrix, which is a table that summarizes the performance of an algorithm (Campbell & Wynne 2011). Each column of the confusion matrix represents the instances in a predicted class, while each row represents the instances in an actual class (or vice-versa). OA is

the total number of correctly classified objects/pixels in a classification result. K is essentially a measure of how well the classifier performed compared to how well a random classification would have performed (i.e. simply generated by chance) (Congalton & Green 2008). OA is easily interpreted because the percentage of classified pixels or objects corresponds to errors of commission and omission, while K can be used to assess statistical differences between classifications (Congalton & Green 2008). In addition to using K to compare the performances of different classifiers with one another, an additional method known as McNemar's test can be employed to determine whether results are significantly different.

McNemar's test (McNemar 1974) is a non-parametric procedure based on a two-by-two cross tabulation of dichotomous data. It is based on the chi-square statistic that takes correctly and incorrectly classified samples as input (the overall accuracies of two separate classifiers in the case of thematic classification) and produces a two-tailed P-value as output. The P-value is used to describe the statistical significance of the difference between the two samples. Using McNemar's test to statistically assess significant differences in classification accuracy has been recommended by Foody & Atkinson (2002) and used by Yan et al. (20015, Whiteside et al. (2011), and Duro, Franklin & Dube (2015).

## **2.12 SUMMARY**

This chapter provided a review of the literature on the use of remote sensing for crop classification. It is clear that the use of multi-temporal optical imagery is the most effective and feasible way of achieving good accuracies, with Landsat-8 imagery being the best source of imagery for the period of study (Sentinel-2 imagery became available during the course of this research, but was not yet available at the time the field surveys were carried out). Landsat-8 imagery meets all the requirements for regional crop classification, with a suitable spatial, spectral, and temporal resolution. Some of the technical aspects relating to crop classification with Landsat-8 imagery that require investigation were outlined in Section 1.2. This includes the effects of pansharpening, the performances of machine learning classifiers, the comparison of OBIA and PBIA, as well as the effects of dimensionality reduction. This chapter expanded on these concepts and is meant to provide a foundation for the following chapters.

The next chapter focuses on the effects of pansharpening and the performances of several machine learning classifiers for crop differentiation using multi-temporal Landsat-8 imagery. The results are then used in Chapter 4 which focuses on the effects of dimensionality reduction on crop classification accuracies.

The next two chapters were published as research articles in *Computers and Electronics in Agriculture*. The content of these articles were kept as published (although the formatting was changed to conform to the rest of the thesis). Given that the same study area and input data were used for both articles, some of the content is duplicated.

## **CHAPTER 3: PANSHARPENED LANDSAT-8 IMAGERY FOR CROP DIFFERENTIATION WHEN USING MACHINE LEARNING AND OBIA**

### **3.1 ABSTRACT**

This paper evaluates the potential of machine learning and object-based image analysis (OBIA) for the differentiation of crops in a Mediterranean climate (Western Cape, South Africa). Several Landsat-8 images covering all calendar seasons and multiple phenological stages were acquired. The remotely sensed images were used to produce a range of spectral values, textural values, vegetation indices, and colour transformations. These spatial variables were input for the decision trees (DTs), k-nearest neighbour (k-NN), support vector machine (SVM), and random trees (RT) classifiers, reaching overall classification accuracies of 85%, 78%, 95%, and 88% respectively. The accuracies achieved were produced by experimenting with both the OBIA and pixel-based image analysis (PBIA) paradigms. The OBIA classification scenarios included a favourable segmentation, an over-segmented image and an under-segmented image. The PBIA scenarios included a standard 30 m spatial resolution image and a pansharpened 15 m spatial resolution image.

### **3.2 INTRODUCTION**

Agricultural productivity is the foundation of developing economies and is critical to food security (Awokuse & Xie 2015). Accurate crop maps may strengthen an agricultural sector's health and therefore ensure food security, as they can update agricultural database statistics and forecast yields (Monfreda, Ramankutty & Foley 2008). Traditional methods for crop mapping and yield forecasting involve routine field visits, which are costly and biased (Castillejo-Gonzalez & López-Granados 2009). Remote sensing offers an unbiased, cost-effective, and reliable way of mapping crops at a local, regional, and national scale. Remotely sensed data play an important role in crop monitoring as it can be easily related to factors such as biomass, climate, plant stress, relative plant health, soil properties, terrain, and light use efficiency (McNairn et al. 2009; Xin et al. 2015). Knowledge of the state of these factors will help farmers gain awareness of crop health and moisture content, which can support decisions regarding the optimization of fertilisation and irrigation (Monfreda, Ramankutty & Foley 2008).

In recent years, optical remote sensing has gained popularity for its use in the identification and monitoring of crop types (Vieira et al. 2012; Simms et al. 2014; Muller et al. 2015; Ozelkan, Chen & Ustundag 2015; Zheng et al. 2015). Multi-temporal data have been shown to improve crop identification as it can better represent crop growth cycles, with optical (as opposed to radio

detection and ranging) multi-temporal data being the preferred data source (Blaes, Vanhalle & Defourny 2005; McNairn et al. 2009; Serra & Pons 2008). Ozelkan, Chen & Ustundag (2015) evaluated multi-temporal Landsat-8 data for the identification of agricultural vegetation and concluded that it was an effective data source. Vieira et al. (2012) tested with Landsat data (TM and ETM+), and showed that multi-temporal optical data allowed accurate crop mapping and that expert knowledge of crop phenological information was of high importance. Similar remarks were made by Zheng et al. (2015) and Muller et al. (2015) who also used multi-temporal Landsat data. This general notion was also supported by Simms et al. (2014) who acquired crop information using MODIS NDVI and ancillary data.

The two different paradigms for image classification are PBI and OBI, which have been compared often in recent years. Castillejo-Gonzalez & López-Granados (2009) compared the performances of PBI and OBI for the identification of crops with Quickbird imagery and concluded that OBI clearly outperformed PBI. Myint et al. (2011) tested the two paradigms using Quickbird imagery for urban land cover and found that OBI outperformed PBI by up to 27.6%. Similar conclusions were also achieved by Bhaskaran, Paramananda & Ramnarayan (2010) and Yan et al. (2015) who saw OBI outperform PBI by overall accuracies of 20% and 36% respectively. Weih & Riggan (2010) used aerial photography and SPOT-5 for land use and land cover supervised classification and showed that by merging high and medium spatial resolution imagery, supervised OBI outperformed both supervised and unsupervised PBI by 10%. Duro, Franklin & Dube (2015) tested both OBI and PBI with SPOT-5 data, and, unlike most other modern literature, concluded that neither method produced significantly better results than the other. Results such as those seen by Duro, Franklin & Dube (2015) may be the result of OBI being preferred over pixel-based classification, provided that the objects of interest are significantly larger than the pixels of the imagery (Pesaresi & Benediktsson 2001; Mathieu, Freeman & Aryal 2007; Blaschke 2010). Landsat-8 imagery will not always be preferred, as certain crops may be in fields smaller than 30 m spatial resolution. In order to mitigate this, the images were pansharpened to a 15 m resolution.

Pansharpening combines the superior spatial resolution of the panchromatic band (required for accurate description of texture and shapes) with the additional spectral resolution from the multispectral bands (required for accurate class discrimination of land covers) (Ghassemian 2016). There seems to be no clear superior method in modern literature; however, the comments made about PCI Pansharpening make it preferable (Zhang & Mishra 2012; Guo-dong et al. 2015). Zhang and Mishra (2012) reviewed all commercially available pansharpening techniques and concluded that PCI Pansharpening constantly produced the best fusion quality for all types of sensors,

images, and spectral bands. Guo-dong et al. (2015) proposed a new fusion method, MS-split, that outperformed Pansharp in four out of five tests. The results obtained by Guo-dong et al. (2015) suggested that MS-split was superior; however, MS-split was not yet commercially available for testing at the time of image processing and Pansharp still outperformed all other methods.

Both OBIA and PBIA are affected differently by different classifiers. In this research, supervised classification was utilized. Supervised classification, the process of using training data to classify objects of unknown identity, was chosen due to better efficiency and more control compared to unsupervised classification (Campbell 2008). Four classifiers were evaluated, namely: decision trees (DTs), k-nearest neighbour (k-NN), random trees (RTs), and SVM. DTs have been tested in multiple cases for land cover classification and have performed well in the cases of Waheed et al. (2006) and Yang et al. (2003). RTs have been successfully used for crop identification, vegetation classification, and change analysis, as seen in the cases of Pal (2005), Gislason, Benediktsson & Sveinsson (2006), and Yuan et al. (2005), while SVM has been successful at classifying agriculture (Karimi et al. 2006; Zheng et al. 2015). k-NN has been included in many research instances for comparison purposes (e.g. Myint et al. (2011); Mountrakis, Im & Ogole (2011); Myburgh & Van Niekerk (2013); Otukey & Blaschke (2010)) because it was the standard classifier for OBIA in eCognition.

Two commonly used methods to assess the accuracy of thematic maps in remote sensing include overall accuracy (OA) and kappa coefficient (K). OA is easily interpreted because the percentage of classified pixels or objects corresponds to errors of commission and omission (Campbell & Wynne 2011), while K can be used to assess statistical differences between classifications. This paper employed the same testing and training samples for each classification to ensure that each classification is independently assessed, warranting the use of K (Foody & Atkinson 2002). Testing for statistically significant differences in classification accuracy by the different approaches was done by means of the McNemar's test, as recommended by Foody & Atkinson (2002) and used by Yan et al. (2015), Whiteside, Boggs & Maier (2011), and Duro, Franklin & Dube (2015).

This paper experimented with the use of multi-temporal Landsat-8 imagery for crop differentiation. Two important, yet under-examined, questions were investigated: 1) Is object-based image analysis beneficial for discriminating crops? 2) What effect does pansharpening have on crop classification?

### 3.3 MATERIALS AND METHODS

#### 3.3.1 Study area

Classification was carried out in the Cape Winelands region, South Africa (Figure 6). The area which stretches from 33°34'39" to 33°52'17" S and 18°32'24" to 18°54'43" E was chosen for three reasons: the availability of multi-temporal cloud-free Landsat-8 data of the area, its variety of crops, and its proximity to the research location (Stellenbosch University), making field validation more efficient and feasible. The area has a Mediterranean climate with cool, wet winters and warm, dry summers, with an average rainfall of 550 mm, while the average annual temperature minima and maxima are 11°C and 22°C respectively (Tererai et al. 2013; Tererai, Gaertner & Jacobs 2015). The area allows a wide array of crops to be grown, the most common of which include canola, grape, lucerne, lupine, olive, pasture, and wheat.

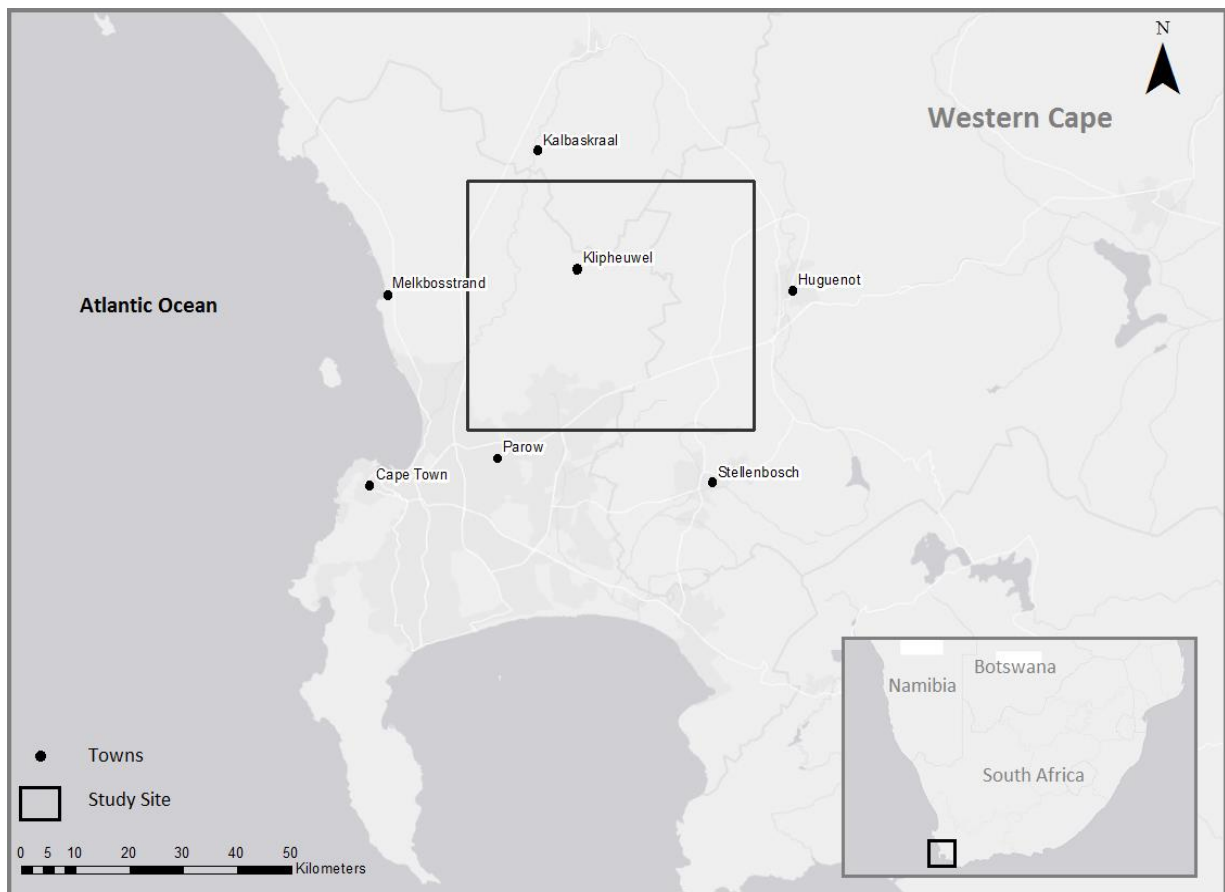


Figure 6 Location of the study area in the Western Cape, South Africa

#### 3.3.2 In situ data

A crop-vector dataset, created through extensive aerial surveys combined with supporting field visits by Spatialintel (SIQ) (Pty), was used to select objects for classifier training and accuracy assessment. The SIQ shapefile, which contains polygons for all agricultural ground in the region, is highly accurate, with a coefficient of variance (CV) of less than 2% on a national level.



Further uncertainty was reduced through field validation by the author's visits to points in the study area correlating to the polygons in the SIQ crop dataset. Stratified random sampling was applied to 150 fields, with a minimum of 20 samples per class. The SIQ data displayed an accuracy of 99.5%.

### 3.3.3 Satellite data and image date selection

Landsat-8 level 1T data were acquired from the USGS (United States Geological Survey). Image dates (from 2015) chosen were: 7 February, 11 May, 12 June, 31 August, and 5 December. Dates chosen were based on the developed crop calendar with phenological data (Figure 7) and analysing times were chosen according to times used in other research (Serra & Pons 2008; McNairn et al. 2009; Peña-Barragán et al. 2011). The temporal conclusion of five months was based on Hao et al. (2015) who found that five months was the optimal time-series. The calendar was developed by using phenological stage information for all crops of interest, obtained from production guidelines provided by the South African Department of Agriculture, Forestry, and Fisheries, as well as additional data sources such as private agricultural companies, interviews with local agricultural experts, and field visits.

	Jan	Feb	Mar	Apr	May	Jun	Jul	Aug	Sep	Oct	Nov	Dec
Canola				Sowing					Harvest			
Grape	Harvest					Pruning		Sowing				
Lucerne			Multiple cutting options (colour and vigour varies)									
Lupine				Sowing				Harvest				
Olive				Harvest								
Pasture				Establishment			Possible summer senescence					
Wheat				Sowing							Harvest	

Figure 7 Phenological information for informational classes. Dark grey represents important phenological stages, light grey indicates the presence of the crop, and white represents bare field. Selected imagery dates are shown with dotted lines.

### 3.3.4 Pre-processing

Landsat-8 data were atmospherically corrected and pansharpened in Geomatica. PCI Pansharp was used as recommended by Zhang (2002a) and Li et al. (2015) to resample the images from 30 m to 15 m spatial resolution. ATCOR (atmospheric and topographic correction) was applied to all images due to its positive effects on land cover classification, as seen in Vanonckelen, Lhermitte & Van Rompaey (2013) and Li et al. (2015).

### 3.3.5 Segmentation

Multi-resolution segmentation (MRS), a region-merging pair-wise algorithm that segments on pixel or object level based on scale, shape, and compactness was used. The ESP (estimation scale parameter) tool developed by Drăguț, Tiede & Levick (2010), which attempts to quantitatively estimate an optimal scale parameter, was run but did not produce a satisfactory scale recommendation. Scale parameters derived from ESP were used as a base for further segmentations. Combining ESP with qualitative analysis by comparing segmentations to shapefiles of digitized and verified crop fields, as well as reviewing past literature of similar segmentation attempts, lead to the eventual optimal segmentation. ESP recommended a scale of 35, which served as the base segmentation. After each run, the scale, shape, and compactness were tweaked until an object delineation was deemed optimal. Based on visual assessment, a favourable delineation of objects was achieved using 0.45, 0.55, and 14 for shape, compactness, and scale respectively. Heavier weighting for the green, red, near-infrared, and shortwave infrared spectral bands were used without any thematic layers. This favourable delineation is seen as E in Figure 8 below.

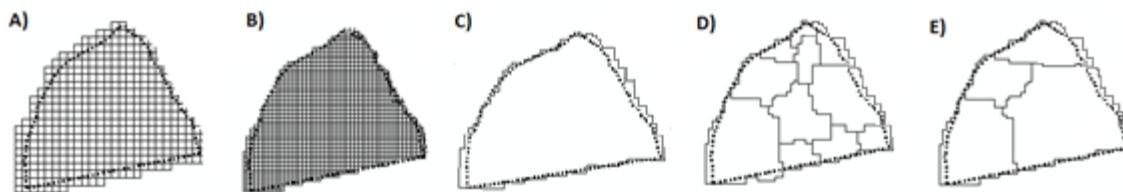


Figure 8 A canola field on which the five different classification methods were used. A) Shows the standard 30 m resolution pixels, B) the Pansharpened 15 m resolution pixels, C) the large object size for both pixel sizes, D) the small object size for both pixel sizes, and E) the preferred objects size for both pixel sizes.

The end parameters for the five different classification scenarios are seen in Table 3.

Table 3 Identification of all classification scenarios.

ID	Approach	Scale	Shape	Compactness
P30	Standard 30 m pixels	-	-	-
P15	Pansharpened 15 m pixels	-	-	-
SS35	Under-segmented objects	35	0.45	0.55
SS07	Over-segmented objects	7	0.45	0.55
SS14	Best segmentation objects	14	0.45	0.55
SPS34	Under-segmented objects	34	0.45	0.55
SPS06	Over-segmented objects	6	0.45	0.55
SPS12	Best segmentation objects	12	0.45	0.55

Note: Included is the parameters used for all three Object Oriented (OO) segmentations. “P” represents “pixel” for both pixel types, “SS” represents “segmentation standard” for segmentations on the standard 30 m pixels, and “SPS” represents “segmentation pansharpened” for the segmentations on the 15 m pansharpened pixels.

### 3.3.6 Features

In addition to the spectral bands provided by the sensor, several other variables such as textural information, vegetation indices, and image transforms were also considered in the classification. Table 2 outlines the various feature types, which resulted in a total of 205 features (41 per image capture date). Most features were created using standard RS software. The tasseled cap transformation images were produced using the coefficients derived by Baig et al. (2014).

Table 4 Features used as input for the DT, NN, SVM, and RT classifiers

Type	Subtype	Features
Spectral features	Mean	Blue, Green, Red, NIR, SWIR 1, SWIR 2, Panchromatic
	Standard deviation	Green, Red, NIR, SWIR 1, SWIR 2
Indices		ARVI, EVI, GCI, GNDVI, Greenness, NDVI, RGRI, SAVI, SRI
Textural features	GLCM	Contrast, Correlation, Entropy, Homogeneity
	GLDV	Contrast, Entropy, Mean
Image transforms	PCA	PC1, PC2, PC3, PC4
	Tasseled cap	Brightness, Greenness, Wetness, Transformation 4, Transformation 5, Transformation 6
	HSI	Hue, Saturation, Intensity

Textural features used include contrast, correlation, and entropy, as recommended by Clausi (2002). The spectral bands coastal aerosol (Band 1), cirrus (Band 8), thermal infrared 1 (Band

10), and thermal infrared 2 (Band 11) were not included since they are designed for other applications, as specified by the USGS (USGS 2015).

### **3.3.7 Classification and accuracy assessment**

Classification and accuracy assessment software used was developed by the Centre for Geographic Analysis in Stellenbosch, South Africa. The software employs four classifiers: DTs, k-nearest neighbour (k-NN), RTs, and SVM. It was developed using C++ and the Microsoft® VisualStudio®2010 development environment to automate the process of classification and accuracy assessment. SVM classification was performed using Libsvm (Chang & Lin 2011) where the radial basis function kernel was chosen as recommended by Hsu, Chen & Chen (2010). The k-NN classification used OpenCV 2.2 (Bradski & Pisarevsky 2000) with a k-value of 1 as used by Qian, Root & Saligrama (2015). The geospatial data abstraction library was used to manipulate shapefiles and raster files, while a 3:2 object split ratio was employed for the classification and accuracy assessment. The software output included OA and K, both of which were loaded into SPSS for the McNemar's test.

## **3.4 RESULTS AND DISCUSSION**

Both the OBIA and PBIA methods achieved satisfactory results (when compared to most modern literature) by using pansharpened imagery (See Table 5). The highest result was obtained with SPS14 using the SVM classifier, which achieved an OA and K of 95.93 and 0.95 respectively. PBIA was not far behind, with P15 achieving 94.30 and 0.93 for OA and K respectively (also with the use of SVM).

Table 5 Overall accuracies and kappa coefficients for each classification and dataset

	DT		NN		RF		SVM		OA		K	
	OA	K	OA	K	OA	K	OA	K	AVG	SD	AVG	SD
P30	74.07	0.69	55.59	0.47	75.36	0.71	79.32	0.75	70.09	10.38	0.73	0.02
P15	85.15	0.82	77.45	0.73	88.75	0.86	94.30	0.93	86.41	6.12	0.84	0.07
SS34	55.56	0.47	51.97	0.43	66.00	0.59	69.33	0.68	60.72	7.16	0.54	0.10
SS06	74.01	0.69	52.30	0.43	74.91	0.70	77.74	0.73	69.74	10.16	0.64	0.12
SS12	74.56	0.70	52.20	0.43	72.76	0.76	80.67	0.77	70.05	10.71	0.67	0.14
SPS35	59.04	0.50	52.87	0.44	68.86	0.63	75.69	0.71	64.12	8.78	0.57	0.11
SPS07	77.71	0.73	73.59	0.68	86.50	0.83	90.73	0.89	82.13	6.81	0.78	0.08
SPS14	81.76	0.78	78.90	0.75	87.54	0.85	95.93	0.95	86.03	6.51	0.83	0.08
AVG	72.54	0.67	61.86	0.56	77.59	0.74	82.96	0.80				
SD	10.33	0.12	11.58	0.14	8.28	0.09	8.96	0.10				

The high overall accuracies for both methods are considered impressive when taking into account the medium spatial resolution, complexity of the classification, and factors such as intra-crop variation. Intra-crop variation can be caused by factors such as different time schedules being followed, moth balling (leaving parts of a field to die), and variations in cover crops. Farmers in the region do not always plant crops on the exact same date, resulting in different phenological stages of crops on image capture dates. Crop fields themselves may also be different because of cover crops, an example of which is the grape class that can have triticale, weeds, wheat, or fynbos as its ground-cover crop. The above results show that even with all of these difficulties, both the OBIA and PBIA are capable of successfully monitoring the crops in the study area with machine learning classifiers.

Table 5's results are expected based on recent literature. OBIA was slightly more accurate than PBIA. OBIA is preferred over PBIA, provided that the objects of interest are significantly larger than the pixels of the imagery, therefore Landsat-8 OBIA was not expected to greatly outperform PBIA due to its medium spatial resolution. Although many of the crop fields classified in this research are larger than the Landsat-8 pixels, it is not often by as much as seen in Table 6. The objects of interest in this case (crop fields) are not significantly larger than the pixels of the imagery, which will explain why OBIA only marginally outperformed PBIA. However, at such a high level (> 90%), the small 1.63% increase in OA and 0.02 increase in kappa is important for developing accurate crop inventories.

Table 6 The average sum of pansharpened pixels per SIQ crop polygon/field

Crop type	Area (m <sup>2</sup> )	Pixel count (15 m)	Pixel count (30 m)
Canola	5623	25	6
Grape	5862	26	6
Lupine	1718	7	1
Olive	1324	5	1
Pasture	5529	24	6
Plum	757	3	1
Wheat	6100	27	6

Pansharpenering approximately quadruples the amount of pixels per crop field (making objects of interest become larger relative to pixel size), which may explain why P15 outperformed P30 by 14.98%, making PBIA with pansharpenering a more effective option for crop differentiation. McNemar's test showed that, without pansharpenering, OBIA is a more effective way to discriminate crops than PBIA using Landsat-8. The McNemar's test on P30 and S14 highest OA's yielded a P-value of 0.0033, which by conventional criteria is considered statistically significant. This was also seen when comparing P30 to P15, which produced a P-value of 0.0071, showing that pansharpenering is beneficial to the classification of crops when using PBIA, as 0.0071 is also considered statistically significant. The final McNemar's test used P15 and S14 OA's and yielded a P-value of 1, showing that OBIA and PBIA do not produce statistically significant results for crop discrimination if the Landsat-8 data is pansharpenered.

Of the three segmentations, the OA results were as anticipated. The under-segmented dataset (S35, the scale recommended by the ESP tool) had the poorest results, most likely due to objects being too large and additional data (from fields such as roads and pathways) being incorporation within them. The under-segmentation also amplifies the effects of intra-crop variation. As mentioned earlier, larger objects include entities such as trees that may be near or within the field, thus reducing the informational classes' spectral purity. S07 and S14 both produced satisfactory accuracies, possibly due to the fields being broken up by objects and because it was possible to exclude noise such as the pathways and trees mentioned above. S14 produced better results than S07, indicating that the qualitative visual assessment used to deem S14 optimal was successful.

All classifiers displayed clear performance patterns (Figure 9). The SVM classifier produced the highest OA, RF the second highest, next was DT, with NN producing the lowest OA in all classification scenarios.

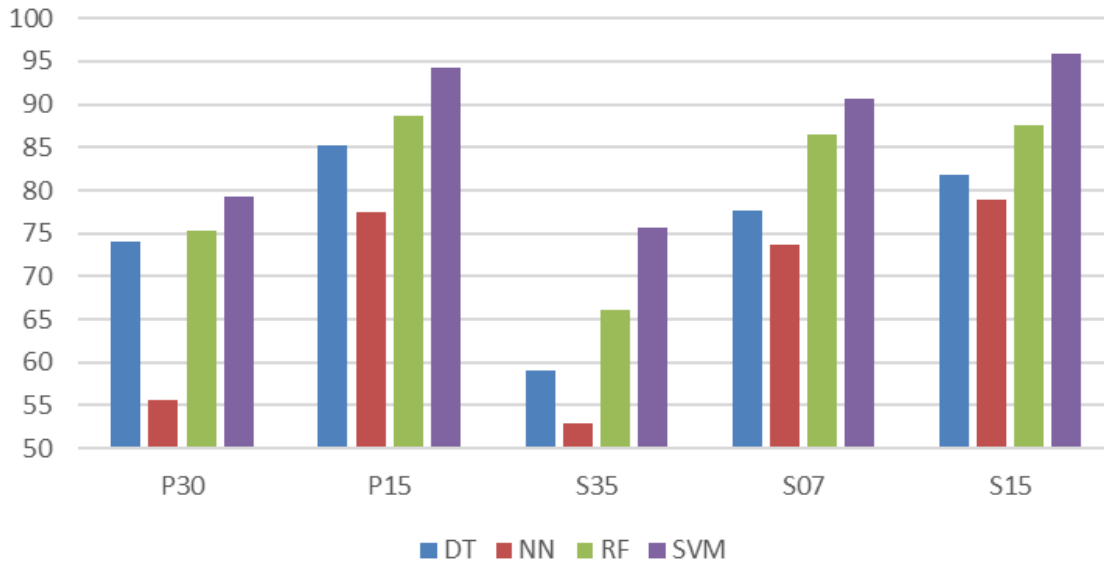


Figure 9 Overall accuracies for all classifiers grouped by dataset

The SVM classifier achieved great results, which can most likely be attributed to the radial basis function kernel recommended by Hsu et al. (2010). NN constantly had the lowest OA and kappa scores, probably because of its reduction of predictive accuracy in higher dimensions. The accuracies of the DT and RF classifiers were usually very similar, with RF not far off from the SVM results. Since the two tree classifiers are also known for being highly accurate classifiers, the likely reasons why they did not perform as well as SVM were that the SVM parameter tuning was better, or that the number and type of informational classes were better suited for SVM.

### 3.5 CONCLUSION

The results produced by this study provide insight into the performance of crop classification under different OBIA and PBIA scenarios with multi-temporal data. The highest accuracy was achieved with the SVM classifier using OBIA of 95.93%, which shows that using Landsat-8 data with a PBIA paradigm, in conjunction with pansharpening, is a feasible and effective way of monitoring crops in a Mediterranean climate. The P-value of 1, generated by McNemar's test when comparing P15 and SPS14, shows that there is no statistical difference in OA when using either pansharpened pixels or well-delineated objects. The lack of a significant statistical difference between P15 and SPS14 suggests that PBIA, with pansharpening, may be a more feasible approach for crop discrimination. It is clear that pansharpening of Landsat-8 is beneficial when classifying crop fields and that correct image segmentation is crucial for achieving high accuracies. The choice of whether or not to pansharpen Landsat-8 imagery has a much more profound effect on crop discrimination than the selection of either OBIA or PBIA.

## **CHAPTER 4: VALUE OF DIMENSIONALITY REDUCTION FOR CROP DIFFERENTIATION WITH MULTI-TEMPORAL IMAGERY AND MACHINE LEARNING**

### **4.1 ABSTRACT**

This study evaluates the use of automated and manual feature selection – prior to machine learning – for the differentiation of crops in a Mediterranean climate (Western Cape, South Africa). Five Landsat-8 images covering the different crop class phenological stages were acquired and used to generate a range of spectral and textural features within an object-based image analysis (OBIA) paradigm. The features were used as input to decision trees (DTs), k-nearest neighbour (k-NN), support vector machine (SVM), and random trees (RT) supervised classifiers. Testing was done by performing classifications (using all spatial variables) and then incrementally reducing the feature counts (based on importance allocated to features by filters), feature extraction, and manual (semantic) feature selection. Classification and regression trees (CART) and random forest (RF) were used as methods to filter feature selection. Feature-extraction methods employed include principal components analysis (PCA) and Tasseled cap transformation (TCT). The classification results were analysed by comparing the overall accuracies and kappa coefficients of each scenario, while McNemar’s test was used to assess the statistical significance of differences in accuracies among classifiers. Feature selection was found to improve the overall accuracies of the DT, k-NN, and RF classifications, but reduced the accuracy of SVM. The results showed that SVM with feature extraction (PCA) on individual image dates produced the most accurate classification (96.2%). Semantic groupings of features for classification also revealed that using the image bands and indices is not sufficient for crop classification, and that additional features are needed. The accuracy differences of the classifiers were, however, not statistically significant, which suggests that, although dimensionality reduction can improve crop differentiation when multi-temporal Landsat-8 imagery is used, it had a marginal effect on the results. For operational crop-type classification in the study area (and similar regions), we conclude that the SVM algorithm can be applied to the full set of features generated.

### **4.2 INTRODUCTION**

Crop maps assist in maintaining the health of an economy’s agricultural sector as they are used to update agricultural statistics and aid in yield forecasting (Castillejo-Gonzalez & López-Granados 2009). An additional benefit of up-to-date crop maps is increased environmental sustainability as these maps are required for modelling greenhouse gas variability in agro-



ecosystems (Monfreda, Ramankutty & Foley 2008). Crop-mapping has traditionally been done using routine field visits. This methodology is costly and can be inaccurate when biased sampling schemes are utilised (Castillejo-Gonzalez & López-Granados 2009). Remote sensing offers an unbiased, cost-effective, and reliable way of mapping crops at a local, regional, and national scale. Crop discrimination using remotely sensed data is, however, not without challenges. Certain crop types have similar spectral signatures, which makes it difficult to differentiate them from one another when using multispectral imagery. Since different crop types have divergent temporal spectral profiles, the consideration of temporal (phenological) variations between crops have been shown to improve classification accuracies (Castillejo-Gonzalez & López-Granados 2009). However, some crop types may display intra-class temporal variability (different phenological growth patterns) from farm to farm due to either natural development variation or diverse crop-management decisions made by farmers (Peña-Barragán et al. 2011).

Nevertheless, the value of multi-temporal data for crop discrimination has been demonstrated by Wardlow, Egbert & Kastens (2007), Ozelkan, Chen & Ustundag (2015), and Zheng et al. (2015). Multi-temporal data allows for the generation of a large number of features (variables) for each image acquisition date, which has been shown to substantially improve results (Heinl et al. 2009). However, the use of multi-temporal data often leads to very high feature counts (Lu & Weng 2007; Heinl et al. 2009). Too many features will lead to the so-called “curse of dimensionality”, whereby the performance of classifiers is hampered by the imbalance between training samples and features (Rodriguez-Galiano et al. 2012). This is driven by the problem of sparsity, where training data becomes too sparse to cope with the large volume of feature space brought on by large numbers of variables (Myburgh & Van Niekerk 2013). Classifiers consequently require an increasing number of training samples as feature dimensionality increases.

Large sets of training samples are not always feasible due to the high costs associated with field visits (Castillejo-Gonzalez & López-Granados 2009). Another approach to mitigate high dimensionality is to carry out feature extraction and/or feature selection (Guyon & Elisseeff 2003). Feature extraction involves the replacement of the original data by a new collection of features representing most of the variance of the original data (Benediktsson & Sveinsson 1997). The most common feature-extraction method is PCA, which transforms the data into a new set of principle components (PCs) that describes the underlying structure of the original dataset (Zhang and Mishra 2012). Other feature-extraction methods include tasseled cap transformation (TCT) and the generation of spectral indices. The TCT is a process whereby spectral data from an optical sensor (predominantly Landsat) is compressed into a few bands associated with a scene's

physical characteristics while suffering minimal information loss (Huang et al. 2002). Spectral indices are essentially arithmetic operators performed on multispectral imagery (or any additional data), which results in a new composite image (Campbell & Wynne 2011). Examples include NDVI (normalised difference vegetation index), SAVI (soil-adjusted vegetation index), and EVI (enhanced vegetation index). PCA, TCT, and spectral indices are commonly used when classifying crops with remotely sensed data (Simms et al. 2014; Campbell et al. 2015; Zheng et al. 2015).

Feature selection involves picking a subset of important features from the original dataset to reduce data dimensionality (Guyon & Elisseeff 2003). The main feature-selection approaches are wrappers, embedded methods, semantic groupings, and filters. A wrapper evaluates various subsets of features during the classification process by making use of the learning algorithm itself (Kojadinovic & Wotk 2000). The advantages of wrappers include interaction between model selection and feature-subset search, and the capability to take feature dependencies into account. However, wrappers have a high risk of overfitting and are also computationally intensive, as every feature subset proposed by the subset selection measure is evaluated in the context of the learning algorithm (Saeys, Inza & Larrañaga 2007). Examples of wrappers include recursive feature elimination (Shahi, Shafri & Hamedianfar 2016), sequential feature selection (Lagrange, Fauvel & Grizonnet 2016), and genetic algorithms (Persello & Bruzzone 2016).

Embedded feature-selection methods are similar to wrappers as they are also used to optimize the performance of a learning algorithm (Guyon & Elisseeff 2003). Embedded techniques learn which features contribute the most to the accuracy of the classification while the model is being created. The difference between an embedded approach and a wrapper is that the former method utilizes an intrinsic model-building metric during learning. Examples of embedded methods include L1 (LASSO) regularization and DTs (Huang et al. 2002). Semantic feature selection simply involves the selection of features according to their type or those deemed most important by an expert. Examples include using only spectral features, only indices, only texture features, etc.

A filter is a pre-processing step that is independent of the learning algorithm (Fourie 2011). This step results in a faster learning pipeline for the feature-selection algorithm (when multiple classifiers are used), but filters tend to not perform as well downstream due to an absence of interaction with the classifier (Kojadinovic & Wotk 2000). Three popular filter methods used in remote sensing are Jeffries-Matusita distance, CART, and RF (Miner, Nisbet & Elder 2009; Rodriguez-Galiano et al. 2012; Hao et al. 2015). CART is a decision-tree machine learning algorithm used for data mining, predictive modelling, and data pre-processing. It uses binary

recursive partitioning to grow DTs, while the Gini and Twoing methods search for important relationships and patterns, allowing better insight into data (Breiman et al. 1984). It can be used to create a short list of predictor variables for use with another predictive method (Miner, Nisbet & Elder 2009). Yu et al. (2006) used CART for detailed vegetation classification with high spatial resolution imagery and found that it improved classification accuracy. Yu et al. (2006) started with two out of 52 variables and found an increase in overall accuracy with the addition of features from 1 to 27, after which accuracies began to decline. Conrad et al. (2011) analysed the effect of CART feature selection on crop classification accuracy using multi-temporal MODIS imagery. They found that CART was able to improve classification accuracy by up to 7% and ascribed this to the prioritization of segments representing active phases of the different crops' phenological development.

RF is a collection of DTs that form an ensemble learning method for classification or feature selection (Pal & Mather 2003). Rodriguez-Galiano et al. (2012) assessed the effect of RF feature selection on Mediterranean land-cover classification (including multiple crop classes) with multi-seasonal imagery and texture. They found that feature selection using RF had a positive effect on image classification (overall accuracy increases of up to 10%) and commented that feature selection reduced the effect of the "curse of dimensionality". Hao et al. (2015; 2016) utilized RF feature selection for crop classification with multi-temporal MODIS imagery and claimed that the technique allowed the identification of the optimal portion of features required for an accurate discrimination between crop types.

Compared to the traditional pixel-based image analyses (PBIA), OBIA approaches have been shown to produce higher classification accuracies in some cases (Castillejo-Gonzalez & López-Granados 2009; Yan et al. 2015), while Duro, Franklin & Dube (2015) found that both paradigms produced similar results. In general, OBIA is preferred only if the objects of interest are significantly larger than the pixels of the imagery (Blaschke 2010).

This study evaluates the use of multi-temporal, object-based supervised classification for the differentiation of crops in a Mediterranean climate (Cape Winelands, South Africa). Five Landsat-8 images were used to generate a large (205) set of features. A small set (159) of fields representing the seven major crops in the region was selected to train and assess the classifiers. The size of the in situ dataset was purposefully limited to evaluate the classifiers' ability to perform with minimal training data (i.e. under sparse training conditions). Filter feature selection (using CART and RF), feature extraction (using PCA and TCT), and thematic feature groupings were applied to the full feature-set to assess whether these techniques improve classification accuracies. The different feature-sets were used to train four machine learning classifiers, namely

DT, k-NN, RF and SVM. The classification results are interpreted in the context of finding an operational solution for the production of accurate crop-type maps in the Cape Winelands region.

### 4.3 MATERIALS AND METHODS

#### 4.3.1 Study area and period

The experiments were carried out in a 1040 km<sup>2</sup> area within the Cape Winelands region, South Africa (Figure 10). The area, which stretches from 33°34'39" to 33°52'17" S and 18°32'24" to 18°54'43" E, was selected due to the availability of multi-temporal cloud-free Landsat-8 data, and the variety of summer and winter crops being produced in the region. The study site has a Mediterranean climate with cool, wet winters and warm, dry summers. The average rainfall is 550 mm, while the average annual temperature minima and maxima are 11 °C and 22 °C respectively (Tererai, Gaertner & Jacobs 2015). A wide range of crops are grown in the area, of which the most common are canola, grape, lucerne, lupine, olive, pasture, and wheat. The period of study was 2015, as this was when in situ data were collected.

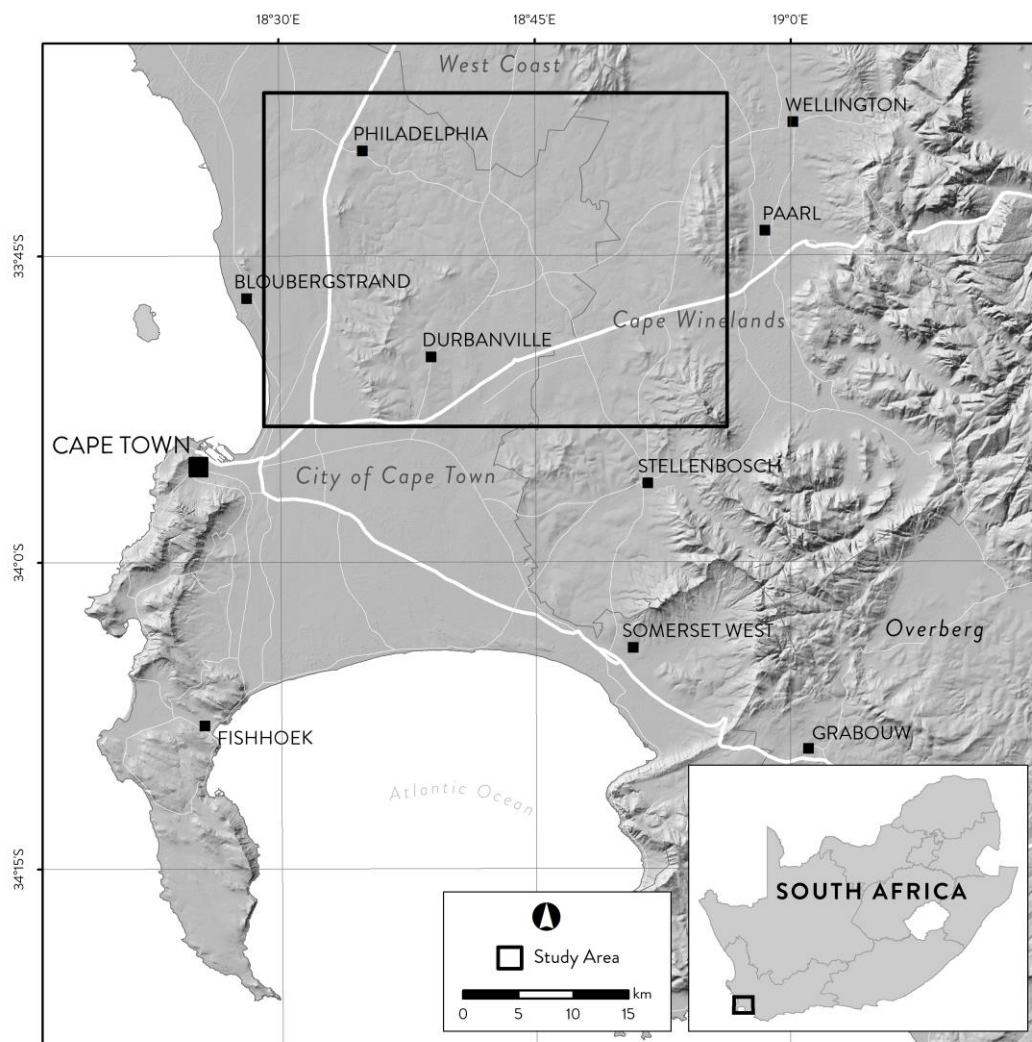


Figure 10 Location of the study area

### 4.3.2 In situ data

A crop-type database in vector geographical information system (GIS) format was obtained from the Western Cape Department of Agriculture. The database contains polygons representing agricultural fields and crop types, as determined during extensive aerial and field surveys in 2013. A stratified random sampling was used to select 159 crop fields from the database. This represented 7.63% (2,340 ha out of 31,443 ha) of the fields occurring in the study area. A minimum of 20 samples (fields) per class (crop type) was set, as recommended by Myburgh & Van Niekerk (2013). A small training-set was purposefully selected to investigate the performance of the classifiers when limited training data are available. Using small sets of training data will reduce the costs associated with operational in situ data collection, especially at regional scales. Because annual crops in the study area are often rotated, the selected fields were visited during a field survey in 2015. Several fields were found to have been incorrectly labelled and the database was updated accordingly.

### 4.3.3 Satellite data and image date selection

As suggested by Hao et al. (2016), five Landsat-8 level 1T images – captured on 7 February, 11 May, 12 June, 31 August, and 5 December 2015 – were acquired from the United States Geological Survey. The image dates were chosen to correspond with phenological data and agricultural production phases (Figure 11) of the crops occurring in the region (Peña-Barragán et al. 2011). The phenological stages for each individual crop were derived from growing guides provided by South Africa’s Department of Agriculture, Forestry, and Fisheries and confirmed by interviews with local farmers.

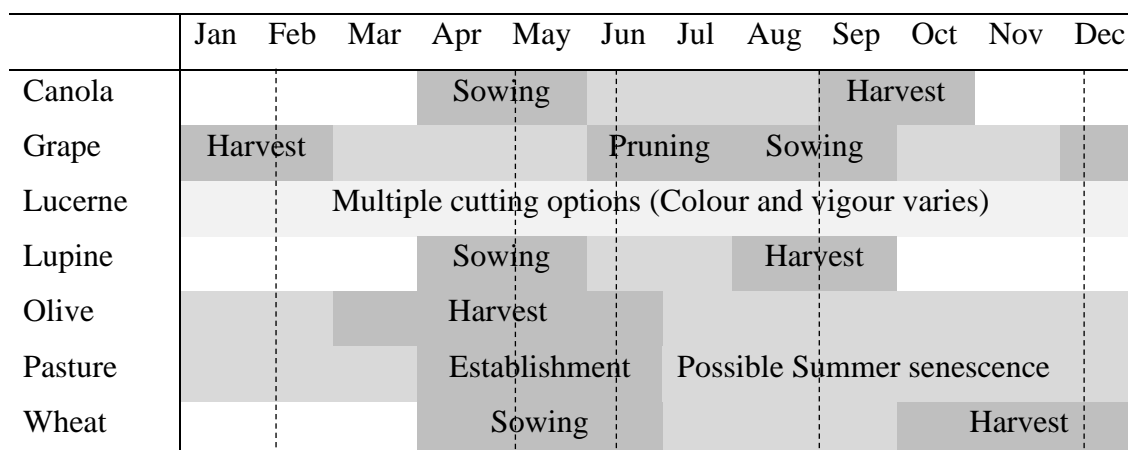


Figure 11 Phenological information on crop types

In Figure 11, dark grey represents important phenological stages, light grey the presence of the crop, and white represents bare field. Selected imagery dates are shown with dotted lines.

#### 4.3.4 Pre-processing

Landsat-8 images were pan-sharpened and atmospherically corrected using the PCI Geomatica software package. As suggested by Gilbertson, Kemp & van Niekerk (2017), PCI PANSHARP was used to resample the multispectral images from 30 m to 15 m spatial resolution (Lin et al. 2015). ATCOR (atmospheric and topographic correction) was applied to all images to convert them to surface reflection.

#### 4.3.5 Segmentation

Multi-resolution segmentation (MRS) was used to group pixels with similar spectral values. MRS uses scale, shape, compactness, and layer weighting as input parameters. The impact of different segmentations on classification accuracy was reported in Gilbertson, Kemp & van Niekerk (2017). Given that the purpose of the present study was to compare different feature selection methods, the best-performing segmentation from Gilbertson, Kemp & van Niekerk (2017) was chosen as a generic set of objects for all classifiers. The image layers and weights used to produce this segmentation were first principle component (25%), panchromatic band (20%), green band (10%), red band (20%), near-infrared band (20%), and short-wave infrared band (5%). Setting image segmentation parameters is considered an ill-structured problem (Verhulp & Van Niekerk 2016) and these weights were set based on a qualitative trial-and-error approach in which each individual layer was assessed according to how well it represented the spectral variations of crops in the study area. Although the estimation scale parameter tool (Drăguț, Tiede & Levick 2010) was used to quantitatively estimate an optimal scale parameter, it did not produce a satisfactory scale recommendation (it resulted in considerable under-segmentation). Instead, a visual assessment was made by comparing segmentations to shapefiles of digitised and verified crop fields. A favourable delineation (slight over-segmentation) of objects was achieved using 0.45, 0.55, and 14 for shape, compactness and scale respectively. Although the chosen parameters (input layers, weights, shape, compactness and scale) are unlikely to be optimal, it was assumed that a sub-optimal segmentation layer would affect all classifiers and feature selection methods equally.

#### 4.3.6 Image feature-set generation

In addition to the Landsat-8 spectral bands, several other features were considered in the classifications (Table 7). Coastal aerosol (band 1), cirrus (band 8), thermal infrared 1 (band 10), and thermal infrared 2 (band 11) were excluded as they were deemed unsuitable or had resolutions that were too low for crop-type differentiation. Nine indices commonly used in vegetation studies were generated from the remaining bands. These bands were also used as

input to PCA, which was applied to the entire dataset (all available spectral bands of all dates) as well as to the spectral bands of the individual image acquisition dates. The PCs to be used for classification were selected by means of a scree test and eigenvalues. Components accounting for 80% or more of the image variance were retained. TCTs were calculated using the coefficients obtained from Baig et al. (2014). Textural features included contrast, correlation, and entropy as recommended by Clausi (2002). The final feature-set consisted of 205 features (38 per image capture date and 15 from PCA on all images dates combined).

Table 7 Features considered in the classifications

Type	Subtype	Features
Spectral features	Mean	Blue, Green, Red, NIR, SWIR 1, SWIR 2, Panchromatic
	Standard deviation	Green, Red, NIR, SWIR 1, SWIR 2
Indices		ARVI, EVI, GCI, GNDVI, Greenness, NDVI, RGRI, SAVI, SRI
Textural features	GLCM	Contrast, Correlation, Entropy, Homogeneity
	GLDV	Contrast, Entropy, Mean
Image transforms	PCA	PC1, PC2, PC3, PC4
	Tasseled cap	Brightness, Greenness, Wetness, Transformation 4, Transformation 5, Transformation 6

#### 4.3.7 Feature selection

Several dimensionality-reduction methods were evaluated. CART and RF, as implemented in Salford Systems data mining and predictive software, were used as tools for filtering feature selection. PCA was used as a feature-extraction technique and was executed in ArcMap. Manual (semantic) feature-subset selection was also carried out.

For RF, Gini importance was selected and the number of trees to build set to 1000. The number of variables to be considered at each node was set to the square root of K (where K is the number of predictors), as recommended by Breiman et al. (1984). Bootstrap sample size was left at AUTO (using a sample that includes only  $\frac{2}{3}$  of the original training data), and a balanced class weighting was applied as recommended by the Salford Systems user's manual.

For CART, the search intensity was set to max (400) and the splitting method was set to Gini, as recommended by Yu et al. (2006). The V-fold cross-validation was set to 10, as was done by Lewis (2000) and recommended by the Salford Systems user's manual. The maximum number of nodes and depth was set to AUTO and no penalties were applied to any variables. The variable importance scores provided by RF and CART was used to select subsets of features. This was done iteratively with intervals of 75, 50, 25, 20, 15, 10, 5, 4, 3, 2, and 1 feature(s).

The final feature-dimensionality reduction-method involved grouping the features into semantic subsets. These were: (1) mean band values (BANDS1); (2) mean band values and band standard deviations (BANDS2); (3) PCs of all spectral bands (PCA1); (4) PCs of spectral bands per acquisition date (PCA2); (5) TCT; (6) indices (INDICES); (7) PCs per image date, TCT, and indices (TRANS); and (8) texture measures (TEXTURE).

#### **4.3.8 Classification and accuracy assessment**

The supervised learning and image classification environment (SLICE) software, developed by the Centre for Geographical Analysis (Myburgh 2012), was used for classification and accuracy assessment. The software makes use of OpenCV 2.2 (Bradski and Pisarevsky 2000) and Libsvm (Chang & Lin 2011) libraries and includes a range of classification algorithms, including DTs, k-NN, RF (called RT in OpenCV), and SVM. In the interest of brevity, the reader is referred to Pal (2005) and Al-doski, Mansor & Shafri (2013) for an overview of these classifiers.

Parameters for DT and RF were set as recommended in the OpenCV library documentation. For DT, the maximum depth was set to 50, K-fold cross-validation was disabled, the minimum number of samples was set to one, and pruning harshness was set to the minimum. For RF, the maximum depth was set to 50, the minimum sample count to one, and the square root of the total number of features (14) was used for the size of the randomly selected subset of features at each tree node. The k-parameter of the k-NN classification was set to one, as suggested by Qian, Root & Saligrama (2015). For SVM, the radial basis function kernel was chosen, as recommended by Hsu, Chang & Lin (2003). The geospatial data abstraction library was used to manipulate the vector and raster files.

A 3:2 sample split ratio was employed for classification and accuracy assessment (i.e. 60 of the 150 samples were randomly excluded from classifier training and used exclusively for assessing the accuracy of the resulting models). The same set of training and testing samples were used for all experiments.

SLICE automatically generates confusion matrixes, and calculates overall accuracies (OA) and the kappa coefficients (K) for each experiment. OA is easily interpreted as it represents the percentage of classified pixels or objects that corresponds to errors of commission and omission (Campbell & Wynne 2011), while K can be used to assess statistical differences between classifications (Foody & Mathur 2004). McNemar's test, ANOVA and t-tests (as implemented in IBM SPSS software) were used for assessing the statistical significance of the accuracies obtained from the experiments, as recommended by Foody & Mathur (2004) and applied by Duro, Franklin & Dube (2015).



## 4.4 RESULTS

The results of the classifications are summarized in Table 8. The first scenario in Table 8 (labelled NONE) represents the classification results when the full set of features were used as input (i.e. no dimensionality reduction applied). Scenarios 2–19 represent the classification results when CART and RF filter methods were applied. The semantic feature groupings are listed as Scenarios 20–27. The total feature count (n) per scenario is also provided.

Table 8 Overall accuracies and kappa coefficients for all classification scenarios (all scenarios are also assigned a unique scenario number)

#	Scenario	n	DT	DT	k-NN	k-NN	RF	RF	SVM	SVM	AVE	AVE
			OA	K	OA	K	OA	K	OA	K	OA	K
1	NONE	205	81.8	0.78	78.9	0.75	87.5	0.82	<b>95.9</b>	0.95	86.0	0.83
2	CART75	75	86.3	0.83	88.1	0.85	89.3	0.87	<b>93.9</b>	0.92	89.4	0.87
3	CART60	60	83.0	0.79	87.1	0.84	88.7	0.86	<b>92.3</b>	0.90	87.8	0.85
4	CART50	50	80.2	0.76	78.4	0.74	84.9	0.82	<b>91.9</b>	0.90	83.9	0.81
5	CART40	40	75.2	0.70	77.7	0.73	84.5	0.81	<b>90.2</b>	0.88	81.9	0.78
6	CART30	30	73.8	0.68	76.9	0.72	82.3	0.79	<b>87.7</b>	0.85	80.2	0.76
7	CART20	20	73.8	0.68	64.6	0.58	79.4	0.75	<b>82.4</b>	0.79	75.1	0.70
8	CART10	10	68.2	0.62	63.4	0.57	72.5	0.67	<b>74.0</b>	0.69	69.5	0.64
10	RF150	150	78.9	0.75	82.0	0.78	85.0	0.82	<b>90.5</b>	0.88	84.1	0.81
11	RF100	100	83.7	0.80	91.6	0.90	89.5	0.87	<b>93.7</b>	0.92	89.6	0.87
12	RF75	75	84.8	0.82	94.9	0.93	89.5	0.87	<b>94.9</b>	0.93	91.0	0.89
13	RF60	60	81.8	0.78	89.9	0.88	88.5	0.86	<b>92.4</b>	0.91	88.2	0.86
14	RF50	50	81.0	0.77	88.2	0.86	86.6	0.84	<b>92.1</b>	0.90	87.0	0.84
15	RF40	40	80.2	0.76	87.5	0.85	86.3	0.84	<b>89.8</b>	0.87	86.0	0.83
16	RF30	30	76.7	0.72	84.4	0.81	79.2	0.75	<b>90.8</b>	0.89	82.8	0.79
17	RF20	20	76.4	0.72	78.0	0.74	79.1	0.75	<b>89.0</b>	0.87	80.6	0.77
18	RF10	10	73.4	0.69	73.5	0.68	78.9	0.75	<b>82.1</b>	0.78	77.0	0.73
20	BANDS1	35	71.3	0.66	88.7	0.86	86.2	0.83	<b>90.5</b>	0.88	84.2	0.81
21	BANDS2	70	72.6	0.67	89.8	0.87	86.0	0.83	<b>92.9</b>	0.91	85.3	0.82
22	PCA1	20	67.5	0.61	83.1	0.79	84.5	0.81	<b>89.1</b>	0.87	81.1	0.77
23	PCA2	20	82.1	0.78	93.0	0.91	90.1	0.88	<b>96.2</b>	0.95	90.4	0.88
24	TCT	30	78.0	0.73	94.5	0.93	84.4	0.81	<b>92.7</b>	0.91	87.4	0.85
25	INDICES	45	67.2	0.61	64.6	0.58	78.6	0.74	<b>87.8</b>	0.85	74.6	0.70
26	TRANS	95	85.7	0.83	84.1	0.81	92.1	0.90	<b>95.2</b>	0.94	89.3	0.87
27	TEXTURE	35	49.8	0.40	56.2	0.48	55.4	0.47	<b>58.1</b>	0.50	54.9	0.46
	MEAN		76.5	0.7	81.6	0.8	83.6	0.8	<b>89.0</b>	0.9	82.7	0.8

Note: Colours range from green (high) to red (low) along rows and consequently visualize accuracies per classifier. Bold numbers represent the highest OA per scenario. The header “n” represents the number of features for each dataset.

The best OA (96.2%) was achieved when the SVM classifier was applied to the PCA2 set of features (Scenario 23, PCA2). This was, however, only marginally (0.3%) higher than when SVM was applied to the entire feature-set (Scenario 1, NONE). According to McNemar’s test, the difference between these results is not statistically significant. Similarly, these results were

not significantly higher than when SVM was applied to Scenario 26 (TRANS), which achieved an OA of 95.2%.

The superior performance of SVM was observed in all of the crop classification scenarios and achieved a mean OA of 89%. This is significantly higher (two-tailed t-test:  $P = 0.02$ ) than the second-best classifier RF (mean OA = 83.6%). Overall DT was the worst performing classifier (mean OA = 76.5%).

The best performing DT scenario was Scenario 2 (CART75), which suggests that DT benefitted from the filtered feature selection, although the difference between Scenario 1 and 2 was not statistically significant ( $P = 0.596$ ). The DT classifier also achieved a relatively high classification accuracy (85.7%) when all of the available image transforms were used (Scenario 26). When the RF was used as filter for feature selection, the best accuracies were achieved with 100 and 75 features. Based on these results, it would seem that CART was better suited to filter features for the DT classifier (compare CART75 and RF75), but only marginally, as the 1.6% difference in OA of Scenarios 2 and 12 was not statistically significant ( $P = 0.311$ ).

The best classification result (94.9%) for the k-NN classifier was achieved when using the 75 most important features, as determined by RF (Scenario 12). In comparison, the CART75 feature-set produced a much poorer classification (88.1%). The second and third best k-NN classifications were achieved with feature-sets TCT (94.5%) and PCA2 (93%) respectively.

The TRANS-subset (Scenario 26) produced the best classification result (92.1%) when RF was used as the classification algorithm. This result is substantially (4.6%) higher than when the full set of features was used (Scenario 1), although this increase was statistically insignificant according to McNemar's test ( $P = 0.286$ ). As with k-NN, the PCA2 feature-set produced a relatively good result (90.1%) when used as input to RF. Other notable RF results include the RF75, RF100, and CART75 feature subsets (89.3–89.5%).

In general, OA decreased with a reduction in feature count (see Figure 12). Slight improvements in accuracy were observed at 75 features for all classifiers (apart from SVM) when CART and RF were used as filters for feature selection. According to McNemar's tests, only the improvement of the k-NN classifier was statistically significant. Interestingly, apart from NN, all classifiers suffered an initial penalty in accuracy when RF was used as feature selection method. At 150 features, the accuracies of SVM, DT and RF were 5.4%, 2.9% and 2.5% lower than when the full set of 205 features was used as input.

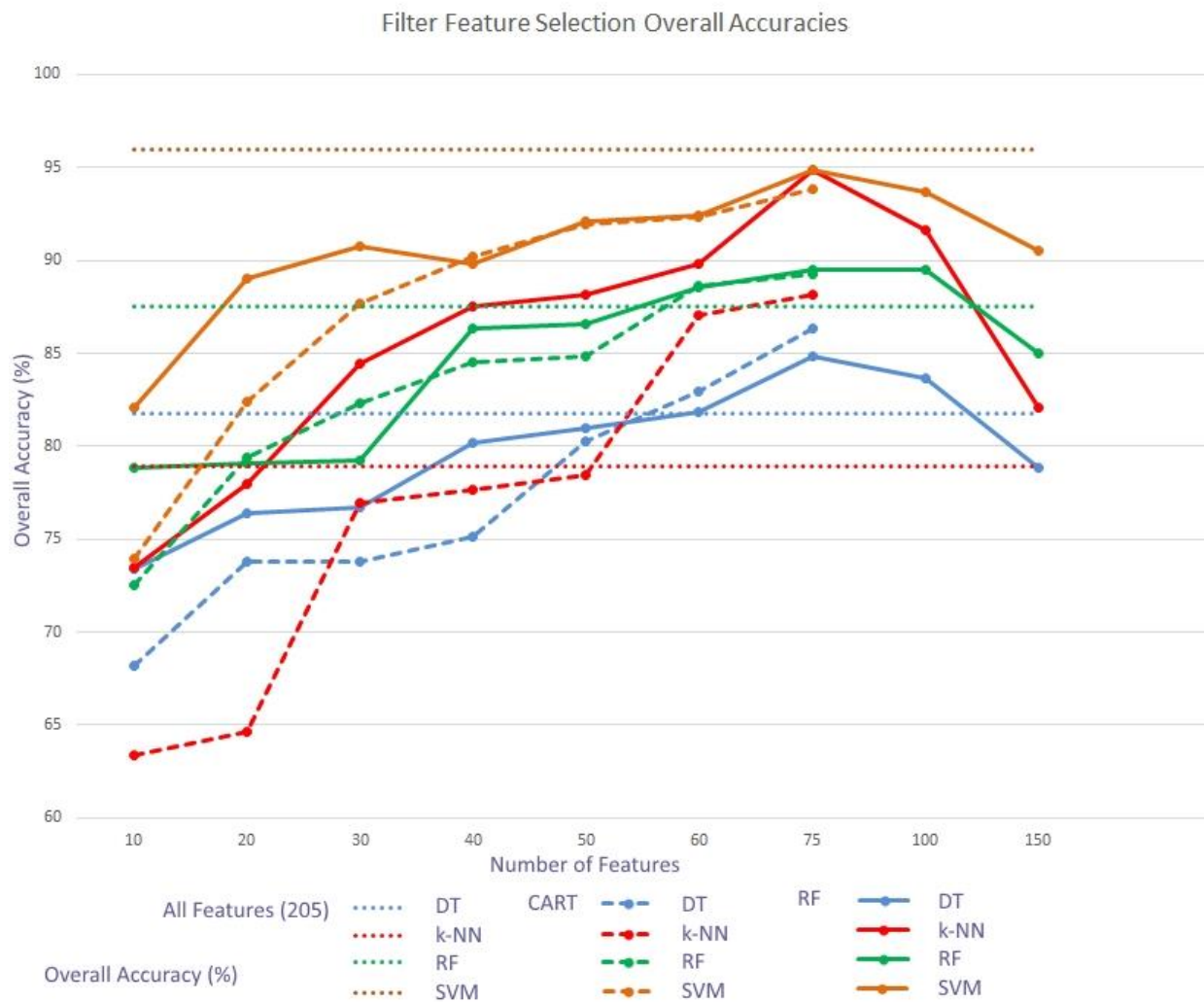


Figure 12 Overall classification accuracies as feature-sets were reduced when using CART and RF as filters

When all the classifiers are considered, the best overall feature-set scenario was when RF was used to select the 75 most important variables (Scenario 12, RF75), with an average OA of 91%. This was only marginally (0.6%) higher than the average of Scenario 2 (CART75), which yielded the second-best overall results for the classifiers evaluated. The difference between the means of these two scenarios were statistically insignificant ( $P = 0.87$ ). This result suggests that there is no difference in the performance of CART and RF as filter methods when multiple classifiers are considered (although clear differences were observed for individual classifiers). According to an ANOVA test, the differences between Scenarios 1, 2, and 12 were not significant, which means that the filter methods did not improve classification accuracies.

Semantic feature groupings provided insight into the importance of certain types of features. Using only the original spectral data (mean band values per object) as input to the classifiers (Scenario 20, BANDS1) resulted in an average OA of 84.2%. The addition of standard deviation values to the objects (Scenario 21, BANDS2) improved the average OA only marginally to 85.3%.

Applying PCA to all features (Scenario 22, PCA1) and choosing the 20 PCs that contributed the most to variation yielded poor results (average OA = 81.1%). In contrast, good results were consistently obtained when PCA was applied to the individual images (Scenario 23, PCA2), with an average OA of 90.4% for all classifiers. Compared to PCA, TCT (Scenario 24) was not as successful (average of 87.4%), especially considering that the PCA feature-set was much (33%) smaller.

Using only indices (Scenario 25) produced relatively poor results (average OA = 74.6%). In contrast, the inclusion of all transforms (Scenario 26) was more successful (average OA = 89.3%). Scenario 27, in which only texture measures were considered, yielded the worst classification results for all four algorithms evaluated.

The mean classification accuracies for all feature-sets give the impression that a feature count of approximately 75 was optimal for this dataset. However, when redundancy was removed using PCA, only 20 features were required.

#### **4.5 DISCUSSION**

From the results, it is clear that SVM outperformed the other classifiers. It produced the classification with the highest individual accuracy (Scenario 23, PCA2), and had the highest mean OA of all four classifiers considered. The relatively strong (95.9%) performance of SVM when all 205 features were used as input (Scenario 1) suggests that SVM was more robust to high dimensionality compared to the other classifiers. This is supported by the observation that SVM was the only classifier that did not benefit from the CART and RF feature selection at 75 features (Scenarios 2 and 12). These results correspond to the findings of Duro, Franklin & Dube (2015), Myburgh (2012), and Poursanidis, Chrysoulakis & Mitraka (2015) who also noted that SVM outperformed other classifiers and was relatively robust to high dimensionality. This is attributed to SVM's use of an optimized sample to generate a kernel (representing the feature space) and for calculating the support vectors (defining the hyperplane). Samples that lie on the edge of the class distribution in feature space are prioritized (Zheng et al. 2015) and are most useful for forming an accurate hyperplane to discriminate classes (Foody & Mathur 2004). The higher the number of input-variables for selecting samples are, the more the classifier is able to develop accurate hyperplanes. Reducing the number of variables can have a negative effect on the sample-set, which can lead to diminished classification results (Lu & Weng 2007; Myburgh & Van Niekerk 2013).

Another explanation for SVM not benefitting from the filter methods may be that CART and RF are ineffective at identifying the most important features for use in SVM. Both CART and RF

are tree-based algorithms; therefore, they will benefit RF and DT more. Interestingly, a slight improvement (0.3%) in accuracy was observed when PCA was used to remove redundant data per image date (Scenario 23). Although this increase was not statistically significant, the accuracies of Scenario 23 are notably higher than that of Scenario 22 in which PCA was applied on all the features. This is attributed to the loss of temporal (phenological) information when PCA is applied to all features.

Variations within crop types (e.g. ground crop, crop condition, temporal variations) have been shown to negatively affect classifications using remotely sensed imagery (Peña-Barragán et al. 2011). SVM is known to be less sensitive to intra-class variations compared to other classifiers (Myburgh & Van Niekerk, 2013) and this attribute was likely a major factor contributing to its superior performance in this study. SLICE's implementation of SVM is particularly powerful as it uses a supervised grid search method to automatically tune (optimize) the C and gamma parameters. This supports the findings of Schwert et al. (2013) and Zheng et al. (2015) who showed that SVM parameter tuning substantially improves classification accuracies.

All the classifiers (apart from SVM) benefitted from filtered feature selection, albeit marginally and only when 60 to 100 features were considered. K-NN benefitted the most, particularly when RF was used (compare Scenarios 1 and 12). DT benefitted the most from CART as feature-selection method (compare Scenarios 2 and 12), likely because both algorithms are based on tree-building (i.e. it functioned almost like a wrapper). Conversely, there is nearly no difference between Scenarios 2 and 12 when RF was used as the classifier, possibly because feature selection is inherent in the RF algorithm.

For k-NN, DT and RF, the use of the 75 most important features (Scenarios 2 and 12) produced the best results, but very similar accuracies were obtained in Scenario 23 (PCA2) in which only 20 variables were considered. This implies that CART and RF do not adequately consider redundancy when used for feature selection. It was found that many of the selected "important" features were strongly correlated. The use of features with high levels of redundancy often negatively affects accuracy (Olden & Poff 2003). It seems that RF fared better than CART in this respect, particularly when the results of k-NN are considered (compare Scenarios 2, 12, and 23). The observation that 75 features generally produced the best results is likely data-specific (combination of training-set size and total number of features), and should not be regarded as an "optimal" number of features to use for crop-type mapping.

The finding that RF feature selection imposed on SVM, DT and RF an initial penalty when the features were reduced from 205 to 150 was unexpected. This suggests that, either some important variables were excluded in the initial purge of the 45 "least important" variables, or

that redundancy increased as a result of the purge. It also brings into question whether feature selection based on variable important lists is effective.

The results of the semantic feature groupings highlighted the importance of using a mixture of feature types. For instance, texture measures have been shown to be very effective in discriminating between crop types (Peña-Barragán et al. 2011), but on its own (Scenario 27) performed poorly in this study. This is attributed to the relatively low (30 m, pan-sharpened to 15 m) spatial resolution of the imagery used. Informative texture properties of crops (e.g. texture differences of woody plants and graminoids; variations in row plantings) are not observable at this resolution (Hall-Beyer 2017). At a 15 m resolution, few pixels are available for texture generation per object and it is likely that high texture at the edges of fields (due to pixels mixed with pixels of roads and adjacent fields) confused the classifiers.

Using only the spectral bands (Scenarios 20 and 21) resulted in high (88.7% and 89.8% respectively) classification accuracies but ultimately fell short of the overall highest OA by over 6.0%, which emphasises the importance of carrying out image transformations for crop-type classifications (Scenario 26). Another notable observation is that the use of only indices (Scenario 25) also resulted in relatively poor classifications. While many multi-temporal crop-mapping studies only consider vegetation indices as features (Wardlow et al. 2007; Hao et al. 2016), our results clearly show that the incorporation of other features substantially improved classification accuracies.

This study focussed on the impact of filtered feature selection, extraction and groupings when Landsat-8 imagery is used as input to machine learning classifiers in an object-based paradigm. It consequently did not pay attention to other factors that may affect classification accuracies. These factors include the use of pixels instead of objects, variations in image segmentations (algorithms and parameters), optimal selection of images (dates and number of images), the use of other sources of optic imagery (e.g. Sentinel-2, SPOT6/7), fusion of other types of data (e.g. synthetic aperture radar), the use of other feature-selection methods (e.g. wrappers), and alternate classification algorithm parameters. Additional research is needed to investigate the impact of these factors. More work is also needed to investigate the value of specific features for recognising and differentiating particular crops and to examine which features have the greatest impact on classification accuracy.

## **4.6 CONCLUSION**

This study evaluated the use of four machine learning classifiers for the differentiation of crops in a Mediterranean climate (Western Cape, South Africa). Because of the costs associated with in

situ data collection, a small set of training samples was used to evaluate how the classifiers will perform under conditions of sparseness – a likely scenario for operational implementations. Filtered feature selection (using CART and RF), feature extraction (using PCA and TCT), and thematic feature groupings were applied to assess whether these techniques can improve classification accuracies. The results showed that filtered feature selection marginally improved classification accuracies of the DT, k-NN, and RF classifiers (particularly when the 75 most important features were selected), but were unable to improve the SVM classifications.

The thematic feature groupings highlighted a number of interesting observations. Using only the spectral bands as input to classification produced relatively poor results (even when SVM was used as classifier). Poorer results were recorded when only indices (e.g. vegetation indices) were considered. This is of particular significance as many crop-type classification studies (and operational implementations) are performed on vegetation indices only (i.e. they mainly focus on the phenology of crops and ignore their spectral and textural characteristics). This study showed that the use of a more diverse set of features (e.g. TCT, PCA, texture) dramatically increased accuracies (on average by more than 10%).

SVM significantly outperformed the other classifiers. The best classifications were obtained when all the features were used as input (95.6%), and when PCA feature extraction was performed per image (96.2%). This shows that SVM is not greatly affected by high-feature dimensionality and that PCA holds much potential for crop-type classification (PCA also benefitted the k-NN and RF classifiers). However, the additional expense of generating and selecting the PCs does not warrant the marginal improvements in accuracies observed. For operational crop-type classification in the study area (and similar regions), we conclude that the SVM algorithm can be applied to the full set of features generated. Hopefully this finding will lead to the generation of more accurate, cost-effective, and timely crop-type maps in the Cape Winelands and improve food security in the region.

## **CHAPTER 5: DISCUSSION**

This chapter summarizes and evaluates the findings of this research. The first section revisits the aims, objectives, and research questions, while the following section reflects on the value of the study. The penultimate section highlights some limitations of the research and makes recommendations for future work. Conclusions are drawn in the final section.

### **5.1 REVISITING AIMS AND OBJECTIVES**

This research aimed to evaluate the use of machine learning and multi-temporal Landsat-8 imagery for mapping crop classes in the Cape Winelands region of South Africa. The research was conducted because countries such as South Africa require accurate crop maps to strengthen their agricultural sectors by providing up to date information regarding about crop extent. Several studies have evaluated Landsat-8 imagery for crop type mapping, but a number of factors required further investigation. OBIA, for instance, has been shown to produce accurate land cover classifications (Schultz et al. 2015), but has not yet been compared to traditional pixel-based methods when using Landsat-8 images as input. There is also evidence that enhancing spatial resolution using pansharpening has positive effects on land cover classifications (Palsson et al. 2012), but no work has been done on its effect on Landsat-8 imagery for crop type mapping. Although many supervised classification algorithms are available, there have not been any comparisons between some of the most popular machine learning classifiers (e.g. DT, k-NN, RF, and SVM) for crop type mapping. Another aspect that has not yet been fully explored within the context of crop type mapping is the impact of dimensionality reduction. Many methods exist (e.g. filters, wrappers, feature extraction) but their value for crop type differentiation has not yet been assessed, especially when multi-temporal Landsat-8 imagery is used.

The literature review (Objective 1) revealed a body of research on the use of remote sensing for crop type discrimination. Much of this research suggests that that high classification accuracy can be achieved if the appropriate techniques are applied, but very little evidence is offered to indicate which combination of techniques will produce the best results when multi-temporal Landsat-8 imagery is used. A series of experiments involving different combinations of techniques were consequently carried out in this study to determine which methods will work best in the Cape Winelands region.

Collecting suitable reference data for classifier training and validation (Objective 2) was accomplished by obtaining a historical crop type map from which a sample of fields was drawn.



The sampled fields were then validated during a field survey. Details of the initial crop type map, sampling, and validation procedure were provided in Section 2.9.

Determining the value of pansharpening (Objective 3) was addressed in Chapter 3. The literature review shed light on which algorithms are the most effective for this purpose. The Pansharp algorithm showed the most potential (Zhang 2002a; Zhang 2002b) and was applied to the imagery. The multi-temporal Landsat-8 data were separated into two datasets: one with standard 30 m spatial resolution and one with 15 m spatial resolution (after pansharpening). The results of the experiments showed that 80.7% was the highest classification accuracy achieved when standard resolution Landsat-8 imagery was used. In contrast, the highest accuracy achieved using pansharpened imagery was 95.9%, a substantial and statistically significant improvement.

Objective 4 was devised in order to evaluate a range of machine learning classifiers (DT, k-NN, RF, and SVM) for producing crop maps with multi-temporal Landsat-8 imagery. As reported in Chapters 3 and 4, SVM produced the highest accuracy (96.2%) and consistently maintained a higher OA than the other classifiers. Overall, RF produced the second best results, followed by the DT and k-NN classification algorithms. It was concluded that SVM has the potential to produce accurate crop maps and that it is best suited for classifying multi-temporal Landsat-8 imagery within the study area when a relatively small number of training samples are used (as was the case in this study).

The comparison of OBIA and PBIAs for crop discrimination was performed in Chapter 3 to address Objective 5. The DT, k-NN, RF, and SVM classifiers were utilized with five datasets: standard pixels, pansharpened pixels, preferred objects, over-segmented objects, and under-segmented objects. For OBIA, the highest OA achieved was 95.9%, which compared favourably to the 94.3% of the best PBIAs classification.

Objective 6 aimed to assess whether dimensionality reduction improves classification results (again using the DT, k-NN, RF, and SVM algorithms) when multi-temporal Landsat-8 imagery is used for mapping crop types. Several dimensionality reduction methods (filter feature selection, feature extraction, and semantic feature grouping) were evaluated in Chapter 4. When all the classifiers are considered, the use of RF as filter method was the most successful (91% average OA). Feature extraction (PCA) also performed consistently well (90.4% average OA) and produced the single best classification result (96.2%) when SVM was used as classifier. However, the 0.3% difference between the feature extraction result and when no dimensionality reduction was performed (i.e. using all features) was marginal when SVM was used as classifier.

Recommendations on the use of Landsat-8 imagery for crop type mapping (Objective 7) will be addressed in Section 5.3 of this chapter.

## 5.2 MAIN FINDINGS AND VALUE OF RESEARCH

The main findings of this research can be summarized as follows:

- Landsat-8 data, in conjunction with pansharpening, is a feasible and effective way of monitoring crops in the study area.
- There was no statistical difference between the accuracies when using pansharpened pixels or when using well-delineated objects, i.e. OBIA and PBIA produced similar results.
- A good image segmentation was critical for achieving high accuracies, which can reduce OBIA's appeal for operational implementations.
- The use of a more diverse set of features (e.g. TCT, PCA, and texture) dramatically increased crop classification accuracy.
- Filter feature selection, feature extraction, and semantic feature selection did not substantially improve crop classifications.
- PCA holds much potential for crop type classification, but must be performed per image and not on the full dataset.
- SVM is relatively robust under conditions of high feature dimensionality and small training datasets.

As demonstrated in Chapter 3, it is clear that pansharpening Landsat-8 imagery is highly beneficial for crop differentiation. This finding agrees with those of Finney (2004) and Ai et al. (2016), who found that pansharpening Landsat data achieved higher classification accuracies for land cover mapping. However, the current study is the first to evaluate the effect of pansharpening of Landsat-8 imagery for crop type classification. The dramatic increases (up to 15%) in accuracy is also unprecedented. This is attributed to the almost quadrupling of the number of pixels per crop field, which increases inter-field variations and helps with crop type discrimination.

In Chapter 3 it was shown that there was no statistically significant difference between pixel-based and object-based crop discrimination when pansharpened Landsat-8 images were used as input to the machine learning classifiers. A good image segmentation (to produce objects that adequately represent fields) was also critical for achieving high accuracies in the OBIA approach. Similar observations were made by Castillejo-Gonzalez & López-Granados (2009), Duro, Franklin & Dube (2015), and Li et al. (2015). Achieving a “good” image segmentation is not a simple task as it often requires a time-consuming and subjective selection of segmentation

parameters through trial and error (Drăguț & Blaschke 2006; Peña-Barragán et al. 2011; Schultz et al. 2015). This study showed that the process of finding suitable image segmentation parameters could be circumvented by simply using a PBIA approach. This finding has practical value for operational implementations as PBIA can more easily be automated.

Chapter 4 showed that a more diverse set of features dramatically increases crop classification accuracy and that the various feature dimensionality reduction methods (filter feature selection, feature extraction, and semantic feature selection) did not significantly improve crop classification when SVM was used as classifier. Although the use of additional features to enhance thematic land cover classification is not new (Lu & Weng 2007; Heinl et al. 2009), the study improved our understanding of the relevance of different features for crop monitoring. Of all the features chosen for image classification (Table 8), the feature type that displayed the most potential was principle components generated with PCA. This finding agrees with Bell, Caviglia-Harris & Cak (2015), Da Silva et al. (2015), and Lee et al. (2016) who demonstrated its effectiveness for reducing dimensionality of remotely sensed data for crop mapping. The current study showed that the application of PCA on individual image capture dates produced the highest OA, which implies that CART and RF do not adequately consider redundancy. It seems that CART and RF selected “important” yet strongly correlated features and that the use of features with high levels of redundancy may have negatively influenced accuracies (Olden & Poff 2003). This suggests that crop type identification can be achieved using a small set of uncorrelated features, but more work is needed to investigate how such features can be automatically selected.

In Chapter 4 it was observed that SVM performed well with the full feature-set (205 features) when compared to DT, k-NN, and RF. SVM was capable of accurate crop classification when using a relatively small set of training samples. This suggests that SVM is comparatively robust to high feature dimensionality and effective with a small training sample. This finding agrees with those of Duro, Franklin & Dube (2015), Myburgh (2012), Zheng et al. (2015), and Grzegozewski et al. (2016), and can likely be attributed to SVM’s use of an optimized sample to generate a kernel (representing the feature space) and for calculating the support vectors (defining the hyperplane).

In summary, the findings of this research provide a good foundation for establishing automated procedures for the operational implementation of crop type mapping in the Cape Winelands.

### 5.3 LIMITATIONS AND RECOMMENDATIONS FOR FUTURE RESEARCH

Other studies have shown that the selection of appropriate image dates is critical to accurate crop classification. In this study, five Landsat-8 images were used, but the many image date combinations and image scenarios may influence classification accuracy. It is consequently recommended that different image capture dates and different image counts be used and compared in future studies.

This study showed that pansharpening of Landsat-8 imagery was very useful for discriminating crops, but only one method (Pansharp) was utilized. Many other pansharpening algorithms are available, with the MS-split technique introduced by Guo-dong et al. (2015) showing great promise. It is recommended that MS-split and other algorithms are assessed for crop type mapping with Landsat-8 imagery.

The comparison of OBIA and PBI in this study showed that the two approaches produced very similar results and that pansharpening had a greater effect on accuracy than the image analysis paradigm used. However, the results did show that a suitable segmentation is important for crop discrimination when OBIA is used. This adds a level of complexity (and source of error) to this approach. This research only evaluated one segmentation algorithm (MRS) and one tool (ESP) to produce a suitable segmentation. Future work should focus on improving image segmentation and providing clear guidelines for obtaining suitable segmentation results. One method that shows much potential is supervised segmentation (Poggi, Scarpa & Zerubia 2005). Alternatively, a super-pixel (over-segmenting and producing objects around the same size) approach can be assessed (Qureshi et al. 2016).

Although all the machine learning classifiers evaluated in this study produced relatively good results (> 85%), it has been shown that different parameterisations can substantially affect algorithm performance (Myburgh & Van Niekerk 2013). In this study, only one set of input parameters per classifier was employed (except for SVM, which included an automated tuning capability). More work is needed to evaluate the effects of using different input parameters. There are also many other classification algorithms available that have proven to produce accurate remote sensing classifications. Notable examples include boosting, oblique tree-based ensembles, artificial neural networks, and other “deep learning” techniques (Ciregan, Meier & Schmidhuber 2012; Maggiori et al. 2017; Poona, Van Niekerk & Ismail 2016; Wang et al. 2017).

In Chapter 4 it was found that feature extraction with PCA led to better classification accuracies compared to those of the CART and RF filter feature selection methods. This is likely because some of the “important” features identified by CART and RF are correlated (i.e. contains duplication). Many factors such as the size of the dataset, the types of features, or parameter

tuning could have influenced these results. Therefore, it is necessary to carry out more experiments on the reduction of features and redundancy for successful crop classification. Research on the efficacy of wrappers (Poona & Ismail 2013; Poona et al. 2016) is needed, while other filter methods such as infinite feature selection and eigenvector centrality feature selection should also be assessed (Wang et al. 2007; Abedinia, Nima & Hamidreza 2017).

## **5.4 CONCLUSIONS**

The research presented in this thesis aimed to evaluate the use of machine learning and multi-temporal Landsat-8 imagery for mapping crops in the Cape Winelands region of South Africa. The aim was addressed by the six objectives outlined in Section 1.3. These objectives were all achieved and three main conclusions were drawn. First, pansharpening Landsat-8 imagery had a much more profound effect on crop discrimination in the study area than the image analysis paradigm (OBIA or PBIA). Second, the SVM classifier is very well suited to crop type mapping as it is less sensitive (compared to DT, k-NN, and RF) to high feature dimensionality (resulting from using multi-temporal imagery and a small set of training data). Third, CART and RF filter feature selection is less effective than PCA feature extraction when reducing dimensionality for crop type identification with multi-temporal imagery, likely because they do not adequately consider feature redundancy. These conclusions provide valuable insights into improving the accuracy of crop type discrimination. It is recommended that the procedures evaluated in this research are operationalized in the Cape Winelands region (and possibly elsewhere) so that crop type maps can be produced on a regular basis. Hopefully this will contribute towards food security and economic growth in the region.

## REFERENCES

- Abedinia O, Nima A & Hamidreza Z 2017. A New Feature Selection Technique for Load and Price Forecast of Electrical Power Systems. *IEEE Transactions on Power Systems* 32(1): 62-74.
- Ai J, Gao W, Gao Z, Shi R, Zhang C & Liu C 2016. Integrating pansharpening and classifier ensemble techniques to map an invasive plant (*Spartina alterniflora*) in an estuarine wetland using Landsat-8 imagery. *Journal of Applied Remote Sensing* 10(2): 26001-26001.
- Al-doski J, Mansor SB & Shafri HZ 2013. Support vector machine classification to detect land cover changes in Halabja City, Iraq. In Business Engineering and Industrial Applications Colloquium (BEIAC). 2013: 353-358.
- Avci ZDU & Sunar F 2015. Process-based image analysis for agricultural mapping: A case study in Turkgeldi region, Turkey. *Advances in Space Research* 56: 1635-1644.
- Awokuse TO & Xie R 2015. Does agriculture really matter for economic growth in developing countries? *Canadian Journal of Agricultural Economics* 63(1): 77-99.
- Abdel-Rahman EM, Ahmed F & Ismail R 2013. Random forest regression and spectral band selection for estimating sugarcane leaf nitrogen concentration using EO-1 Hyperion hyperspectral data. *International Journal of Remote Sensing* 34(2): 712-728.
- Avci ZDU & Sunar F 2015. Process-based image analysis for agricultural mapping: A case study in Turkgeldi region, Turkey. *Advances in Space Research* 56(8): 1635-1644.
- Baig MB, Zhang L, Shuai T & Tong Q 2014. Derivation of a tasseled cap transformation based on Landsat-8 at-satellite reflectance. *Remote Sensing Letters* 5(5): 423-431.
- Barrett EC 2013. Introduction to environmental remote sensing. Routledge.
- Bauer ME 1975. The role of remote sensing in determining the distribution and yield of crops. *Advances in Agronomy* 27: 271-304.
- Bell AR, Caviglia-Harris JL & Cak AD 2015. Characterizing land-use change over space and time: Applying principal components analysis in the Brazilian Legal Amazon. *Journal of Land Use Science* 10(1): 19-37.
- Benedetti R & Rossini P 1993. On the use of NDVI profiles as a tool for agricultural statistics: The case study of wheat yield estimate and forecast in Emilia Romagna. *Remote Sensing of Environment* 326: 311-326.

- Benediktsson JA & Sveinsson JR 1997. Feature extraction for multisource data classification with artificial neural networks. *International Journal of Remote Sensing*. 18(4): 727-740.
- Benz UC, Hofmann P, Willhauck G, Lingenfelder I & Heynen M 2004. Multi-resolution, object-oriented fuzzy analysis of remote sensing data for GIS-ready information. *ISPRS Journal of photogrammetry and remote sensing* 58(3): 239-258.
- Bhaskaran S, Paramananda S, & Ramnarayan M 2010. Per-pixel and object-oriented classification methods for mapping urban features using Ikonos satellite data. *Applied Geography* 30: 650-665.
- Bittencourt H & Clarke R 2004. *Feature selection by using classification and regression trees*. The international Archives of the Photogrammetry, Proceedings of the 20<sup>th</sup> Congress of the International Society for Photogrammetry and Remote Sensing held 2004 in Istanbul. University of Turkey: 66-70.
- Blaes X, Vanhalle L & Defourny P 2005. Efficiency of crop identification based on optical and SAR image time series. *Remote Sensing of the Environment* 96: 352-365.
- Blaschke T 2010. Object-based image analysis for remote sensing. *ISPRS Journal of Photogrammetry and Remote Sensing* 65: 2-16.
- Blaschke T & Lang S 2006. *Object-based image analysis for automated information extraction-a synthesis*. In Measuring the Earth II ASPRS Fall Conference held 2006 in San Antonio. University of Antonio: 6-10.
- Bradski GR & Pisarevsky V 2000. *Intel's Computer Vision Library: applications in calibration, stereo segmentation, tracking, gesture, face and object recognition*. In Computer Vision and Pattern Recognition. Proceedings. IEEE Conference held 2000 in Head Island. 796-797.
- Breiman L 2001. Random forests. *Machine learning* 45(1): 5-32.
- Breiman L, Friedman J, Stone CJ & Olshen RA 1984. *Classification and regression trees*. 1<sup>st</sup> ed. Wadsworth, Belmont: CRC Press.
- Brown JC, Kastens JH, Coutinho AC, de Castro Victoria D & Bishop CR 2013. Classifying multiyear agricultural land use data from Mato Grosso using time series MODIS vegetation index data. *Remote Sensing of Environment* 130: 39-50.
- Campbell J 2008. *Introduction to Remote Sensing*. 4<sup>th</sup> ed. New York: Taylor and Francis.
- Campbell J & Wynne R 2011. *Introduction to Remote Sensing*. 5<sup>th</sup> ed. New York: Taylor and Francis.

- Campbell M, Congalton RG, Hartter J & Ducey M 2015. Optimal land cover mapping and change analysis in north-eastern Oregon using Landsat imagery. *Photogrammetric Engineering & Remote Sensing* 81(1): 37-47.
- Castillejo-Gonzalez I & López-Granados F 2009. Object and pixel-based analysis for mapping crops and their agro-environmental associated measures using QuickBird imagery. *Computers and Electronics in Agriculture* 68(2): 207–215.
- Chang CC & CJ Lin 2011. LIBSVM: A library for support vector machines. *ACM Transactions on Intelligent Systems and Technology* 2(3): 27-30.
- Ciregan D, Meier U & Schmidhuber J 2012. Multi-column deep neural networks for image classification. *In Computer Vision and Pattern Recognition (CVPR)* 1: 3642-3649.
- Clausi DA 2002. An analysis of co-occurrence texture statistics as a function of grey level quantization. *Canadian Journal of Remote Sensing* 28(1): 45-62.
- Collingwood A, Franklin SE, Guo X & Stenhouse G 2009. A medium-resolution remote sensing classification of agricultural areas in Alberta grizzly bear habitat. *Canadian Journal of Remote Sensing* 35(1): 23-36.
- Congalton RG & Green K 2008. *Assessing the accuracy of remotely sensed data: principles and practices*. 2<sup>nd</sup> ed. New York: Taylor and Francis Group CRC press.
- Conrad C, Colditz R, Dech S, Klein D, Vlek P 2011. Improved irrigated crop classification in Central Asia using temporal segmentation and MODIS time series. *International Journal of Remote Sensing* 32 (23): 8763-8778.
- Crist EP & Cicone RC 1984. A Physically-Based Transformation of Thematic Mapper Data-The TM Tasseled Cap. *IEEE Transactions on Geoscience and Remote Sensing* 22(3): 256-262.
- DAFF [Department of Agriculture, Forestry and Fisheries] 2015. Plant Production - Brochures and Production guidelines. Available at: <http://www.daff.gov.za/daffweb3/Branches/Agricultural-Production-Health-Food-Safety/Plant-Production/Production-Guidelines>
- Da Silva CA, Nanni, MR, Cezar E, Gasparotto ADC, da Silva AA, Silva GFC, Facco CU & Demattê JM 2015. Principal Component Analysis in Monitoring Soybean Fields of Brazil through the MODIS Sensor. *Journal of Agronomy* 14(2): 72-79.
- Duro DC, Franklin SE & Dube MG 2015. A comparison of pixel-based and object-based image analysis with selected machine learning algorithms for the classification of agricultural landscapes using SPOT-5 HRG imagery. *Remote Sensing of Environment* 118: 259-272.



- Drăguț L & Blaschke T 2006. Automated classification of landform elements using object-based image analysis. *Geomorphology* 81: 330-344.
- Drăguț L, Tiede D & Levick SR 2010. ESP: a tool to estimate scale parameter for multiresolution image segmentation of remotely sensed data. *International Journal of Geographical Information Science*. 24(6): 859-871.
- Drăguț L, Csilik O, Eisank C & Tiede D 2014. Automated parameterisation for multi-scale image segmentation on multiple layers. *ISPRS Journal of Photogrammetry and Remote Sensing* 88: 119-127.
- Elachi C & Van Zyl JJ 2006. *Introduction to the physics and techniques of remote sensing*. 2<sup>nd</sup> ed. John Wiley & Sons.
- Finney KM 2004. Utilizing Pansharpened Landsat-7 Imagery to Detect Urban Change in the Vancouver Census Metropolitan Area: 1999-2002. *Graduate Program in Spatial Analysis Research Paper*. Toronto, Ontario, Canada, Ryerson University. 2004.
- Foody G & Atkinson P 2002. Uncertainty in Remote Sensing and GIS. *Uncertainty in remote sensing and GIS*. Chichester: Wiley.
- Foody GM & Mathur A 2004. Toward intelligent training of supervised image classifications: directing training data acquisition for SVM classification. *Remote Sens of the Environment* 93(1): 107–117.
- Fourie C 2011. A one class object-based system for sparse geographic feature identification. Master's Thesis. Stellenbosch: Stellenbosch University.
- Gamon J & Surfus J 1999. Assessing leaf pigment content and activity with a reflectometer. *New Phytologist* 143: 105-117.
- Gao BC 1996. NDWI—A normalized difference water index for remote sensing of vegetation liquid water from space. *Remote sensing of environment* 58(3): 257-266.
- Gao J 2009. *Digital Analysis of Remotely Sensed Imagery*. New York: McGraw Hill.
- Ghassemian H 2016. A Review of Remote Sensing Image Fusion Methods. *Information Fusion* 0(1): 1-15.
- Ghodekar HR, Deshpande AS & Scholar PG 2016. Pansharpening Based on Non-Subsampled Contourlet Transform. *International Journal of Engineering Science* 1: 2831.

- Gilbertson JK, Kemp J & van Niekerk A 2017. Effect of pan-sharpening multi-temporal Landsat 8 imagery for crop type differentiation using different classification techniques. *Computers and Electronics in Agriculture* 134: 151-159.
- Gislason PO, Benediktsson JA, & Sveinsson JR 2006. Random forests for land cover classification. *Pattern Recognition Letters* 27(4): 294-300.
- Gitelson A, Kaufman Y & Merzlyak M 1994. Use of a green channel in remote sensing of global vegetation from EOS-MODIS. *Desert Research* 58(3): 289-298.
- Gitelson AA, Kaufman YJ, Stark R & Rundquist D 2002. Novel algorithms for remote estimation of vegetation fraction. *Remote sensing of Environment* 80(1): 76-87.
- Gitelson AA, Gritz Y & Merzlyak MN 2003a. Relationships between leaf chlorophyll content and spectral reflectance and algorithms for non-destructive chlorophyll assessment in higher plant leaves. *Journal of plant physiology* 160(3): 271-282.
- Gitelson AA, Viña A, Arkebauer TJ, Rundquist DC, Keydan G & Leavitt B 2003b. Remote estimation of leaf area index and green leaf biomass in maize canopies. *Geophysical Research Letters* 30(5). 277-281.
- Gitelson AA, Viña A, Ciganda V, Rundquist DC & Arkebauer, TJ 2005. Remote estimation of canopy chlorophyll content in crops. *Geophysical Research Letters* 32(8).
- Grzegozewski DM, Johann JA, Uribe-Opazo, MA, Mercante E & Coutinho AC 2016. Mapping soya bean and corn crops in the State of Paraná, Brazil, using EVI images from the MODIS sensor. *International Journal of Remote Sensing* 37(6): 1257-1275.
- Guan H, Yu J & Luo L 2012. Random Forests-Based Feature Selection for Land-Use Classification Using LIDAR Data and Orthoimagery. *Remote Sensing and Spatial Information Sciences* 39: 7-11.
- Guan X, Huang C, Liu G, Meng X & Liu Q 2016. Mapping Rice Cropping Systems in Vietnam Using an NDVI-Based Time Series Similarity Measurement Based on DTW Distance. *Remote Sensing* 8(1): 19-25.
- Guo-dong Y, Xin-yu X, Xiang Z & Hong-wei Z 2015. MS-split and analysis of the comparison it with another three image fusion approaches. *International Journal of Signal Processing, Image Processing and Pattern Recognition* 8(10): 331-342.
- Guyon I & Elisseeff A 2003. An introduction to variable and feature selection. *The Journal of Machine Learning Research* 3:1157-1182.

- Hall-Beyer M 2017. Practical guidelines for choosing GLCM textures to use in landscape classification tasks over a range of moderate spatial scales. *International Journal of Remote Sensing* 38(5): 1312-1338.
- Hao P, Zhan Y, Wang L, Niu Z & Shakir M 2015. Feature selection of time series MODIS data for early crop classification using random forest: A case study in Kansas, USA. *Remote Sensing* 7(5): 5347-5369.
- Hao P, Wang L, Zhan Y, Niu Z & Wu M 2016. *Using historical NDVI time series to classify crops at 30m spatial resolution: A case in Southeast Kansas*. In Geoscience and Remote Sensing Symposium (IGARSS) held July 2016 in Beijing: 6316-6319.
- Heinl M, Walde J, Tappeiner G & Tappeiner U 2009. Classifiers vs. input variables—The drivers in image classification for land cover mapping. *International Journal of Applied Earth Observation and Geoinformation* 11(6): 423-430.
- Hess L, Ratana P, Huete A, Potter C & Melack J 2009. *Use of MODIS enhanced vegetation index to detect seasonal patterns of leaf phenology in central Amazon várzea forest*. In 2009 IEEE International Geoscience and Remote Sensing Symposium held July 2009 in Cape Town: 4-1007.
- Hoffer RM, Johannsen CJ & Baumgardner MF 1966. Agricultural applications of remote multispectral sensing. *In Proceedings of the Indiana Academy of Science*. 76: 386-396.
- Huang C, Wylie B, Yang L, Homer C, & Zylstra 2002. Derivation of a tasseled cap transformation based on Landsat 7 at-satellite reflectance. *International Journal of Remote Sensing* 23(8): 1741-1748.
- Huang HH, Liu XY & Liang Y 2016. Feature Selection and Cancer Classification via Sparse Logistic Regression with the Hybrid L 1/2+ 2 Regularization. *PloS one* 11(5):149-675.
- Huete A, Justice C & Liu H 1994. Development of vegetation and soil indices for MODIS-EOS. *Remote Sensing of the Environment* 49:224-234.
- Hunt ER, Doraiswamy PC, McMurtrey JE, Daughtry CS, Perry EM & Akhmedov B 2013. A visible band index for remote sensing leaf chlorophyll content at the canopy scale. *International Journal of Applied Earth Observation and Geoinformation* 21: 103-112.
- Hunt ER, Daughtry CS, Mirsky SB & Hively WD 2014. Remote sensing with simulated unmanned aircraft imagery for precision agriculture applications. *Selected Topics in Applied Earth Observations and Remote Sensing* 7(11): 4566-4571.

- Hsu CC, Chang CC & Lin CJ 2003. A practical guide to support vector classification [online]. Available from: <http://www.csie.ntu.edu.tw/~cjlin/papers/guide/guide.pdf> [Accessed 26 September 2017].
- Hsu CC, Chen MC & Chen LS 2010. Integrating independent component analysis and support vector machine for multivariate process monitoring. *Computers & Industrial Engineering*. 59(1): 145-156.
- Jackson R & Huete AR. 1991. Interpreting vegetation indices. *Preventive Veterinary Medicine* 11: 185-200.
- Johnson BA, Scheyvens H & Shivakoti BR 2014. An ensemble pansharpening approach for finer-scale mapping of sugarcane with Landsat 8 imagery. *International Journal of Applied Earth Observation and Geoinformation*. 33: 218-225.
- Jordan CF 1969. Derivation of leaf area index from quality of light on the forest floor. *Ecology* 50: 663–666.
- Jiang Z, Huete AR., Didan K, & Miura T 2008. Development of a two-band enhanced vegetation index without a blue band. *Remote Sensing of Environment* 112(10): 3833-3845.
- Jiang Z 2008. Development of a two-band enhanced vegetation index without a blue band. *Remote Sensing of Environment* 112(10): 3833–3845.
- Karimi Y, Prasher SO, Patel RM & Kim SH 2006. Application of support vector machine technology for weed and nitrogen stress detection in corn. *Computers and electronics in agriculture* 51(1): 99-109.
- Kaufman Y & Tanr D 1992. Atmospherically resistant vegetation index (ARVI) for EOS-MODIS. *Geoscience and Remote Sensing* 30(2): 261-270.
- Kauth RJ & Thomas GS 1976. *The tasseled cap - a graphic description of the spectral-temporal development of agricultural crops as seen by Landsat*. In LARS Symposia: 159. 1976.
- Khazenie N & Richardson K 1993. Comparison of texture analysis techniques in both frequency and spatial domains for cloud feature extraction. *International Archives of Photogrammetry and Remote Sensing* 29: 1009-1015.
- Kojadinovic I & Wotzka T 2000. Comparison between a filter and a wrapper approach to variable subset selection in regression problems. Proceedings of the European Symposium on Intelligent Techniques.

- Kosaka N, Akiyama T, Tsai B & Kojima T 2005. Forest type classification using data fusion of multispectral and panchromatic high-resolution satellite imageries. *International Geoscience and Remote Sensing Symposium 4*: 2980-2985.
- Kumar P, Prasad R, Gupta DK, Mishra VN & Choudhary A 2015. Support vector machine for classification of various crop using high resolution LISS-IV imagery. *Bulletin of Environmental and Scientific Research* 4(3): 34-29.
- Kusumaningrum R & Arymurthy AM 2011. Color and Texture Feature for Remote Sensing–Image Retrieval System: A Comparative Study *IJCSI* 8(5): 125-135.
- Lagrange A, Fauvel M & Grizonnet M 2016. Large-scale feature selection with Gaussian mixture models for the classification of high dimensional remote sensing images. *HAL archives*. 1.
- Lang MW, Kasisckhe ES, Prince SD & Pittman KW 2008. Assessment of C-band synthetic aperture radar data for mapping and monitoring coastal plain forested wetlands in the Mid-Atlantic Region, USA. *Remote Sensing of the Environment* 112: 4120-4130.
- Lawrence R & Wright a 2001. Rule-Based classification systems using Classification and regression trees (CART) analysis. *Photogrammetric Engineering and Remote Sensing* 1137-1142.
- Lee J, Cai X, Lellmann J, Dalponte M, Malhi Y, Butt, N, Morecroft M, Schönlieb CB & Coomes DA 2016. Individual tree species classification from airborne multi-sensor imagery using robust PCA. *IEEE Journal of Selected Topics in Applied Earth Observations and Remote Sensing* 9(6): 2554-2567.
- Lewinski S 2007. Applying fused multispectral and panchromatic data of Landsat ETM+ to object oriented classification. *New Developments and Challenges in Remote Sensing* 1: 233-240.
- Lewis RJ 2000. *An Introduction to Classification and Regression Tree (CART) Analysis. Presented at Annual Meeting of the Society for Academic Emergency Medicine. In Annual Meeting of the Society of Academic Emergency Medicine held 2000 in San Francisco.* 0-41.
- Li Q, Wang C, Zhang B & Lu L 2015. Object-Based Crop Classification with Landsat-MODIS Enhanced Time Series Data. *Remote Sensing* 7(12): 16091-16107.
- Liaw A & Wiener M 2002. Classification and regression by random forest. *R news* 2(3): 18-22.
- Liang S, Fang H, Morissette JT, Chen M, Shuey CJ, Walthall CL & Daughtry CS 2002. Atmospheric correction of Landsat ETM+ land surface imagery. Validation and applications. *IEEE transactions on Geoscience and Remote Sensing* 40(12): 2736-2746.

- Lin C, Wu CC, Tsogt K, Ouyang YC & Chang CL 2015. Effects of atmospheric correction and pansharpener on LULC classification accuracy using WorldView-2 imagery. *Information Processing in Agriculture* 2(1): 25-36.
- Lee E, Kastens JH & Egbert SL 2016. Investigating collection 4 versus collection 5 MODIS 250 m NDVI time-series data for crop separability in Kansas, USA. *International Journal of Remote Sensing* 37(2): 341-355.
- Loh WL 2011. *Classification and regression trees*. 1<sup>st</sup> ed. John Wiley & Sons, Inc.
- Long JA, Lawrence R., Greenwood MC, Marshall L & Miller PR 2013. Object-oriented crop classification using multi-temporal ETM+ SLC-off imagery and random forest. *GIScience & Remote Sensing* 50(4): 418-436.
- Long F Zhang H & Feng DD 2003. *Fundamentals of content-based image retrieval*. In Feng DD, Siu WC, Zhang HJ (eds) *Multimedia Information Retrieval and Management*. Signals and Communication Technology. Springer, Berlin, Heidelberg
- Lu D & Weng Q 2007. A survey of image classification methods and techniques for improving classification performance. *International Journal of Remote Sensing* 28(5): 823-870.
- Lück W, Mhangara P, Kleyn L & Remas H. 2010. Land Cover Field Guide, version 2.0. Report prepared for Chief Directorate: National Geospatial Information, CSIR Satellite Applications Centre: Earth Observation Service Centre, Pretoria.
- Maggiori E, Tarabalka Y, Charpiat G & Alliez P 2017. Convolutional Neural Networks for Large-Scale Remote-Sensing Image Classification. *IEEE Transactions on Geoscience and Remote Sensing* 55(2): 645-657.
- Mather PM 2004. *Computer Processing of Remotely-Sensed Images: An Introduction*. Chichester: Wiley.
- Mathieu R, Freeman C & Aryal J 2007. Mapping private gardens in urban areas using object-oriented techniques and very high-resolution satellite imagery. *Landscape and Urban Planning* 81: 179-192.
- McFeeters SK 1996. The use of the Normalized Difference Water Index (NDWI) in the delineation of open water features. *International Journal of Remote Sensing*. 17(7): 1425-1432.

- McNairn H, Champagne C, Shang J, Holmstorm D & Reichert G 2009. Integration of optical and synthetic aperture radar (SAR) imagery for delivering annual crop inventories. *ISPRS Journal of Photogrammetry and Remote Sensing* 64(1):434-449.
- McNemar Q 1974. Correction to a correction. *Journal of Consulting and Clinical Psychology* 42(1): 145.
- Miner G, Nisbet R & Elder J 2009. *Handbook of statistical analysis and data mining applications*. Academic press.
- Monfreda C, Ramankutty N & Foley JA 2008. Farming the planet: Geographic distribution of crop areas, yields, physiological types, and net primary production in the year 2000. *Global biogeochemical cycles* 22(1): 45-54.
- Mountrakis G, Im J & Ogole C 2011. Support vector machines in remote sensing: A review. *ISPRS Journal of Photogrammetry and Remote Sensing* 66(3): 247-259.
- Mulla DJ 2013. Twenty-five years of remote sensing in precision agriculture: Key advances and remaining knowledge gaps. *Biosystems Engineering* 114(4): 358-371.
- Muller H, Rufin P, Griffiths P, Siqueira A & Hostert P 2015. Mining dense Landsat time series for separating crop land and pasture in a heterogeneous Brazilian landscape. *Remote Sensing of Environment* 156:490-499.
- Myburgh G 2012. The impact of training set size and feature dimensionality on supervised object-based classification: a comparison of three classifiers. Master's Thesis. Stellenbosch: Stellenbosch University.
- Myburgh G & Van Niekerk A 2013. Effect of feature dimensionality on object-based land cover classification: A comparison of three classifiers. *South African Journal of Geomatics* 2(1):13-27.
- Myint SW, Gober P, Brazel A, Grossman-Clarke S & Weng Q 2011. Per-pixel vs. object-based classification of urban land cover extraction using high spatial resolution imagery. *Remote sensing of environment* 115(5): 1145-1161.
- Nolin AW & Payne MC 2007. Classification of glacier zones in Western Greenland using albedo and surface roughness from the multi-angle imaging Spectroradiometer (MISR). *Remote Sensing of the Environment* 107: 264-275.
- Oguro Y & Suga Y 2003. Monitoring of a rice field using landsat 5 TM and landsat 7 ETM+ data. *Characterization of Satellite Sensors* 32(11): 2223–2228.
- Olden JD & Poff NL 2003. Redundancy and the choice of hydrologic indices for characterizing streamflow regimes. *River Research and Applications* 19(2): 101-121.

- Oruc M, Marangoz AM & Buyuksalih G 2004. *Comparison of pixel-based and object-oriented classification approaches using Landsat-7 ETM spectral bands*. In Proceedings of XX ISPRS Congress held 2004 in Istanbul. 1: 5.
- Otukei JR & Blaschke T 2010. Land cover change assessment using decision trees, support vector machines and maximum likelihood classification algorithms. *International Journal of Applied Earth Observation and Geoinformation*. 12: 27-S31.
- Otukei JR, Blaschke T, Collins M & Maghsoudi Y 2011. *Analysis of ALOS PALSAR and TerraSAR-X data for protected area mapping: A Case of the Bwindi impenetrable National Park, Uganda*. IEEE International geoscience and Remote Sensing Symposium (IGARSS) held July 2011 in Vancouver: 348-351.
- Ozelkan E, Chen G & Ustundag BB 2015. Multiscale object-based drought monitoring and comparison in rainfed and irrigated agriculture from Landsat-8 OLI imagery. *International Journal of Applied Earth Observation and Geoinformation* 44: 159-170.
- Pal M & Mather P 2003. An assessment on the effectiveness of decision tree methods for land cover classification. *Remote Sensing of the Environment* 86(4):554-565.
- Pal M 2005. Random forest classifier for remote sensing classification. *International Journal of Remote Sensing*. 26(1): 217-222.
- Palsson F, Sveinsson JR, Benediktsson JA & Aanaes H 2012. Classification of pansharpened urban satellite images. *IEEE Journal of Selected Topics in Applied Earth Observations and Remote Sensing* 5(1): 281-297.
- Pauw T & Van Niekerk A 2012. Automated wetland classification using OBIA: Agulhas Plain, South Africa.
- Peña JM, Gutiérrez PA, Hervás-Martínez C, Six J, Plant RE & López-Granados F 2014. Object-based image classification of summer crops with machine learning methods. *Remote Sensing* 6(6): 5019-5041.
- Peña-Barragán JM, Ngugi MK, Plant RE & Six J 2011. Object-based crop identification using multiple vegetation indices, textural features and crop phenology. *Remote Sensing of Environment* 115(6): 1301-1316.
- Pesaresi M & Benediktsson JA 2001. A new approach for the morphological segmentation of high resolution satellite imagery. *Geoscience and Remote Sensing* 39(2): 309-320.



- Persello C & Bruzzone L 2016. Kernel-Based Domain-Invariant Feature Selection in Hyperspectral Images for Transfer Learning. *IEEE Transactions on Geoscience and Remote Sensing* 54(5): 2615-2626.
- Poggi G, Scarpa G & Zerubia JB 2005. Supervised segmentation of remote sensing images based on a tree-structured MRF model. *IEEE Transactions on Geoscience and Remote Sensing* 43(8): 1901-1911.
- Poona NK & Ismail R 2013. *Reducing hyperspectral data dimensionality using random forest based wrappers*. In Geoscience and Remote Sensing Symposium (IGARSS) IEEE International, held July 2013 in Munich. 1470-1473
- Poona N, Van Niekerk A & Ismail R 2016. Investigating the utility of oblique tree-based ensembles for the classification of hyperspectral data. *Sensors* 16(11): 1918.
- Poona NK, van Niekerk A, Nadel RL & Ismail R 2016. Random forest (RF) wrappers for waveband selection and classification of hyperspectral data. *Applied spectroscopy* 70(2): 322-333.
- Poursanidis D, Chrysoulakis N & Mitraka Z 2015. Landsat 8 vs. Landsat 5: A comparison based on urban and peri-urban land cover mapping. *International Journal of Applied Earth Observation and Geoinformation*. 35: 259-269.
- Qian J, Root J & Saligrama V 2015. Learning Efficient Anomaly Detectors from k-NN Graphs. *Artificial Intelligence and Statistics* 4(1): 790-799.
- Qian Y, Zhou W, Yan J, Li W & Han L 2015. Comparing machine learning classifiers for object-based land cover classification using very high-resolution imagery. *Remote Sensing* 7:153-168.
- Qureshi WS, Payne A, Walsh KB, Linker R, Cohen O & Dailey MN 2016. Machine vision for counting fruit on mango tree canopies. *Precision Agriculture* 1:1-21.
- Richardson A, Goodenough DG & Chen H 2014. *Hierarchical unsupervised nonparametric classification of polarimetric SAR time-series data*. In Geoscience and Remote Sensing Symposium (IGARSS), 2014 IEEE International held July 2014 in Cuebec City: 4730-4733.
- Rodriguez-Galiano VF, Chica-Olmo M, Abarca-Hernandez F, Atkinson PM & Jeganathan C 2012. Random Forest classification of Mediterranean land cover using multi-seasonal imagery and multi-seasonal texture. *Remote Sensing of Environment* 121: 93-107.
- Rondeaux G, Steven M & Baret F 1996. Optimization of soil-adjusted vegetation indices. *Geography* 55(2): 95-107.

- Roy DP, Wulder MA, Loveland TR, Woodcock CE, Allen RG, Anderson MC & Helder D 2014. Landsat-8: Science and product vision for terrestrial global change research. *Remote Sensing of Environment* 145 (2): 154-172.
- Saeys Y, Inza I & P Larrañaga 2007. A review of feature selection techniques in bioinformatics. *Bioinformatics* 19: 2507-2517.
- Sakamoto T, Yokozawa M, Toritani H, Shibayama M, Ishitsuka N, & Ohno H 2005. A crop phenology detection method using time-series MODIS data. *Remote sensing of environment* 96(3): 366-374.
- Salmon JM, Friedl MA, Froking S, Wisser D & Douglas EM 2015. Global rain-fed, irrigated, and paddy croplands: A new high-resolution map derived from remote sensing, crop inventories and climate data. *International Journal of Applied Earth Observation and Geoinformation* 38: 321-334.
- Schiewe J 2002. Segmentation of high-resolution remotely sensed data-concepts, applications and problems. *International Archives of Photogrammetry Remote Sensing and Spatial Information Sciences* 34(4): 380-385.
- Schultz B, Immitzer M, Formaggio AR, Sanches IDA, Luiz AJB & Atzberger C 2015. Self-guided segmentation and classification of multi-temporal landsat-8 images for crop type mapping in south-eastern brazil. *Remote Sensing* 7(11): 14482-14508.
- Schwert B, Rogan J, Giner NM, Ogneva-Himmelberger Y, Blanchard SD & Woodcock C 2013. A comparison of support vector machines and manual change detection for land-cover map updating in Massachusetts, USA. *Remote Sensing Letters* 4(9): 882-890.
- Serra P & Pons X 2008. Monitoring farmers' decisions on Mediterranean irrigated crops using satellite image time series. *International Journal of Remote Sensing* 29(9): 2293-2316.
- Shahi K, Shafri HZM & Hamedianfar A 2016. Road condition assessment by OBIA and feature selection techniques using very high-resolution WorldView-2 imagery. *Geocarto International* 1: 1-18.
- Siegmund A & Menz G 2005. Fernes nah gebracht - Satelliten- und Luftbildeinsatz zur Analyse von Umweltveränderungen im Geographieunterricht. *Geographie und Schule*: 154: 7.
- Simms D, Waite T, Taylor J & Juniper G 2014. The application of time-series MODIS NDVI profiles for the acquisition of crop information across Afghanistan. *International Journal of Remote Sensing* 35(16): 6234-6254.

- Singh K, Agrawal KN & Bora GC 2011. Advanced techniques for weed and crop identification for site-specific weed management. *Biosystems Engineering*. 109(1): 52-64.
- SIQ 2014. Producer independent crop estimate system (PICES) [Online]. Available from: <http://www.siq.co.za/pices.php> [Accessed: 7 April 2015].
- Smith LI 2002. A tutorial on principal components analysis. Cornell University, USA, 51, 52.
- Song C, Woodcock CE, Seto KC, Lenney MP & Macomber SA 2001. Classification and change detection using Landsat TM data: when and how to correct atmospheric effects? *Remote sensing of Environment* 75(2): 230-244.
- Steinwart I & Christmann A 2008. *Support vector machines*. Springer Science & Business Media.
- Srinivasan GN & Shobha G 2008. Statistical Texture Analysis. *World Academy of Science Engineering, and Technology* 36: 1264-1269
- Stephenson G & van Niekerk 2009. *A cost effective, rule based technique to improve forestry inventory on a national scale*. Paper delivered at the IEEE international Geoscience and Remote Sensing Symposium (IGARSS) held July 2009 in Cape Town: 11-330.
- Suykens JA & Vandewalle J 1999. Least squares support vector machine classifiers. *Neural processing letters* 9(3): 293-300.
- Taghvaeian S, Fox G, Boman R & Warren J 2015. *Evaluating the Impact of Drought on Surface and Groundwater Dependent Irrigated Agriculture in Western Oklahoma*. A Tribute to the Career of Terry Howell, Sr. Conference Proceedings: 1-8.
- Tang H, Wu EX, Ma QY, Gallagher D, Perera GM & Zhuang T 2000. MRI brain image segmentation by multi-resolution edge detection and region selection. *Computerized Medical Imaging and Graphics* 24(6): 349-357.
- Tererai F, Gaertner M, Jacobs SM & Richardson DM 2013. Eucalyptus invasions in riparian forests: effects on native vegetation community diversity stand structure and composition. *Ecological Management* 297:84-93.
- Tererai F, Gaertner M & Jacobs SM 2015. Resilience of invaded riparian landscapes: The potential role of soil-stored seed banks. *Environmental Management* 55:86-99.
- USGS 2015. Landsat instruments and data products [Online]. Available from: <http://landsat.usgs.gov/landsat8.php> [Accessed 15 February 2015].

- Van Niekerk A 2010. A comparison of land unit delineation techniques for land evaluation in the Western Cape, South Africa. *Land Use Policy* 27(3): 937-945.
- Vanonckelen S, Lhermitte S & Van Rompaey A 2013. The effect of atmospheric and topographic correction methods on land cover classification accuracy. *International Journal of Applied Earth Observation and Geoinformation* 24: 9-21.
- Verhulp J & Van Niekerk A 2016. Effect of inter-image spectral variation on land cover separability in heterogeneous areas. *International Journal of Remote Sensing*. 37(7): 1639-1657.
- Vieira MA, Formaggio AR, Renno CD, Atzberger C, Aguiar DA & Mello MP 2012. Object-based Image Analysis and Data Mining applied to a remotely sensed Landsat. *Remote Sensing of Environment* 123: 553-562.
- Viña A, Gitelson AA, Nguy-Robertson AL & Peng Y 2011. Comparison of different vegetation indices for the remote assessment of green leaf area index of crops. *Remote Sensing of Environment* 115(12): 3468-3478.
- Waheed T, Bonnell RB, Prasher SO & Paulet E 2006. Measuring performance in precision agriculture: CART-A decision tree approach. *Agricultural Water Management* 84(1): 173-185.
- Wardlow BD, Egbert SL & Kastens J 2007. Analysis of time-series MODIS 250 m vegetation index data for crop classification in the US Central Great Plains. *Remote Sensing of Environment* 108(3): 290-310.
- Wardlow BD, Egbert SL 2008. Large-area crop mapping using time-series MODIS 250 m NDVI data: An assessment for the US Central Great Plains. *Remote Sensing of Environment*. 112(3): 1096-1116.
- Wang X, Yang J, Teng X, Xia W & Jensen R 2007. Feature selection based on rough sets and particle swarm optimization. *Pattern Recognition Letters* 28(4): 459-471.
- Wang X, Li X, Tan M & Xin L 2015. Remote sensing monitoring of changes in winter wheat area in North China Plain from 2001 to 2011. *Transactions of the Chinese Society of Agricultural Engineering* 31(8): 190-199.
- Wang L, Zhang J, Liu P, Choo KKR & Huang F 2017. Spectral-spatial multi-feature-based deep learning for hyperspectral remote sensing image classification. *Soft Computing* 21(1): 213-221.

- Weih RC & Riggan ND 2010. Object-based classification vs. pixel-based classification: Comparative importance of multi-resolution imagery. *The International Archives of the Photogrammetry, Remote Sensing and Spatial Information Sciences* 38(4): 7-14.
- Whiteside TG, Boggs GS, & Maier SW 2011. Comparing object-based and pixel-based classifications for mapping savannahs. *International Journal of Applied Earth Observation and Geoinformation* 13(6): 884-893.
- Wilson EH & Sader SA 2002. Detection of forest harvest type using multiple dates of Landsat TM imagery. *Remote Sensing of Environment* 80: 385–396.
- Xin Q, Broich M, Suyker AE, Yu L & Gong P 2015. Multi-scale evaluation of light use efficiency in MODIS gross primary productivity for croplands in the midwestern United States. *Agricultural and Forest Meteorology* 201: 111-119.
- Xu H 2006. Modification of normalised difference water index (NDWI) to enhance open water features in remotely sensed imagery. *International Journal of Remote Sensing* 27(14): 3025-3033.
- Yan G, Mas JF, Maathuis BHP, Xiangmin Z & Van Dijk PM 2015. Comparison of pixel-based and object-oriented image classification approaches—a case study in a coal fire area, Wuda, Inner Mongolia, China. *International Journal of Remote Sensing* 27(18): 4039-4055.
- Yang L, Xian G, Klaver JM & Deal B 2003. Urban land-cover change detection through sub-pixel imperviousness mapping using remotely sensed data. *Photogrammetric Engineering & Remote Sensing* 69(9): 1003-1010.
- Yang Z, Willis P & Mueller R 2008. Impact of band-ratio enhanced AWIFS image to crop classification accuracy. *The Future of Land Imaging: Going Operational Denver* 17(1): 18-20.
- Yoon GW, Cho SI, Jeong S & Park JH 2003. Object oriented classification using Landsat images. *Forest* 47: 37-50.
- Yu QP, Gong P, Clinton N, Biging G, Kelly M & Schirokauer D 2006. Object-based detailed vegetation classification with airborne high spatial resolution remote sensing imagery. *Photogrammetric Engineering and Remote Sensing* 72(7): 799-811.
- Yuan F, Sawaya KE, Loeffelholz BC & Bauer ME 2005. Land cover classification and change analysis of the Twin Cities (Minnesota) Metropolitan Area by multi-temporal Landsat remote sensing. *Remote sensing of Environment* 98(2): 317-328.

- Zhao S, Wang Q, Yao Y, Du S, Zhang C, Li J & Zhao J 2016. Estimating and validating wheat leaf water content with three MODIS spectral indexes: a case study in Ningxia Plain, China. *Journal of Agricultural Science and Technology* 18(2): 387-398.
- Zhang Y 2002a. Problems in the fusion of commercial high-resolution satellite as well as Landsat 7 images and initial solutions. *International Archives of Photogrammetry Remote Sensing and Spatial Information Sciences* 34(4): 587-592.
- Zhang Y 2002b. A new automatic approach for effectively fusing Landsat 7 as well as IKONOS images. *In IEEE/IGARSS 2*: 24-28.
- Zhang Y & Mishra RK 2012. A review and comparison of commercially available pansharpening techniques for high resolution satellite image fusion. *In Geoscience and Remote Sensing Symposium (IGARSS), 2012 IEEE International 1*:182-185.
- Zheng B, Myint SW, Thenkabail PS & Aggarwal RM 2015. A support vector machine to identify irrigated crop types using time-series Landsat NDVI data. *International Journal of Applied Earth Observation and Geoinformation* 34:103-112.